A gene regulation mechanism that allows synthesis of two ferredoxin : NADP oxidoreductase isiforms from a single gene in the cyanobacterium Synechocystis sp. PCC 6803

Amin Nasser

Université Paris VI - Pierre et Marie Curie

Ecole doctorale iViv - ED387

Doctorat en

BIOLOGIE

Auteur

Amin NASSER

Titre

Un mécanisme de régulation génétique permettant la synthèse de deux isoformes de la ferrédoxine:NADPoxydoréductase, à partir d'un seul gène, chez la cyanobactérie *Synechocystis* sp. PCC 6803

Soutenance le 13 juillet 2012

Jury:

Rapporteures	Karine LAPOUGE
	Amel LATIFI
Examinatrices	Sophie CRIBIER
	Pascale ROMBY
Directrice de thèse	Ghada AJLANI

Acknowledgments

I would like to thank all the people that contributed to the success of this work. However, it is difficult to cite everyone who assisted, contributed or encouraged me during my thesis, and I hope that being in a hurry or sometimes stressed did not prevent me for thanking them at the appropriate moment.

I'll start by thanking my PhD committee for accepting the task of evaluating my thesis. I would like to express my thankfulness to Dr. *Amel LATIFI* and Dr. *Karine LAPOUGE* for accepting, in the midst of their activities, to constitute the reading committee.

I would like to record my gratitude to my supervisor, Dr. *Ghada AJLANI* for her guidance, encouragements and support over these years. Thank you for your enthusiasm, your competence, your passion for science and for cyanobacteria. Thank you for your limitless advises, your knowledge and skills; thanks for sharing all that with me, which were very fruitful for shaping up my ideas and research.

Thank you for giving me the chance of discovering the magnificent world of cyanobacteria. Thanks for your heartfelt support along the way. Thanks for being a mentor and a friend. Thanks for all the good moments as well as for the hard ones, that taught me a lot. Thanks for your matchless kindness and for you humor, which are undoubtedly of good help all the time. Thank you for all the "philosophical" debates that gave me the chance to see the world from a new perspective and with a critical eye.

Thank you for all that and for many other things...

I doubt that I will ever be able to convey my appreciation fully, but I owe you my eternal gratitude.

I gratefully thank Dr. *Bruno ROBERT* for accepting me in his laboratory and for offering me a financial support for an additional year.

A very special thanks goes also to *Adrienne GOMEZ de GRACIA*, for her skills and for all the help with the experiments. Thank you for the countless discussions, the advices and for the critical sense of humor during these years.

My thanks also go to all the members of the team, for their kindness, their help and all the good moments

A special acknowledgement goes to Dr. *Violaine DAVID* for her competence, her kindness, for all the scientific and nonscientific discussions and for her humor, which I really appreciate. Your invitation to "Zakhlé" is still open.

I would like to thank Dr. *Andrew GALL, Dr. Andrew PASCAL*, Dr. *Daniel PICOT*and Dr. *Pierre SETIF* for their constructive comments and their critical reading of my dissertation.

Many thanks to all the IBMC members I met in Strasbourg, where I spent one of the best parts of my thesis. Thanks to Dr. *Pascal ROMBY*for accepting me in her laboratory, for her kindness, for all the stimulating discussions and for giving me the opportunity to discover the wonderful world of RNA. Thanks to Dr. *Stefano MARZI*for the supervision and all the discussions. Thanks to *Anne-Catherine* for the technical help. A special thanks to *Cédric, Redmond, Sara, Mélodie, Patrick, Delphine, Efi*and many others for the help as well as for being good friends.

Many thanks to all my friends who have been around during my thesis and who have been of a good help at different occasions and have influenced my thesis in one way or another. In particular, thanks to *Fakih and Mroue*for being around and helpful since my first day in France, Thanks to *Zeinab*for being an extraordinary neighbor, to*Michal*for all the discussions and for the"funny" adventure in the US, toDenis for his humor and the discussions, thanks to *Denise, Qian, Sana, Anja, Maria, Kevin, Tiona, Ali, Arthur, Sylvia, Antoine, Christophe, Mazen, Nancy Zarour, Oula, Rana and NancyAbouzeid.*

I owe my family a special gratefulness,for showing me the joy of intellectual pursuit ever since I was child and later for giving me the chance of going to France. Thank you for all the "long-distance" encouragements and support.

Finally, I would like to thank everyone who was important to the successful realization of my thesis, as well as expressing my apology that I could not mention personally every one.

Amin

Table of contents

List of figures

List of tables

This work was carried out at the

Laboratoire bioénergétique membranaire et stress (LBMS)

Address

iBiTec-S, Batiment 532,

CNRS, CEA-Saclay,

91191Gif-sur-Yvette Cedex, FRANCE

Résumé

Les cyanobactéries sont des bactéries dont le métabolisme dépend essentiellement de la photosynthèse. Représentantes actuelles de l'ancêtre cyanobactérien des chloroplastes, elles synthétisent des molécules organiques, à partir de gaz carbonique, de nitrates ou d'azote atmosphérique (dans les souches fixatrices d'azote).

Ainsi la photosynthèse oxygénique assure la conversion de l'énergie lumineuse en énergie biochimique (NADPH et ATP) tout en rejetant de l'oxygène. La formation photosynthétique du NADPH à partir des électrons provenant des photosystèmes est catalysée par la ferrédoxine:NADP oxydoréductase (FNR). La FNR peut aussi oxyder le NADPH afin de fournir des électrons à certaines voies métaboliques. Différentes isoformes de FNR, codées par une famille de gènes nucléaires, sont présentes dans les plastes des plantes.

Dans un travail antérieur, notre laboratoire a identifié, chez la cyanobactérie *Synechocystis* sp. PCC6803, deux isoformes de FNR, codées par l'unique gène *petH* (FNR_L de 46 kDa et FNR_S de 34 kDa). Grâce à un domaine supplémentaire dont la séquence est similaire à celle des linkers du phycobilisome (complexe macromoléculaire collecteur de lumière), la grande isoforme FNR_L se trouve attachée au phycobilisome. Ce domaine est absent dans la petite isoforme FNR_S. Des tests de croissance de mutants, exprimant uniquement une des isoformes, ont suggéré que FNR_L est impliquée dans la fonction photosynthétique (transfert linéaire d'électrons) et que FNR_S est impliquée dans la fonction respiratoire et dans le transfert cyclique d'électrons. Il est donc établi que, chez certaines cyanobactéries, une double fonction est assurée par l'unique gène *petH*, produisant deux isoformes de FNR. Ces isoformes ont des localisations différentes, en raison de leurs capacités d'interaction avec le phycobilisome. Le processus aboutissant à la synthèse de FNR_L ou de FNR_S par le gène *petH*, implique deux sites d'initiation de traduction distants de 337 nucléotides. Le premier permet la synthèse de FNR_L alors que le second permet celle de FNR_S.

L'objet de ce travail de thèse est l'élucidation du mécanisme qui permet, en fonction des conditions de croissance, des initiations de traductions alternatives. Ce mécanisme est dorénavant bien décrypté grâce à une combinaison d'approches (de génétique classique, de biochimie et de biologie moléculaire) résumée ci-après.

Etant donné que *petH* est un gène indispensable à la survie de *Synechocystis*, la première partie du travail concerne l'expression d'un allèle ectopique placé dans le locus *psbA2*. Cette insertion est neutre pour *Synechocystis* car une autre copie de ce gène, *psbA3*, assure sa fonction en son absence. Les allèles exprimés comprennent la région codante de *petH* placée soit sous le contrôle de la région 5' non codante de *psbA2*, soit sous le contrôle de la région 5' non codante propre au gène *petH*. La région 5' non codante de *petH* contient la région promotrice telle qu'elle a été définie par van Thor et al. en 1999. L'allèle ectopique portant la région 5' non codante de *psbA2* étant incapable d'induire la traduction de FNR_S, nous avons conclu que la région 5' non codante de *petH* est indispensable à la synthèse de FNR_S. Des délétions dans la région 5' non codante de *petH* ont montré que chaque isoforme est codée par un transcrit spécifique. Ceci a été confirmé par la cartographie de l'extrémité 5' des transcrits en conditions standard (où FNR_L s'accumule) et en conditions de carence en azote (où FNR_S s'accumule). En effet deux ARNm avec des séquences "leader" similaires (32 et 53 bases) sont transcrits en conditions standard, alors qu'en conditions de carence en azote un ARNm portant une séquence "leader" plus longue (126 bases) est transcrit. La présence de promoteurs spécifiques à chaque transcrit a été confirmée par des insertions de cassette portant des terminateurs de transcription dans différents sites de la région 5' non codante.

Nous avons aussi montré, par une série de mutations ponctuelles ainsi que par des expériences de retard de migration de fragments d'ADN comprenant le promoteur *petH*, que la synthèse de l'ARNm le plus long était sous le contrôle du régulateur transcriptionnel NtcA.

Nos résultats montrent également que, contrairement à ce qui a été décrit par van Thor et al., l'organisation transcriptionnelle de *petH* dans *Synechocystis* était similaire à celle décrite chez la cyanobactérie *Anabaena* sp. PCC7120 (Valadaress et al. 1999).

De plus, des fusions transcriptionnelles du promoteur *lac* de *Escherichia coli* avec les différentes régions transcrites de *petH* ont permis de montrer que la régulation traductionnelle ne nécessite pas de facteur spécifique à *Synechocystis* sp. et qu'elle peut être accomplie par des structures secondaires adoptées par la région leader des ARNm. De telles structures pouvant activer l'initiation de traduction de FNR_S et inhiber celle de FNR_L.

Afin de tester cette hypothèse, nous avons utilisé le programme mfold pour modéliser la structure secondaire de l'extrémité 5' des ARN messagers de *petH*(Zucker, 2003). Alors que plusieurs structures ont été proposées, une seule d'entre elles a été validée par les résultats des délétions effectuées dans la région codant l'extrémité 5' du transcrit *petH*.

L'hypothèse a aussi été testée *in vitro* par des expériences de cartographie des complexes d'initiation de traduction "Toeprinting". Dans l'ARNm le plus long, le complexe a été localisé dans la région initiatrice de FNR_L (AUG-1) alors que dans les ARNm plus courts, celui-ci a été localisé dans la région initiatrice de FNR_S (AUG-113). Ce résultat confirme l'hypothèse d'une simple structuration de l'extrémité 5' du transcrit dans le choix du codon d'initiation.

Des expériences de cartographie visant à déterminer la structure des transcrits sont en cours, afin de mieux comprendre ce nouveau mécanisme de régulation au niveau moléculaire.

Abbreviations

A	Absorption
A_1	Phylloquinone; an electron acceptor in photosystem I
Amp^r	Ampicillin resistance
APC	Allophycocyanin
ASD	Anti-Shine-Dalgarno
a.u.	Arbitrary unit
b_6f	Cytochrome b_6f
CET	Cyclic electron transfer
CRP	**c**AMP **r**eceptor **p**rotein
cyt	Cytochrome
Da	Dalton
EDTA	Ethylene diaminetetraacetic acid
(F_X, F_A, F_B)	(4Fe-4S) Clusters, the terminal acceptor of PSI
Fd	Ferredoxin
FNR	Ferredoxin:NADP(H) oxidoreductase
FNR_L	Large FNR isoform
FNR_S	Small FNR isoform
Ile	Isoleucine
Km^r	Kanamycin resistance
L_C	Core-linker polypeptide
L_{CM}	Core-membrane-linker polypeptide
LET	Linearelectron transfer
L_R	Rod-linker polypeptide
L_{RC}	Rod-core-linker polypeptide
Mb	Megabase
Met	Methionine
$NADP^+$ (NADPH)	Nicotinamide adenine dinucleotide phosphate
NDH	NADPH dehydrogenase
OD	Optical density
orf	Open reading frame
P680	Primary electron donor of photosystem II
P700	Primary electron donor of photosystem I
PBP	Phycobiliprotein
PBS	Phycobilisome
PC	Phycocyanin
PCB	Phycocyanobilin
PCC	Pasteur Culture Collection
PE	Phycoerythrin
PQ	Plastoquinone
PSI	Photosystem I

PSII	Photosystem II
Q_A	Primary electron acceptor quinone of photosystem II
Q_B	Secondary electron acceptor quinone of photosystem II
ROS	Reactive oxygen species
RTO	Respiratory terminal oxidase
SD	Shine-Dalgarno
SDS	Sodium dodecyl sulfate
SDS-PAGE	Polyacrylamide gel electrophoresis in the presence of SDS
Sm^r	Spectinomycin resistance
Sp^r	Streptomycin resistance
Synechocystis	*Synechocystis* sp. PCC 6803
TIR	Translationinitiation region
Tsp	Transcriptionstart point
UTR	Untranslated region
WT	Wild type
Y_Z	Tyrosine residue of photosystem II (secondary donor Tyr)
$\alpha^{AP\text{-}B}$	Allophycocyanin $\alpha^{AP\text{-}B}$subunit
α^{APC}andβ^{APC}	Allophycocyanin$\alpha^{APC}$and β^{APC}subunits
α^{PC} andβ^{PC}	Phycocyanin$\alpha^{PC}$and β^{PC}subunits
β^{18}	Allophycocyanin β^{18}subunit
Ω cassette	Spectinomycin and Streptomycin resistance cassette bracketed by transcription terminators

I. Introduction

I.1. Cyanobacteria

Formerly known as blue-green algae, cyanobacteria are considered to be among the oldest organisms on earth in evolutionary terms. Putative microfossils, that are 3.5 billion years old, have been found and were attributed to cyanobacteria (Schopf, 1993). The main reason for the evolutionary endurance of these organisms is their successful combination of effective metabolic pathways (Vermaas, 2001). All cyanobacteria are able to grow using CO_2 as the sole carbon source. They are among the very few groups that can perform oxygenic photosynthesis and respiration simultaneously in the same cell compartment. In addition, some cyanobacterial species are able to fix atmospheric nitrogen. Therefore cyanobacteria survive under a wide range of environmental conditions and inhabit almost every conceivable environment (freshwater, marine and terrestrial).

Cyanobacteria form a group of gram-negative bacteria that is genetically heterogeneous. This heterogeneity is observed in their genome size (2.4 to 13 Mb) and GC content (32 to 71%). They represent one of the major phylogenetic lines of bacteria and show a distant relationship to gram-positive bacteria (Madigan et al., 1996). The morphological diversity of the cyanobacteria is considerable - both unicellular and multicellular filamentous forms exist, and considerable variation within these morphological types occurs(**Figure I.1**). Cyanobacterial cell size ranges from those of typical bacteria (0.5-1 μm in diameter) to cells as large as 60 μm in diameter as in the case of the cyanobacterium*Oscilliatoria princeps.*

Cyanobacteria differ in fatty acid composition when compared to other prokaryotes. Like plant plastids, they frequently contain polyunsaturated fatty acids, while bacteria usually contain almost exclusively saturated and monounsaturated fatty acids. All cyanobacteria, like plant chloroplasts, contain chlorophyll and carotenoids as photosynthetic pigments. They all synthesize chlorophyll *a* and most of them also contain characteristic bilin pigments called phycobilins, which function as accessory

pigments in photosynthesis. These pigments are responsible for the diverse color range observed in these species (blue, green, red and black). Distinct cyanobacterial lineages produce alternative chlorophyll pigments (in addition to chlorophyll *a*); these include three prochlorophyte species that produce chlorophyll *b*(*Prochlorotrix hollandica*, *Prochloron didemni*, and *Prochlorococcus marinus*) and the species *Acaryochloris marina*, which produces chlorophyll *d*.

According to 16S rRNA phylogenetic analysis, cyanobacteria constitute a diverse phylum of organisms within the bacterial radiation that are close to plant chloroplasts on the phylogenetic tree. Such analysis supports the endosymbiotic theory for the origin of plant plastids.(Giovannoni et al., 1988; Turner et al., 1999)

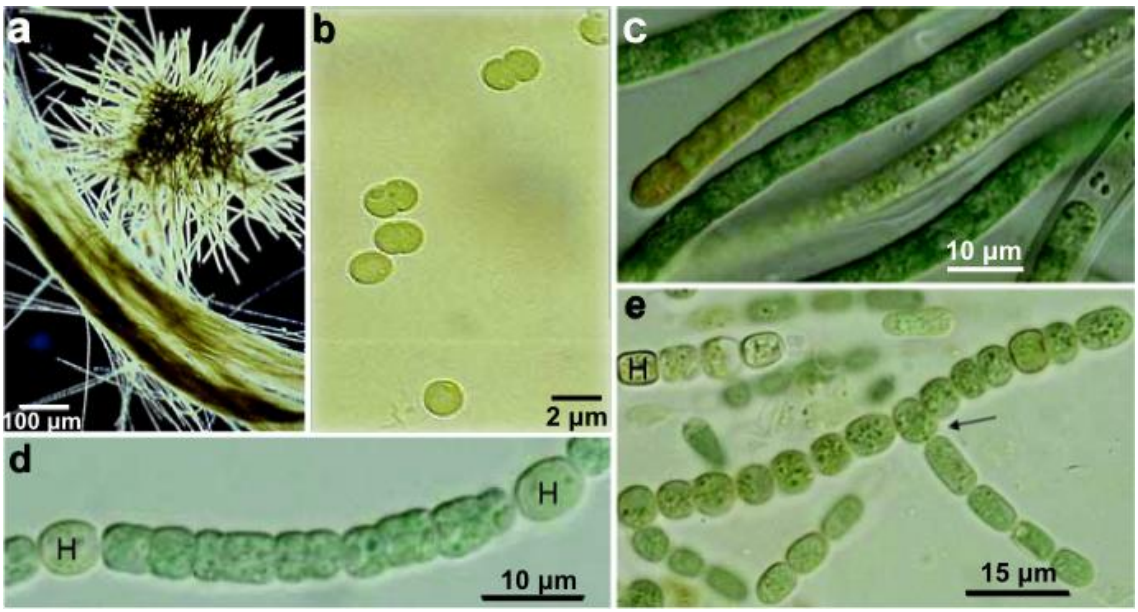

Figure I.1 Micrographs of cyanobacteria strains illustrating their morphological differences.
a. The filamentous bloom-forming *Trichodesmium thiebautii*. **b.** The unicellular *Synechocystis* sp. PCC 6803. **c.** The filamentous *Symploca* PCC 8002. **d.** The filamentous, non-branching, and *Nostoc* PCC 7107 (note heterocysts, H). **e.** The filamentous, heterocysts (H) and branching (arrow) *Fischerella* PCC 7521 (H – heterocyst). From (Cox et al., 2005), with some modifications.

I.2. *Synechocystis* sp. strain PCC 6803

Our model organism is the unicellular cyanobacterium *Synechocystis* sp. strain PCC 6803 (hereafter referred to as *Synechocystis*). *Synechocystis* was originally isolated from a freshwater lake in California by R. Kunisawa(Stanier et al., 1971).It is the first photosynthetic organism and the second bacterium to have its genome fully sequenced (Kaneko et al., 1996). *Synechocystis* is the most popular laboratory strain serving as a model in the research fields of photosynthesis, stress response and metabolism (Ikeuchi and Tabata, 2001). There are two major reasonsfor its importance: it is naturally transformable by exogenous DNA (Grigorieva and Shestakov, 1982), and it can grow heterotrophically in the presence of glucose, which permits the selection of photosynthesis-deficient mutants(Rippka et al., 1979; Ikeuchi and Tabata, 2001).

Synechocystis is a unicellular coccoid or spherical cyanobacterium (**Figure I.1-b** and**Figure I.2**).Its circular genome is about 3.5 Mb,with an average GC content of 47.7%(Kaneko et al., 1996).

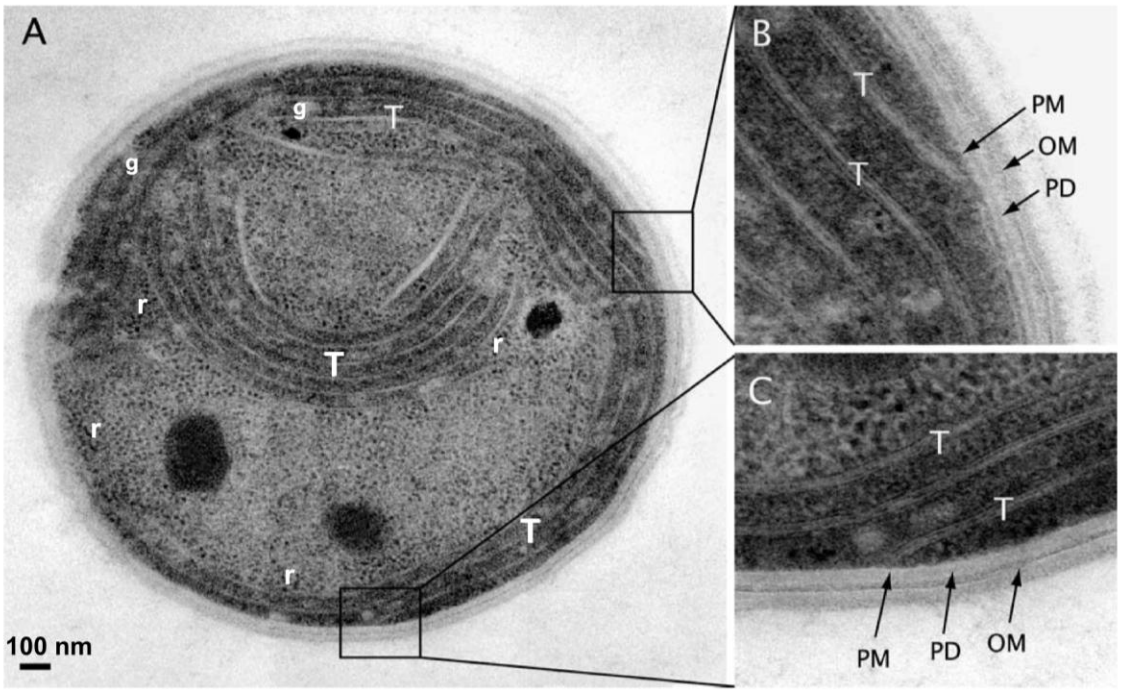

Figure I.2 Electron micrograph of a thin section through *Synechocystis* sp. PCC 6803.
A.Thin section showing intracellular structures present in *Synechocystis* sp. PCC 6803.
Band **C**. Enlargements of the boxed areas in A, showing close proximity of thylakoid membrane (T) and plasma membrane (PM). *g:* glycogen granule; *r* ribosomes; *OM:* outer membrane; *PD:* peptidoglycan layer. From (Liberton et al., 2006).

As all gram-negative bacteria, *Synechocystis* has a cell envelope consisting of a plasma membrane, a peptidoglycan layer and an outer membrane (**Figure I.2**). In addition, as in all cyanobacteria exceptfor*Gloeobacter violaceus*, *Synechocystis* contains an internal membrane system,the thylakoid, where photosynthetic and respiratory electron-transfer reactions occur (**Figure I.2**).

Components of both photosynthetic and respiratory systems, as well astheir electron transferpathwaysare introduced in the following section.

I.3. Bioenergetics

It is believed that photosynthesis arose early in the evolution of life on earth,more than 3.5 billion years ago. At the beginning photosynthetic life was almost certainly anoxygenic (purple bacteria, green sulfur bacteria). Oxygenic photosynthesis was later initiated by cyanobacteria,which revolutionized the energetic and enzymatic fundamentals of life, by releasing oxygen into the atmosphere. Photosynthesis literally means "synthesis with light"; it is the process by which the electromagnetic energy from a photon is converted into biochemical energy. Madiganet al. classified photosyntheticbacteriainto five major groups or phyla (Madigan et al., 1996); four are anoxygenic, which means that they don't produce molecular oxygen -theseinclude purple bacteria, green-sulfur bacteria, green-nonsulfur bacteria and heliobacteria. The single oxygen-evolving, or oxygenic, group of photosynthetic bacteria are the cyanobacteria (Madigan et al., 1996).

In addition to light, oxygenic photosynthesis requires water and CO_2 as substrates, from which it produces oxygen and sugars. Organisms performing oxygenic photosynthesis are photoautotrophs,becausethey derive all their cellular carbon (organic components) from CO_2 and light. The synthesized organic components may then be ingested and used by heterotrophs, which are the organisms that derive their cellular carbon from organic compounds(Madigan et al., 1996).

Species capable of performing photosynthesis are present in prokaryotic and eukaryotic lineages. In photosynthetic eukaryotes(plants), photosynthesis is localized in subcellular organelles known as chloroplasts. These structures usually have the size of a bacterium (a few micrometers in diameter) and evidence suggests that chloroplasts originated from cyanobacteria by endosymbiosis (Raven, 1970). It is assumed that a cyanobacterial-like cell was a symbiont within a protoeukaryotic cell and then became a semi-autonomous part of the host. This explains the similarity between cyanobacteria and the photosynthetic eukaryotes.

Oxygenic photosynthesis is carried out in double bilayer membraneswith closed ends called thylakoids (from the Greek: sac-like); the compartment inside these "sacs" is called lumen (**Figure I.2**). The thylakoid membranes are suspended in the chloroplast stroma in eukaryotic cells and in the cytoplasm of cyanobacteria. These membranes are

independent from the outer membrane in both cases. Thylakoids contain the electron transport chain and allow for the accumulation of an electrochemical gradient, these are the key elements for photosynthesis.

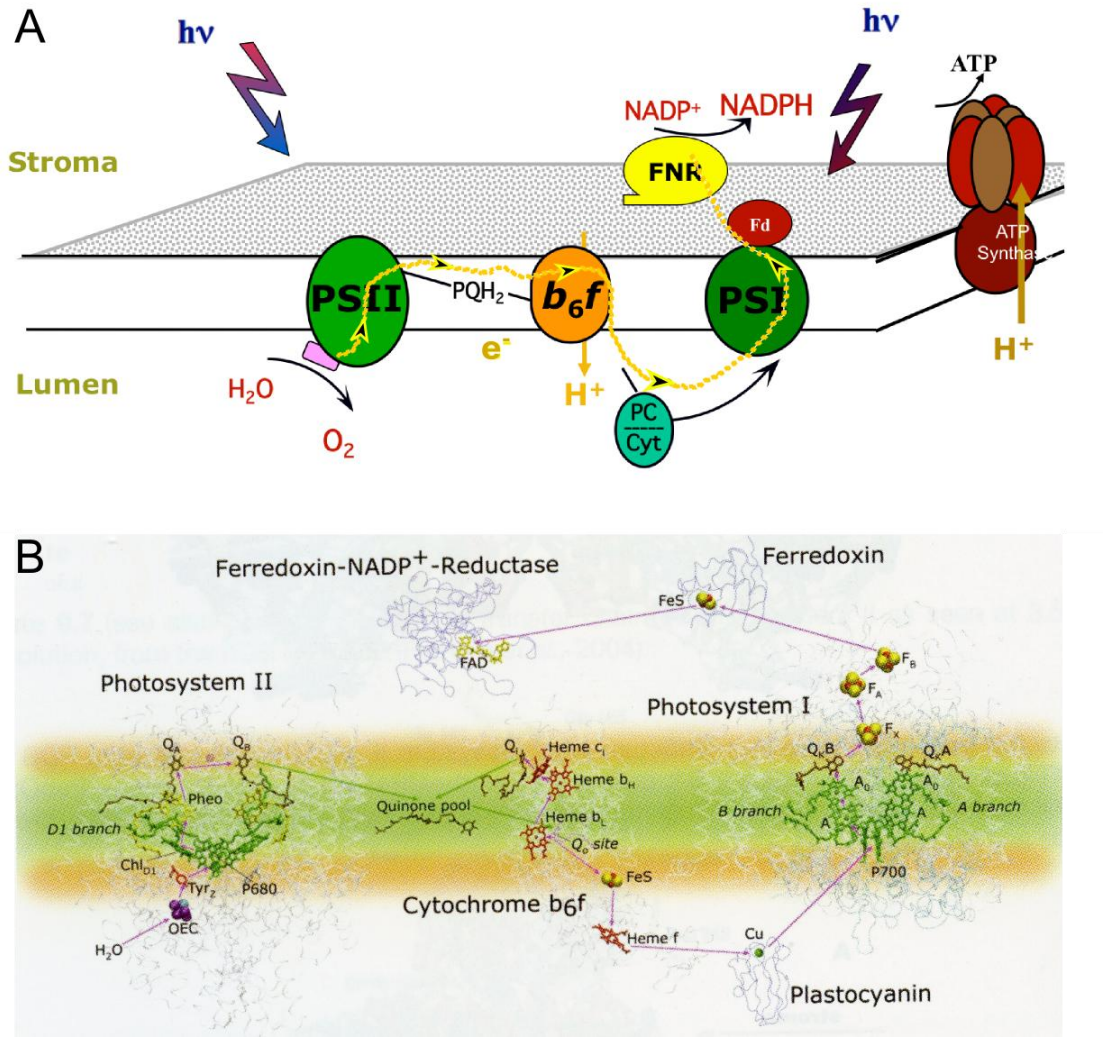

Figure I.3 The photosynthetic complexes present in the thylakoid membrane.
A. Scheme of the protein complexes that drive oxygenic photosynthesis in thylakoids. Black-yellow arrows indicate the trajectory of the electrons during linear photosynthetic electron transport.
B. Representation of the cofactors involved in photosynthetic electron transport.
From left to right: photosystem II (PSII), the cytochrome b_6f complex (b_6f), photosystem I (PSI), and the ATP synthase as well as the soluble electron carriers plastocyanin (PC), cytochrome *c6* (Cyt) (only in A), ferredoxin (Fd) and the ferredoxin:NADP+ oxidoreductase (FNR). From (DeRuyter and Fromme, 2008).

Two modes of photosynthetic electron transfer exist: linear electron-transfer (LET) and cyclic-electron transfer (CET). While CET is involved in redox-state regulation, LET is the major mode of electron transfer in organisms performing oxygenic photosynthesis.

I.3.1. Linear photosynthetic electron transfer

LET involves two photosynthetic reaction centers called photosystem I (PSI) and photosystem II (PSII) (**Figure I.3-A**). It implicates water oxidation to molecular oxygen by PSII, as a first step, then the reduction of $NADP^+$ to NADPH *via* PSI, as a final step. The membrane-protein complex called cytochrome b_6f (cyt b_6f) mediates electron transport between PSII and PSI in the thylakoid. During this process an electrochemical proton gradient is produced across the thylakoid membrane. This gradient is used, by ATP synthase, to produce ATP (**Figure I.3-A**). NADPH and ATP are then used to fix CO_2 in the Calvin cycle, among other anabolic reactions.

In the following sections, we will introduce the four integral membrane-protein complexes, PSII, cyt b_6f, PSI and ATP-synthasethat are involved in photosynthetic electron transfer and ATP synthesis.

The **photosystem II**reaction center (PSII) is composed mainly of two similar protein subunits referred to as D1 and D2. It carries out the first step of LET, which is the light-catalyzed oxidation of water. This reaction provides almost all earth's atmospheric molecular oxygen.

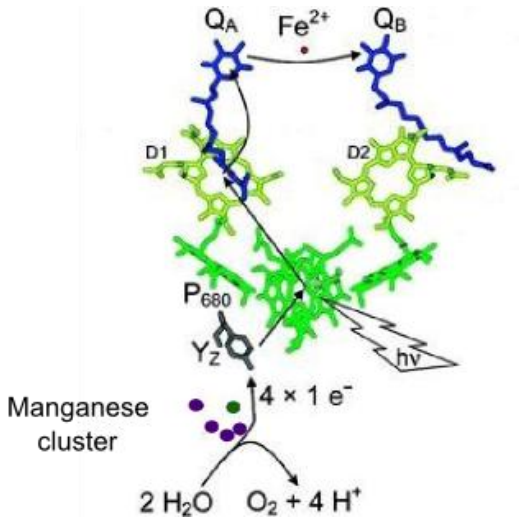

Figure I.4 Photosystem II reaction-center cofactors.
The PSII reaction center cofactors involved in light harvesting, electron transfer and water oxidation. Water oxidation produces oxygen and the extracted electrons accumulate as reduced plastoquinones that will be transferred to cytb_6f. Purple dots represent the magnesium atoms in the manganese cluster. Green dot represent the chloric atom of the manganese cluster. From (McEvoy and Brudvig, 2006).

The reaction starts with the excitation of P680, the primary chlorophyll donor of PSII (**Figure I.4**). Upon absorption of a photon,an electron is transferred from an excited

state of P680 to a pheophytin that in turn reduces a D2-bound plastoquinone called Q_A(Barber et al., 1987). Q_A^- reduces a second D1-bound plastoquinone Q_B, and after two charge-separation events doubly-reduced Q_B^{2-} picks up two hydrogen ions to form plastoquinol (PQH2). PQH2 then leaves PSII to transfer electrons to cyt b_6f;the Q_B site is refilled from the PQ pool in the membrane. On the donor side of PSII, $P680^+$ oxidizes a Tyr residue, Y_Z, which in turn oxidizes a cluster of four manganese atoms. The manganese cluster is able to accumulate four oxidizing equivalents that are necessary to release one oxygen molecule (O_2) from two waters(Hankamer et al., 1997).

The **cytochrome *b_6f*** complex transfers electrons from plastoquinone (PQ) to PSI. Cyt $b_6f$contains at least five essential cofactors: two *b*-hemes, two*c*-hemes (*f*and c_i) and a characteristic high-potential 2Fe-2S center (the Rieske iron-sulfur protein) (**Figure I.5**). The cyt b_6f complex also contains two PQ-binding sites, Q_o (luminal side) and Q_i (cytoplasmic side). Plastoquinol is oxidized at the luminal side of the membrane, transferring two electrons and releasing two protons into the lumen.The first electron is transferred to the Rieske iron-sulfur protein,then onto cyt *f* and finally to plastocyanin (or to cyt c_6). The second electron is transferred *via* two *b*-hemes (b_L and b_H) to the Qi site where another PQ is reduced. As a consequence only one electron will be delivered to PSI while two protons will cross the thylakoid membrane (Trumpower, 1990; Stroebel et al., 2003).

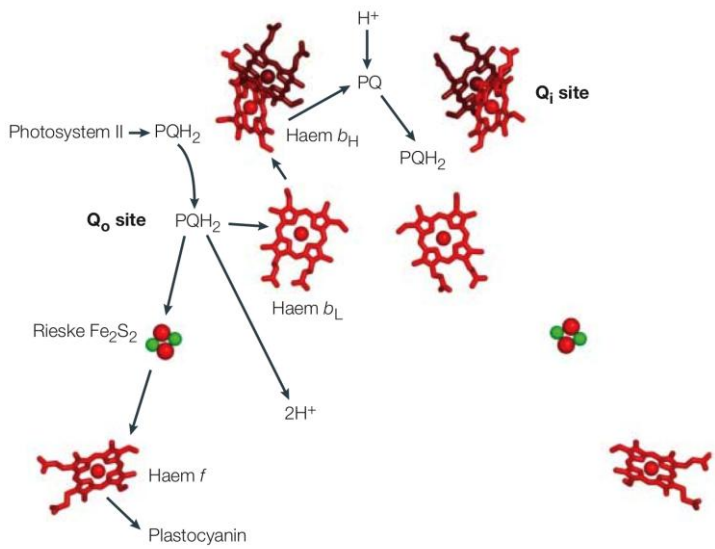

Figure I.5 Cytochrome-*b_6f* cofactors.
Cyt b_6f oxidizes plastoquinone, using the extracted electrons to reduce soluble electron carriers such as plastocyanin or cyt c_6. From (Stroebel et al., 2003).

Photosystem I (PSI) functions at the reducing end of the photosynthetic electron transfer chain (Golbeck, 1993). The reaction center is formed mainly by two large,homologous subunits called PsaA and PsaB. These subunits harbor most of the PSI pigments and all the cofactors up to F_X. The primary chlorophyll in PSI is a chlorophyll *a* called P700 (Krauss et al., 1993). Photoexitation of P700 results in its oxidation to $P700^+$ and the reduction of a phylloquinone A_1. An electron from plastocyanin (or cyt c_6) reduces $P700^+$ to P700, while A_1^- passes its electron to three iron-sulfur clusters, FeS-X (F_X), FeS-A (F_A) and FeS-B (F_B) (**Figure I.6**). The electron is then transferred to the soluble **Ferredoxin** (Fd), which itself reduces NADP+ into NADPH*via* the enzyme called ferredoxin:NADP oxidoreductase (FNR) (**Figure I.3**).This FNR enzyme constitutes the subject of this thesis.

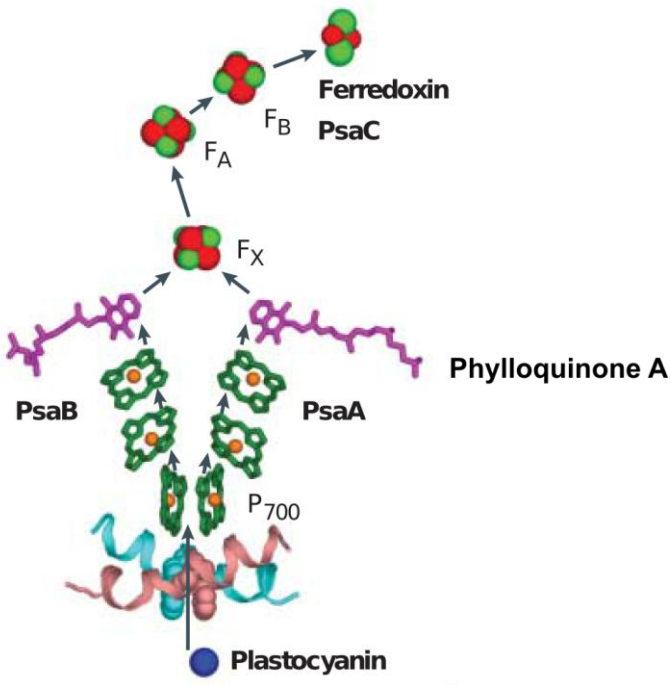

Figure I.6 Photosystem I cofactors.
PSI uses light to oxidize P700 and reduce ferredoxin. $P700^+$ oxidizes a reduced plastocyanin (or cyt c_6). From (Ben-Shem et al., 2003).

This chain of electron transfers also results in the formation of a proton gradient across the thylakoid membrane. Protonflowfrom the lumen through the integral membrane,part of the **ATP-synthase,**provides energy for ATP synthesis (**Figure I.3-A**).

I.3.2. Electron redirection and cyclic photosynthetic electron flow

Duringphotosynthetic LET, O_2, ATP and reduced NADPH are produced. However, stress conditions, like high-light or low CO_2, may lead to electron redirection towards other compounds. In these cases, electrons can be transferred from PSI to molecular oxygen, which resultsin the photoreduction of O_2, *via* superoxideanion (O_2^-), to form H_2O_2 in plant chloroplastes(Mehler-reaction) (Mehler, 1951). This reaction produces reactive oxygen species (ROS), known to cause a significant damage to the cell. In photosynthetic organisms PSII is the preferential target of ROS resulting in photoinhibition (Hackenberg et al., 2009). ROS are quickly detoxified by the combined action of superoxide dismutase and peroxidases. O_2 photoreduction in cyanobacteria is quite different from that in plants. In*Synechocystis*, O_2 is reduced directly to water in a reaction mediated by A-type flavoproteins, which avoids ROS accumulation(Vicente et al., 2002).

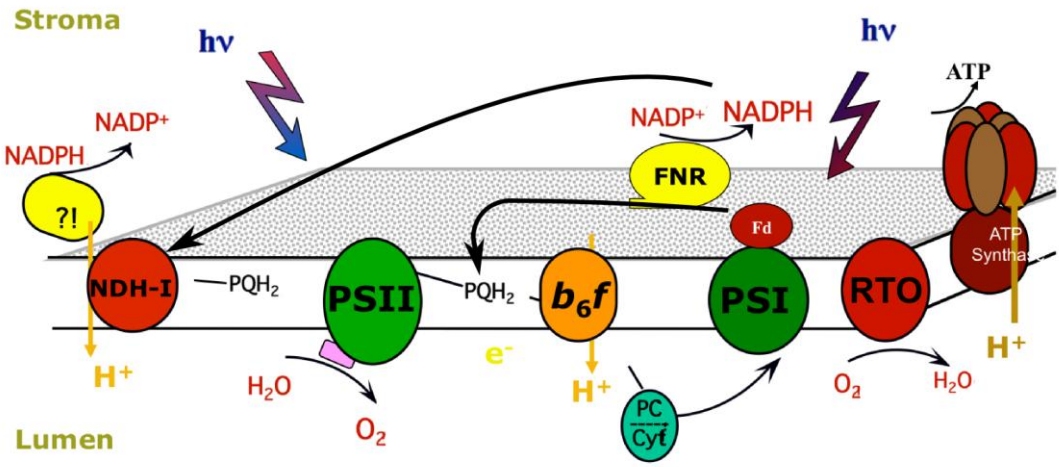

Figure I.7 Schematic view of cyanobacterial thylakoid membrane.
The different complexes implicated in photosynthesis are depicted. The two major pathways of cyclic-electron transfer are indicated with black arrows. They involve the respiratory NDH-1 complex and/or the Fd. Respiratory complexes such as cytochrome oxidase, Cox and NAD(P)H dehydrogenase I, NDH-1 are represented in addition to the photosynthetic complexes.

Another pathway of electron redirection is called CET (**Figure I.7**). In this alternative electron pathway ATP is generated with no NADPH accumulation. Two pathways for CET have beenproposed; both involve PSI, cyt b_6f, and the PQ pool. Several partners were proposed to catalyze the donation of electrons from the acceptor side of PSI (Fd, FNR, NADPH) back into the PQ pool, reduced PQ transfer electrons to cyt b_6f, which

inturn transferthem to PSI and so on (Shikanai, 2007). Onepathway involveselectron redirection from Fd to the PQ pool (**Figure I.7**-black arrow) while another pathway involvesits redirection from NADPH to the NDH-I complex (introduced in the next section) then to the PQ pool(Shikanai, 2007)(**Figure I.7**-black arrow).

I.3.3. Respiratory electron transfer

Cyanobacteria are known not only to perform oxygenic photosynthesis but also oxygenic respiration. One of the unique aspects of cyanobacteria is that oxygenic photosynthesis and respiration are not separated in different organelles, as in plants, but are active in the same compartment. Several components used for photosynthesis,such as NADPH, PQ and cyt b_6f,are also part of the respiratory electron-transport chain.

The respiratory electron-transport chain involves three major complexes. The NAD(P)H:quinone oxidoreductase (NDH-I) that oxidizes NADPH, the cyt b_6f that accept electronsfrom NDH-1 and the respiratory terminal oxidase (RTO)(**Figure I.7**).

The **NAD(P)H:quinone oxidoreductase** complex (NDH-I)is an homologue of the mitochondrial respiratory complex I.It is a proton-translocating NAD(P)H:quinone oxidoreductase. NDH-I is a multisubunit membrane enzyme characterized by the presence of flavin mononucleotides (FMN) and several iron-sulfur clusters (Fe-S). NDH-Iin*E. coli*, which is considered to be a model for proton-pumping NADH:quinone oxidoreductases, contains 14 subunits. Homologues of 11 of the 14 subunits were identified in *Synechocystis*(Battchikova and Aro, 2007). Several types of NDH-I complexes, which differ in structure, exist in cyanobacteria. This structural variety allows many functions like respiration, CET around PSI and CO_2 uptake (Battchikova and Aro, 2007). It is important to mention that the NADPH-oxidase subunitof the NDH-1 complex is not yet identified in cyanobacteria.

The **Respiratory Terminal Oxidases** (RTO) reduce the O_2 into water as the last reaction in oxygenic respiration. Three RTO exist in cyanobacteria: cytochrome *c* oxidase (Cox), quinol oxidase (Cyd), and an alternative RTO (ARTO) (Pils and Schmetterer, 2001). As for photosynthesis, respiratory electron transfers lead to an electrochemical proton gradient that will be used to produce ATP by the ATP-synthase.

I.4. The phycobilisome

Photosynthetic organisms developed auxiliary-antennacomplexes, or light-harvesting complexes, that extends the absorbance capacityof the light harvesting apparatus(DeRuyter and Fromme, 2008). These antenna complexes are generally localized close to the photosystems, which allows excitation energy transfer to the reaction-center chlorophylls. The structure and the composition of these antenna complexes differ between organisms. Theycan be divided into integral-membrane antenna and external-membrane antenna(that are associated to the membrane without crossing it)(Blankenship, 2002). Cyanobacteria and some algal species developed an external water-soluble antenna complex, the phycobilisome.

The **Phycobilisome** (PBS) is a giant protein complex (7-1510^3 kDa), it is 3 to 6 times larger than thebacterial ribosome (2.410^3 kDa). PBS are produced in massive amounts in a number of photosynthetic organisms and constitute up to 50% of the soluble protein of the cell (Grossman et al., 1993). PBS are located on the cytoplasmic side of the thylakoid membrane, which allows them to transfer light energy efficiently to PSII. The PBS allows species to absorb visible light in the wavelength range of 500-660 nm,which extends the spectral range for photosynthetic-light harvesting to the region between the blue and the red absorption bands of chlorophylls. Different morphological types of PBS exist: hemidiscoidal, hemiellipsoidal, bundle-shaped, and block-shaped (Wehrmeyer, 1982; Sidler, 1994).

In the following sections aredescribed the structure and the function of the hemidicsoidal PBS, which is the most common type and the one found in *Synechocystis*(Bryant et al., 1979; Rosinski et al., 1981).

I.4.1. Phycobilisome structure

Although a PBS contains hundreds of subunits, it is an efficient molecular machine that transfers energy with an efficiency of up to 95% (Glazer, 1989). The PBS is composed of chromophore-containing proteins called phycobiliproteins and smaller amounts of colorless polypeptides called linkers.

A PBSis composed of two subdomains: the core, that interacts with the thylakoid membrane, and the peripheral rods that radiate from the core (**Figure I.8-A**). Three different types of hemidiscoidal PBS have been identified depending on their core structure. (1) The tricylindrical core PBS, like the one in *Synechocystis* represented inFigure I.8, (2) the bicylindrical core PBS (*Synechococcus* sp. PCC 6301 and PCC7942) and (3) the pentacylindrical core PBS (*Anabaena* sp. PCC 7120). Several cyanobacteria, like *Synechocystis* sp. strain BO 8402, have been reportedto containbiliproteins that are not organized into PBSstructures (Reuter et al., 1994).

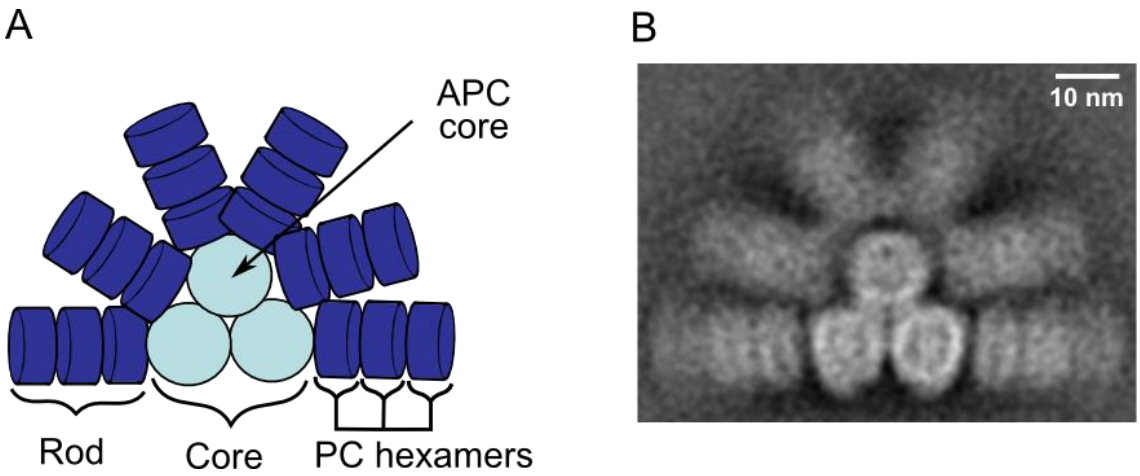

Figure I.8The hemidiscoidal PBS of *Synechocystis* sp. PCC 6803.
A.Schematic representationof a tri-cylindrical core PBS, from which six rods, composed of three hexamers each, radiate.
B. Image of negatively stained PBS, from *Synechocystis*, produced by single-particle electron microscopy(Arteni et al., 2009).
PC, phycocyanin; APC, allophycocyanin.

Phycobiliproteins

Phycobiliproteins (PBP) are the main PBS component (80% of the PBS by mass)(de Marsac and Cohen-bazire, 1977).They are water-soluble proteins to which open-chain tetrapyroles, known as phycobilins, are bound. PBP are basically formed by two subunits, the α and the β subunits. PBP are divided into four groups based on their visible absorption properties: allophycocyanin (APC), forms the major component of the PBS core; phycocyanin (PC),are always present close to the core at the base of the rods (core-proximal side);phycoerythrins (PE) and phycoerythrocyanin (PEC),when presentare found at the core-distal ends of the rods.

Note that the same chromophore, phycocyanobilin (PCB), is typically associated with the PC and APCsubunits. The color difference (blue for PC and turquoise for APC) is due to PCB interaction with different proteins. Different chromophores are found in PE and PEC.

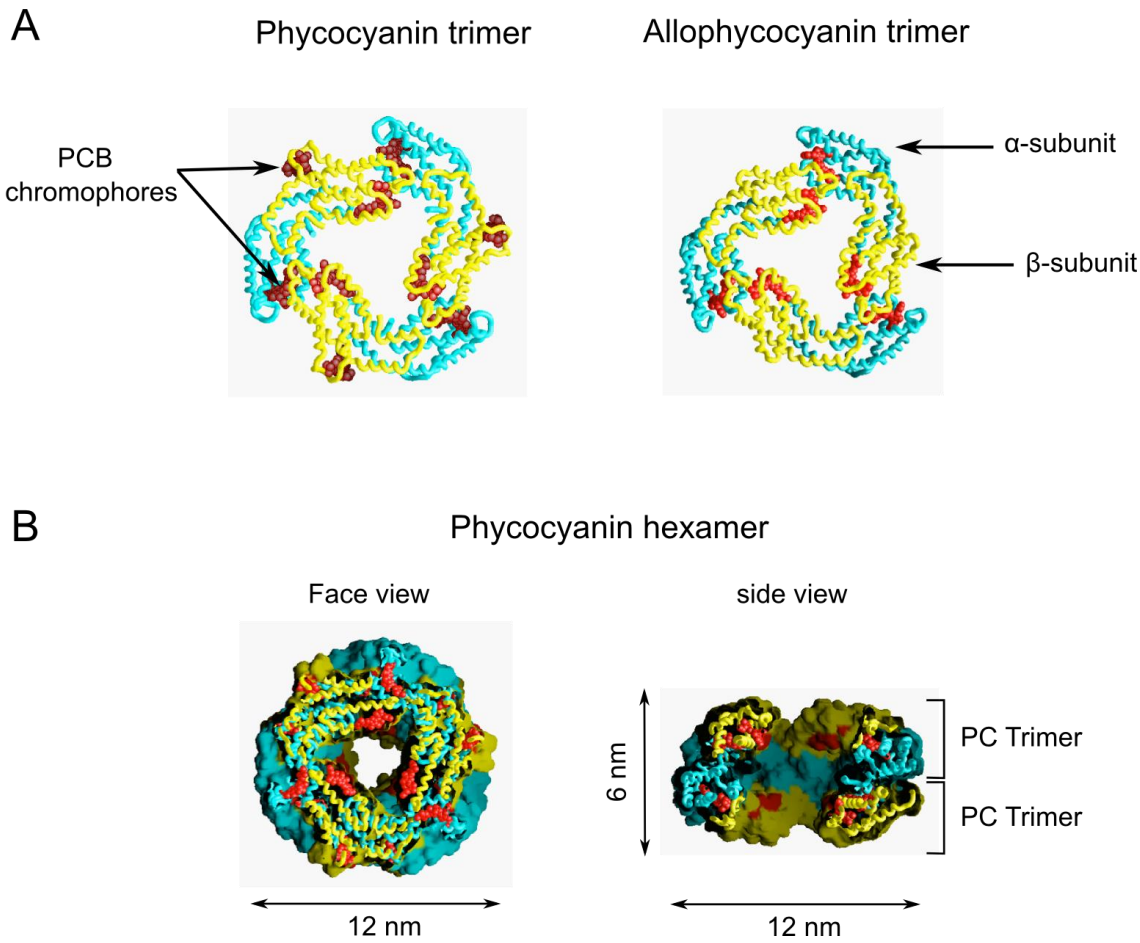

Figure I.9 Crystallographic models of phycocyanin and allophycocyanin.
A. Phycocyanin and allophycocyanin trimers. α-subunits are blue, β-subunits are yellow and the chromophores are red. **B.** Representation of a section in the molecular surface of a phycocyanin hexamer. The models were kindly provided by D. Picot.

a. Phycobiliprotiens of the core

The PBS core is always composed of APC, theturquoise-colored PBP, arranged into discs and cylinders. APC assemble into trimeric discs composed ofα^{APC} and β^{APC} subunits $(\alpha^{APC}\beta^{APC})_3$ (**Figure I.9**). A portion of the core contains divergent types of α and β subunits likeα-allophycocyanin-B ($\alpha^{AP\text{-}B}$) and β^{18}.

The $\alpha^{APC}$and the β^{APC}subunits (18kDa each) are encoded by the *apcBA* operon, while the *apcD* and the *apcF* genes encode $\alpha^{AP\text{-}B}$(18kDa) andβ^{18}(19 kDa), respectively.

b. Phycobiliproteins of the rods

Depending on the organism and on the growth conditions, PBS rods might contain phycocyanin (PC), phycoerythrin (PE) or phycoerythrocyanin (PEC). In *Synechocystis* only PC, the blue colored PBP, is present. PC assembled into hexameric discs composed by the α^{PC} and the β^{PC} subunits $(\alpha^{PC}\beta^{PC})_6$(**Figure I.9**).

The *cpcBA* operon encodesα^{PC} (18kDa) and β^{PC} (19 kDa).

Linker polypeptides

Different linkers are specifically associated to each PBP type (**Figure I.10**). These linkers are important for the PBS assembly and for the optimization of energy transfer (de Marsac and Cohen-bazire, 1977). It was suggested that linkers bind to the central cavity of PBP discs(Yu and Glazer, 1982; Reuter et al., 1999).

According to their function, linker polypeptides are divided into four groups:(i) The core-membrane linker (L_{CM}), a multifunctional polypeptide mainly involved in the attachment of the core to the thylakoid membrane. (ii) The core linker (L_C) stabilizes the core assembly.(iii) The rod-core linker (L_{RC}) allows the attachment of the rods to the core. (iv) The rod linkers (L_R) involved in rod assembly.

Furtherinformationof thePBSlinkers present in *Synechocystis*are summarized in the following table:

Table I.1Linker polypeptides present in the*Synechocystis*phycobilisome.

Name	Abbreviation	Gene	Role	Molecular weight
Core-membrane linker	L_{CM}	*apcE*	Binding to membrane	100 kDa
Small-core linker	L_C	*apcC*	Stabilizes the core	8 kDa
Rod-core linker	L_{RC}	*cpcG1*, *cpcG2*	rod-core attachment	27 kDa
Rod linker	L_R^{30}, L_R^{33}	*cpcC2*, *cpcC1*	Incorporates phycobiliprotein hexamers into rods	30 kDa/33kDa
Small-rod linker	L_R^{10}	*cpcD*	Minimizes rod heterogeneity	10 kDa

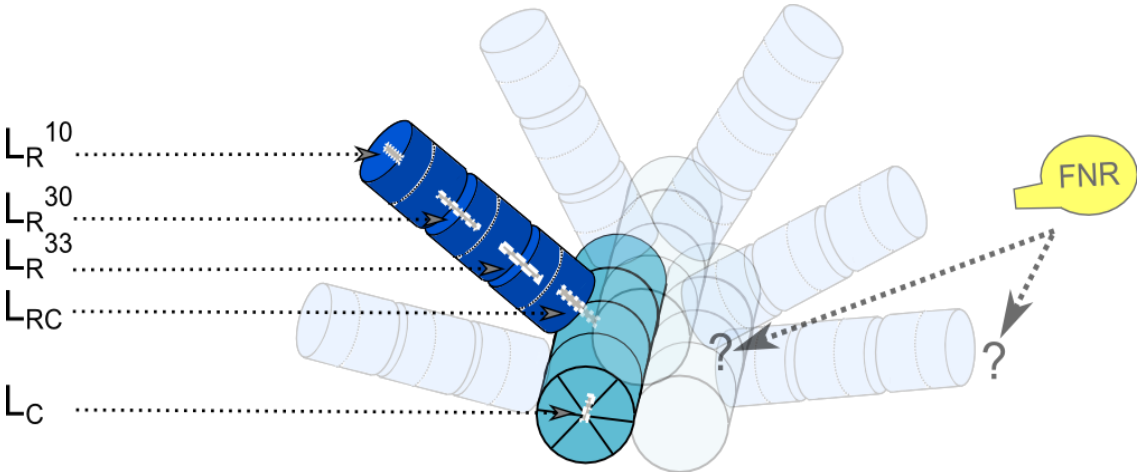

Figure I.10 Schematic representation of phycobilisome rod attachment to the core cylinder.
The scheme shows the linkers (except for the L_{CM}) present in the *Synechocystis* PBS. L_R and $L_C$represent the core and the rod linkers, respectively. FNR_L (in yellow) is also represented with its potential PBS-binding sites.

The Ferredoxin:NADP(H) oxidoreductase

Ferredoxin:NADP(H) oxidoreductase is the enzyme that catalyzes the last step of LET.In many cyanobacteria FNR is attached to the PBS; an average of two FNR per PBS was found in *Synechocystis*(van Thor et al., 1999). The FNRN-terminal domain is similar to L_R^{10}, which explains its attachment to the PBS. The structure and the function of FNR will be introduced in section I.5.

Phycobilisome Assembly

Stacking of PBP discs, made up of APC trimers and PC hexamers, with the help of linkers, ends up withPBS assembly.

L_{CM} together with $L_C$assembles APC discs into cylinders and into a core substructure. The rod-core linkage position is always occupied by a PC hexamer (importantsince some organisms produce PE or PEC in addition to PC); this core proximal PC hexamer is attached to the core by L_{RC}(**Figure I.10**). L_R^{33} attaches the proximal PC hexamer to the intermediary hexamer, which in turns is attached to the distal PC hexamers *via* L_R^{30}. L_R^{10} is thought to be attached to the distal PC hexamer without being involved in PC-hexamer stacking (**Figure I.10**) and is believed to minimize rod-length heterogeneity(de Lorimier et al., 1990).

I.4.2. Phycobilisome function

The main role of PBS is to absorb light energy and transfer it to the PSII reaction center.However, PBS are also used as nutrientsourcesunder starvation conditions.

Energy transfer and light adaptation

Light energy harvested at the PBSrod periphery migrates through the rods to the core and then to the PSII chlorophyll *a*. The energy transfer is efficient (95%) and unidirectional (Glazer, 1989).

PBS composition may alter in response to changing environmental conditions such as light intensity or quality. It has been shown that cyanobacteria can modulate the size (Lönneborg et al., 1985; Garnier et al., 1994) and/or the number of their PBS (Grossman, 1990)in order to adapt their light absorption efficiency to light quantity. In addition, some cyanobacteria, like *Fremiella diplosiphon*, adjust their PBP composition to optimize light absorption under different light colors, a processcalled complementary-chromatic adaptation. Suchstrains introducephycocyanin (PC) or phycoerythrin(PE)in their PBS rods when grown under red or green light conditions, respectively(Kehoe, 2010).

Phycobiliproteins as a nutrient source

PBS are not only light-harvesting antenna, they also serve as protein storage that is used under nutrient-limited conditions. Under these conditions, cyanobacteria adjust the photosynthetic apparatus in a process known as chlorosis or bleaching,during which PBSare degraded(Allen and Smith, 1969). Cyanobacteria respond differently to nutrient-limited conditions,while *Synechococcus* PCC7942 degrades PBS under nitrogen and sulfur starvation (Collier and Grossman, 1992), *Synechocystis*degrade PBS only under nitrogen starvation(Richaud et al., 2001).

The degradation of PBSs under nitrogen-starvation conditions is a rapid and ordered processindicating the existence of effective and regulated degradation machinery. It has been shown that *nblA*, coding a protein of about 60 amino acids, is a key gene for PBS degradation (Collier and Grossman, 1994). *nblA* exists in all PBS-containing organisms (except for marine cyanobacteria) and its expression is highly upregulated under nitrogen starvation and high-light conditions (Luque and Forchhammer, 2008). The mechanism by which NblA triggers PBS degradation is not yet elucidated. It was

proposed that NblA binds to the α-subunits of PBP *via* its C-terminus and to ClpC (HSP100 chaperone partner of the Clp protease) *via* its N-terminus, which triggers PBS degradation (Karradt et al., 2008) (**Figure I.11**).It was also proposed that NblA may penetrate between the PCtrimers of the rods, thereby disrupting the rod structures and making them susceptible to proteolytic degradation (Dines et al., 2008)(**Figure I.11**).

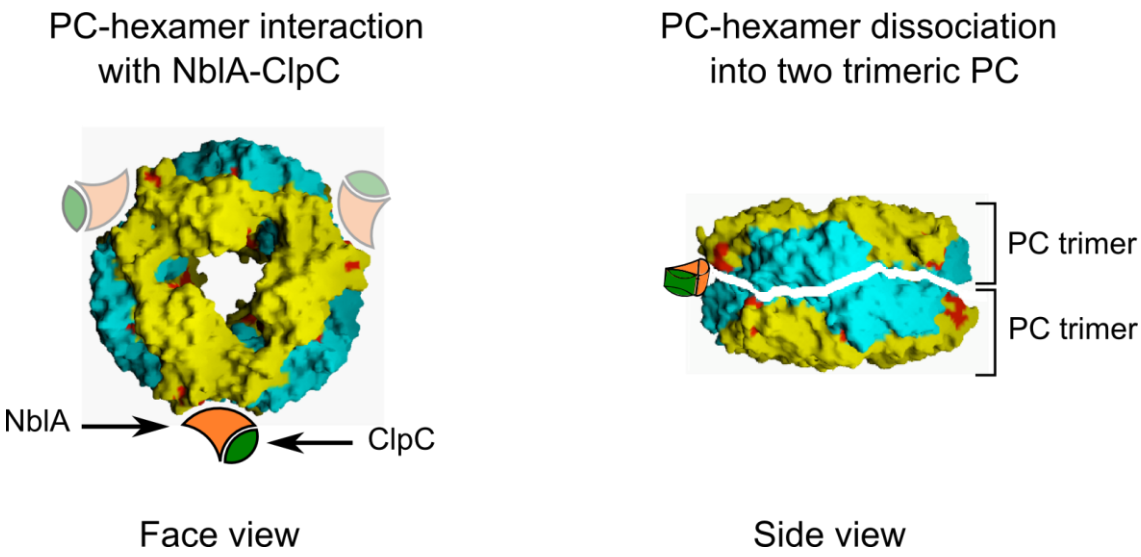

Figure I.11Phycocyanin-NblAbinding models.
NblA binds to the trimer-trimer interface of phycocyanin, which is formed by the α-subunits (colored blue) and the β-subunits (shown in yellow).
Left, a PC-hexamer is represented interacting with NblA and ClpC (orange and green, respectively). Three NblA-binding sites are present per hexamer.
Right, during the process of phycobilisome degradation, PC-hexamers dissociate into two trimeric sub-structures.

I.5. The Ferredoxin:NADP(H) oxidoreductase

Ferredoxin:NADP(H) oxidoreductase (FNR) is a flavoprotein that catalyzes the last step of linear electron transfer between Fd and NADPH. FNR acceptstwo electrons, one at time, from ferredoxinand carries out the two-electron reduction of $NADP^+$ to NADPH (Blankenship, 2002). The overall reaction catalyzed by FNR is as follows:

$$2Fd_{red} + NADP^+ + H^+ \rightarrow 2Fd_{ox} + NADPH$$

I.5.1. Structure and function

The crystallographic structure of different FNR has been determined from plant-chloroplasts as well as from cyanobacteria. These enzymes have similar structures including two "classical" domains (ca. 150 residues each): the N-terminal forms the FAD-binding domain and the C-terminal forms the NADPH-binding domain (Karplus and Faber, 2004) (**Figure I.12**).

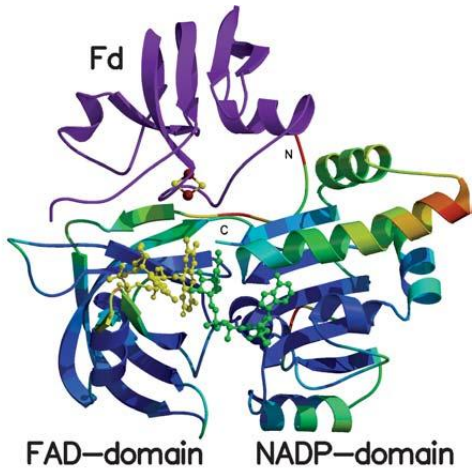

Figure I.12 Structural model of the ferredoxin:NADP oxidoreductase with bound ferredoxin.
Stereo-ribbon diagram of spinach FNR showing β-strands as arrows and α-helices as spirals. The bound FAD and NADPH molecules are shown as yellow and green ball-and-stick models, respectively. The ferredoxin ribbon is purple, and the FNR ribbon is color coded to convey information about the mobility of the chain, with a gradient from deep blue for the best ordered parts of the structure, to red for the most mobile parts of the structure.The N- and C-termini of FNR are labeled, as are the FAD domain and the NADP domain. From(Karplus and Faber, 2004).

In order to perform electron transfer between Fd and NADP+, FNR must have a functional group that accepts one electron from the Fd and retains it while a second Fd

provides a second electron. This functional group is a flavin adenine dinucleotide (FAD); FNR is therefore a flavoprotein. FAD binds to the**FAD-bindingdomain**and transfers the two acquired electrons to the NADP present in the **NADPH-bindingdomain**(**Figure I.12**).

Ferredoxin binding. Protein-protein interaction is important for electron transfer between Fd and FNR. It has been shown that Fd binds to a concave region of the FAD-binding domain, bringing its [2Fe-2S] cluster into close proximity to the FAD and allowing electron transfer between these cofactors (Kurisu et al., 2001) (**Figure I.12**).

I.5.2. Isoforms

As mentioned before, FNR exists in plants plastids and in cyanobacteria. I will first introduce plantFNR isoforms and then describe those of cyanobacteria.

Plant isoforms

FNR isoforms are tissue specific in plant. They are about 35 kDa (Zanetti and Aliverti, 1991). The leaf isoforms (photosynthetic;pFNR) are primarily required for $NADP^+$ reduction and the root isoforms (heterotrophic; hFNR) oxidize NADPH and generate reduced Fd. In addition, different isoformswere found in maize (Okutani et al., 2005) and in wheat leaves (Gummadova et al., 2007).

In all photosynthetic organisms *petH* is the gene that encodes FNR. FNR isoforms are encoded by a multiple *petH*gene family in plants.

Cyanobacterial isoforms

Only one *petH*gene copy is foundin cyanobacteria except for *Acaryochloris marinus*,where 3 *petH* gene copies are present.

In most PBS-containing cyanobacteria, FNR are larger than those found in plants, they are about 45 kDa (Schluchter and Bryant, 1992). In addition to the enzymatic domain, similar to the one found in plants, an N-terminal domain exist and FNR is associated with PBS. It has been shown that the N-terminal domain is homologous to L_R^{10}, the PC associated PBS-linker.Thesimilarity is 78% in the cyanobacterium *Synechococcus* PCC 7002 and 75% in *Synechocystis*(Schluchter and Bryant, 1992; Fillat et al., 1993; van Thor et al., 1999).

FNR binding to the PBS was confirmed in several works (Schluchter and Bryant, 1992; van Thor et al., 1999; Thomas et al., 2006)but a controversy exists concerning its location on the PBS rod(Gomez-Lojero et al., 2003). It was suggested that FNR binds to core-distal PC hexamers.(Schluchter and Bryant, 1992; Gomez-Lojero et al., 2003). However, van Thor et al. proposed that FNR binds to core-proximal PC hexamers (van Thor et al., 1999) (**Figure I.10**). FNR binding to the PBS is not characteristic for all PBS-containing organisms; FNR is not attached to PBSin red algae and few cyanobacteria (Morsy et al., 2008).

A recentstudy in our laboratory showed that, under specific conditions, *Synechocystis* and some other cyanobacteria generate a smaller FNR isoform. The large isoform, 47 kDa, was named FNR_L while the small isoform, 34 kDa, was named FNR_S.

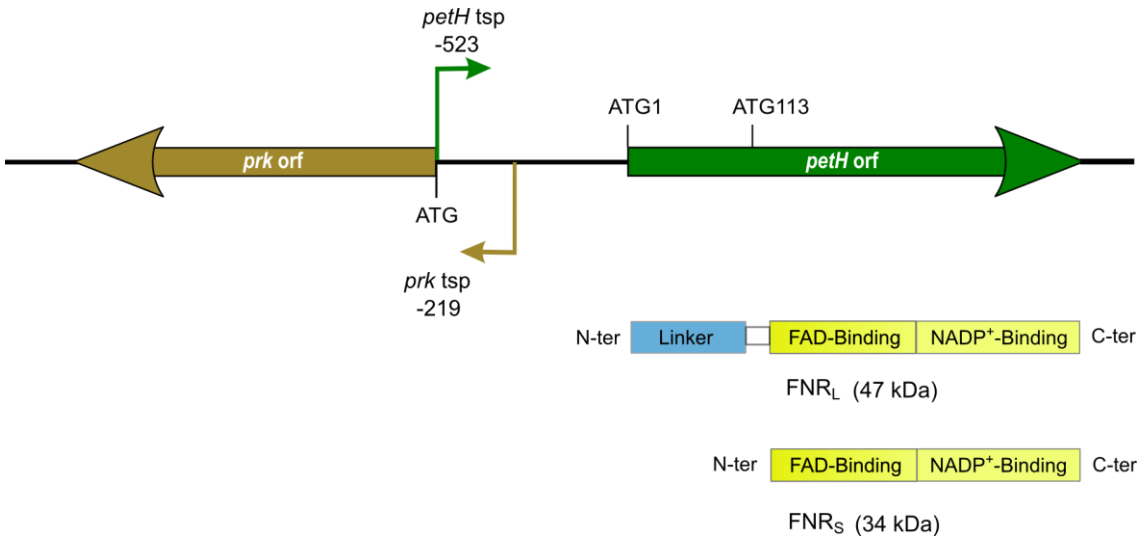

Figure I.13Representation of the *prk* and *petH*genetic organization as well as the *petH* gene products.
Upper, Divergent transcription of *prk* and *petH* resulting in complementary regions between their transcripts was described in (van Thor et al 1998). Green and brown boxes represent *petH* and *prk* orfs, respectively. Bent arrows indicate the position of the transcription start points (tsp) of *petH* (green) and *prk* (brown). The numbers -532 and -219 are relative to the first translation-initiator codon of *petH* (ATG-1) and *prk* (ATG), respectively.
Lower, FNR_S and FNR_L functional domains. In addition to the catalytic domain (yellow), FNR_L possess an N-terminal domain (blue) that resembles the L_R^{10} PBS-rod linker.

$FNR_L$is detected under photoautotrophic conditions,or standard conditions (light and CO_2), while FNR_S accumulates when photosynthesis slows down; like under chemoheterotrophic (dark and glucose), mixotrophic (dim-light and glucose)or starvation conditions. It was also showed that the small isoform was present only in facultative heterotrophic cyanobacteria.Therefore, it was suggested that FNR_L is related

to photosynthetic metabolism ($NADP^+$ reduction) while FNR_S is more adapted to provide electrons for heterotrophic metabolism (NADPH oxidation)(Thomas et al., 2006).

It was also showed that the two FNR isoforms are translated from two distinct methionines codons, ATG-1 and ATG-113 for FNR_L and FNR_S, respectively (**Figure I.13**).FNR_Sbeing produced by an in-frame internal translation initiation, within the FNR_Lopen reading frame (orf) (Thomas et al., 2006).

The following section introduces mutants that demonstrated the presence of an alternative translation-initiation site and that were extensively used during my PhD.

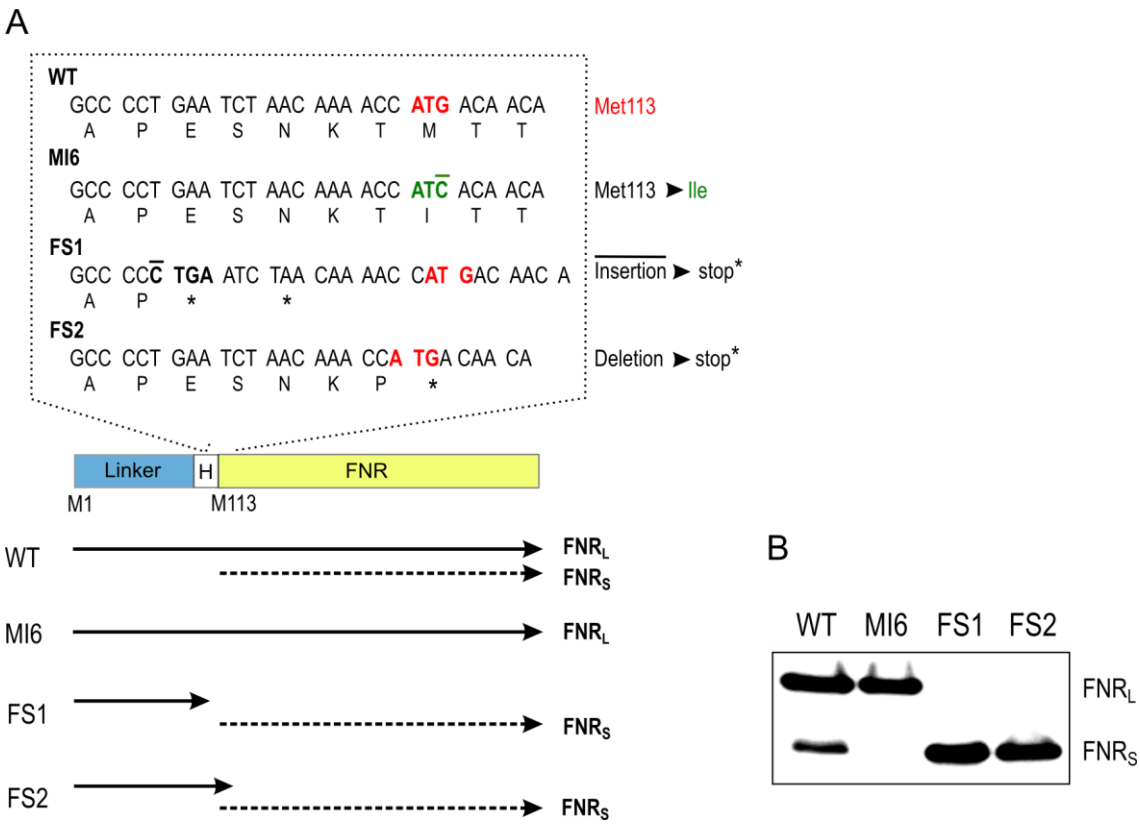

Figure I.14 FNR_S is translated from Met-113 in *Synechocystis* sp. PCC 6803.
A. (Upper) Schematic representation of FNR_L with the linker (blue), hinge (H), and enzymatic domains (Yellow), Met-1 and Met-113 are shown. Met-113 was changed to isoleucine (ATC) in MI6. Frameshifts in FS1 and FS2 result in translation termination (*). (Lower) Translated polypeptides are indicated for each mutant. From (Thomas et al., 2006) with some modifications.
B. FNR Immunodetection in total protein extracts from WT, MI6, FS1 and FS2 strains. Only FNR_L is present in MI6 and only FNR_S is present in FS1 and FS2.

ferredoxin:NADP oxidoreductase mutants

Missense or frame-shift mutations were introduced in the *petH* gene of *Synechocystis* resulting in mutants that accumulatedonly one of the isoforms.

A missense mutation, in mutant MI6, changed Met113 to an Ile(**Figure I.14-A**). Frame-shift mutations, created by the insertion or the deletion of a single base, created stop codons causing premature translation termination upstream and downstream from Met113 resulting in FS1 and FS2, respectively(**Figure I.14-A**).

Under standard conditions, the WT accumulates mainly FNR_L with only trace amounts of FNR_S; MI6 contained only FNR_L, while in FS1 and FS2 only $FNR_S$is detected(**Figure I.14-B**).

FS1 (like FS2) showed slower growth under photoautotrophic conditions and slightly better growth under chemoheterotrophic conditions compared to WT. MI6 grew photoautotrophically like the WT but encountered difficulties to grow under chemoheterotrophic conditions. This confirmed that FNR_S is better adapted to sustain heterotrophic growth (NADPH oxidation) while $FNR_L$was more suited to autotrophic growth ($NADP^+$ reduction).

petHtranscription

van Thor et al.describeda monocistronictranscript for *petH*and mapped thetranscription start point (tsp) 523 bases upstream from ATG-1,in *Synechocystis*(van Thor et al., 1998). They also showed that the *petH*tsp is situated within the open-reading frame of the *prk* gene (encodingphosphoribulokinase), which is transcribed in the opposite orientation with respect to*petH* (**Figure I.13**). The*prk*tspwas mapped 219 nucleotides upstream from the *prk*initiation codon, resulting in a 223-bases overlap between the*petH* and the*prk* transcripts (**Figure I.13**).

In the filamentous cyanobacterium *Anabaena*sp. PCC 7120, *petH* produces two mRNA, one is constitutive (starts at nucleotide -63 from Met-1) and the other one is induced in the absence of combined nitrogen (starting at nucleotide-188 from Met-1) (Valladares et al., 1999).Therefore,*petH* transcription in *Anabaena* sp. PCC 7120 was thought to be markedly different from that of *Synechocystis*(Thomas et al., 2006).

Since I was interested in understanding the genetic regulation of *petH*,which depending on growth conditions produces the large or the smallFNR isoform,I exploredthe gene regulation aspects that affect protein synthesis.

I.6. Gene regulation

Bacteria respondto environmental challenges at morphological and functional levels. This sort of adaptation is often controlled at the genetic level, the process by which geneexpression is turned on (or off), under specific conditions, is called gene regulation.

Gene expression can be regulated when RNA is synthesized; this is called transcription regulation and is by far the most common. Another type occurs after gene transcription and is referred to as post-transcriptional regulation.

Transcription regulation is considered to be the most efficient gene regulation pathway, since transcribing RNA without using them seems wasteful. The products of so-called "regulatory genes" often regulate the transcription of bacterial genes and operons. These products are often proteins, called activators orrepressors, that bind to promoters thus inducing or inhibiting transcription, respectively.

Post-transcriptional regulation constitutes a second level of gene regulation. It occurs when the regulated gene encodes a protein; it implicates regulation of the transcribed mRNA eitherby inhibiting(or activating) its translation or by controlling its decay rate. Secondary and tertiary structures of the mRNA play a crucial role in this process. The key step of this sort ofpost-transcriptionnal regulation (also called translation regulation) is translation initiation. Translation regulation involves different factors such as: small-noncoding RNA, which are the major players in post-transcriptional regulation; riboswitches and proteins that could compete with the ribosome.

In bacteria, translation andtranscription are coupled. Translation initiation occurs as soon as the mRNA is synthetized. In many cases, it is difficult to distinguishbetween transcriptional and translationalregulations; this is exploited, by bacteria, to provide unique regulation mechanisms.

I.6.1. Transcriptional regulation

Transcription initiation

The promoter is a DNA sequence that allows the RNA polymerase to recognize the beginning of a transcription unit. Promoterssequences are not identical but they often

share a certain consensus. The promoter has two important elements: a short AT-rich region (consensus TATAAT) centered at about 10 bases upstream from thetsp, know as -10 Pribnow-box (or -10 box) and a region centered at about 35 bases upstream from the tsp called -35 box (consensus TTGACA) (**Figure I.15**). With some exceptions (Kammerer et al., 1986; deHaseth et al., 1998), the general rule holds that the greater the similarity is, of the -35 and -10 regions, to the consensus the better the promoter functions (deHaseth et al., 1998). RNA polymerase recognizes these promoters through its σ subunit. In bacteria severalσ factors exist conferring promoter selectivity for the RNA polymerase. The *E. coli*σ^{70} factoris the most known and studied; it recognizes the previously described promoter and controls a large number of genes that are denoted housekeeping genes. Under stress conditions,*E. coli*produces other sigma factors, that differ in function and structure,like σ^{S}that recognizes stress-specific gene promoters.

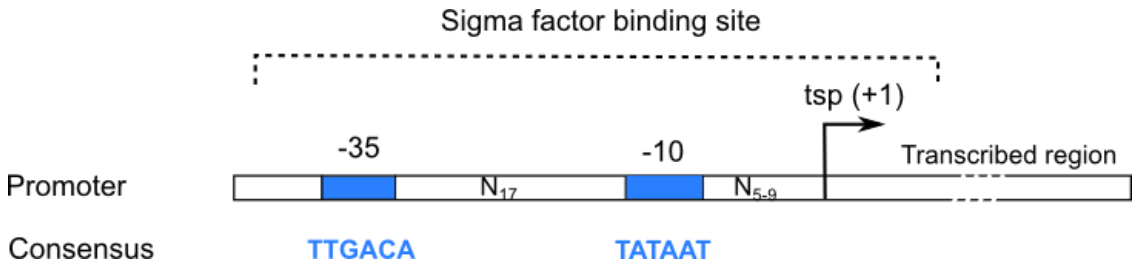

Figure I.15Structure of the σ^{70}-bacterial promoter.
Consensus sequences,-35 and -10 boxes, are indicated in blue. "N" indicates the number of nucleotides separating the different domains. Dotted line indicates the region where σ^{70} recognizes the transcription unit.

In cyanobacteria only the σ^{70}-factor type exists,nine genes (*sigA* to *sigI*)encodesigma-factor homologues in *Synechocystis*(Imamura et al., 2003). They are structurally and functionally subdivided into three groups and each group contains one or more σ factors. Group 1 and 2 are structurally similar, however group 1 (*sigA*) is essential for cell viability, which is not the case for group 2 (*sigB* to *sigE*).

Group 1 and 2 σ factors recognize promoters possessing the following elements:a -10 box and a -35 box (as in the *psbA* promoter), a -10 box and an enhancer-motif associated with transcriptional factors (as in the *glnB*alternative promoter) (Asayama et al., 2004) or an extended -10 boxpreceded by TGTG or GC sequences (as in the dark-inducible *lrtA* promoter)-(Imamura et al., 2004; Imamura and Asayama,

2009). It was suggested that these two groups of sigma factors are linked by a network of mutual regulation that could allow them to act in concert in the global transcriptional control of the bacterium (Lemeille et al., 2005).

Group 3 σ factors(SigF to SigI),which arestructurally different from groups 1 and 2,recognizea different promoter type (*pilA*, *pixJ1* and *sigF* promoters) with no clear consensus sequences (Asayama and Imamura, 2008; Imamura and Asayama, 2009). Promoter recognition by group 3 σ factorsis still unclear.

Transcription factors

Transcriptionfactors are usually proteins that act by interacting with gene promoters. Activators usually bind upstream from the promoter's-35 boxand contact the RNA polymerase while repressors often bind to the promoter sequence itself,whichprevents the RNA polymerase access. Note that some regulators, like NtcA (introduced later), could act as a repressor or activator on the same gene depending on the conditions.

cAMP receptor proteinin E. coli

The best-studied bacterial transcription factor is the **c**AMP **r**eceptor **p**rotein (CRP), also called **c**atabolite gene **a**ctivator **p**rotein (CAP). CRP is a global transcriptional regulator that controls the expression of many genes in *E. coli*.

CRP is implicated in the regulation of many processes such as carbon-sourcestransport, the tricarboxylic-acid cycle (TCA), the pyruvate-dehydrogenase (PDH) and aerobic respiration(Shimada et al., 2011). A minimum of 378 target promoters, on the *E. coli* genome, have been proposed to be under the control of CRP (Shimada et al., 2011).

CRP regulates genes by binding to their promoters by its C-terminal helix-turn-helix motif. It binds to a specific region "the CRP-box" consisting of a palindromic DNA sequence (consensus TGTGA N_6 TCACA) (Berg and von Hippel, 1988). However, the DNA-binding of CRP is activated when cAMP, which level depends upon cell physiology, binds to the CRP N-terminal domain (Passner and Steitz, 1997). cAMP-CRP is a dual regulator acting as an activator or a repressor of gene expression depending on its binding site location.

Nitrogen control A in cyanobacteria

Nitrogen control A (NtcA) is a global transcriptional regulator and the central player in nitrogen and carbon metabolism control in cyanobacteria. It is ubiquitous and exclusive to cyanobacteria (Frias et al., 1993). NtcA belongs to the CRP family (Körner et al., 2003) and controls the expression of genes involved in nitrogen and carbon metabolism including its own. NtcA regulates genes transcription by acting as an activator or a repressor.

Like CRP, NtcA is a dimeric protein, of about 50 kDa, composed of two identical subunits; each one contains 220 amino acids. NtcA binds to DNA by its C-terminal domain containing a helix-turn-helix motif (Vega-Palas et al., 1992). A consensus DNA sequence to which NtcA binds was identified as GTA N_8 TAC (Luque et al., 1994), the two external GT and AC being the most important nucleotides(Vázquez-Bermúdez et al., 2002). Deviation fromthe consensus sequence or/and the spacer length (N8) have been identified and result in decreasing the NtcA binding affinity to the promoter(Jiang et al., 2000; Luque et al., 2001). Figure I.16shows different potential NtcA-binding sites in different cyanobacteria.

2-oxoglutarate (2-OG), the molecule that signals the carbon/nitrogen balance, binds to NtcA (Llácer et al., 2010) and increases its activity (Vázquez-Bermúdez et al., 2002). In fact, *ntcA* is expressed at a basal level under standard conditions. In the absence of nitrogen, 2-OG accumulates, which activates NtcA that in turns increases its own transcription as well as that of genes essential for nitrogen metabolism (Luque et al., 1994).It was proposed that a perfect NtcA-binding site is located 40.5 nucleotides upstream from the tsp to be activated (Luque et al., 1994)(**Figure I.16**). NtcA-activated promoters represent a class of promoters that function in many cases without a recognizable -35 box (deHaseth et al., 1998) like the previously mentioned,*glnB*alternative promoter of *Synechocystis*(Asayama et al., 2004). In some cases the NtcA-binding site was shown to overlap the -35 box (Herrero et al., 2001; Mitschke et al., 2010). A large number of genes in different cyanobacteria bear a canonical NtcA-activated promoter(Herrero et al., 2001). Bioinformaticstudies proposed that NtcA-binding sites could be found up to 238 nucleotides upstream from the tsp, although experimental demonstration for a regulation by NtcA still remains to be establishedfor such sites (Luque and Forchhammer, 2008).

In the case of NtcA-repressed promoters, NtcA-binding sitesare located downstream from the -40.5 position (**Figure I.16**), which blocks the access of the RNA polymerase to these promoters. Several genes like *gifA* and *gifB*, encoding two homologous polypeptides involved in the inactivation of type I Glutamine synthase,and *rbcL* that encodes the ribulose bisphosphate carboxylase/oxygenase (RubisCO), have been reported to be repressed by NtcA in *Synechocystis*and in *Anabaena*sp. PCC 7120(García-Domínguez et al., 2000; Galmozzi et al., 2010).

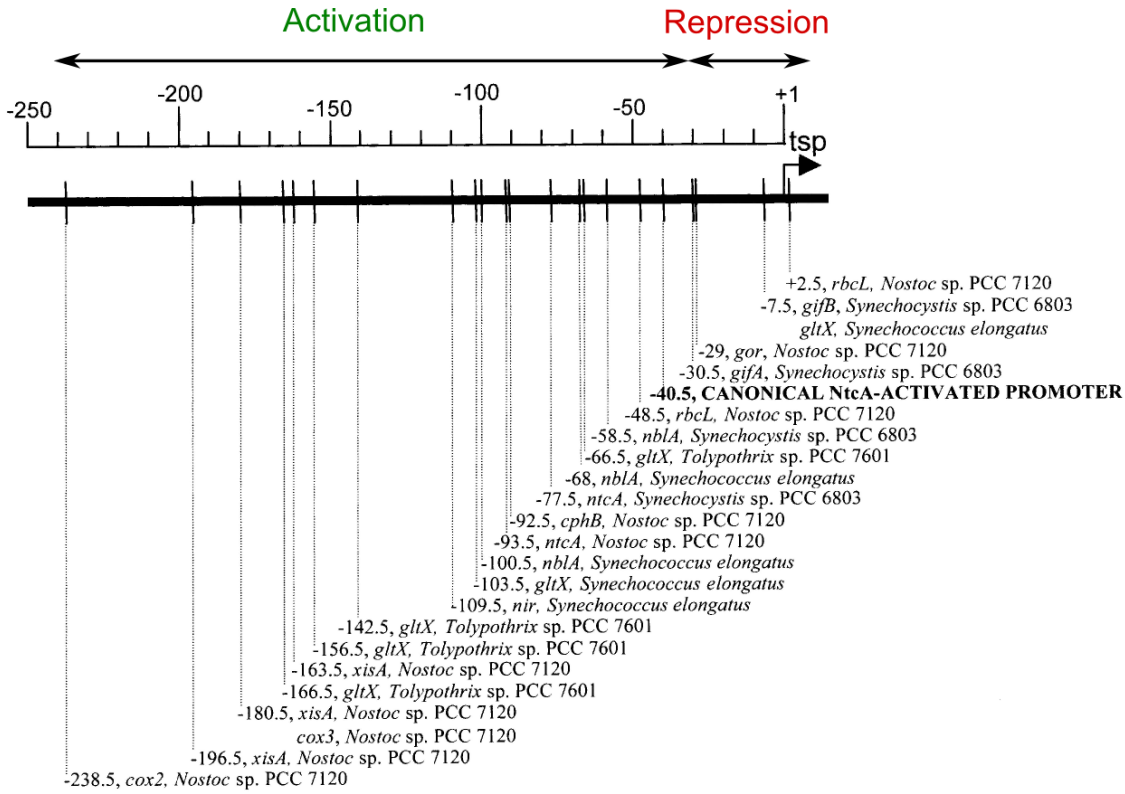

Figure I.16 NtcA-binding siteslocation in different cyanobacterial promoters.
NtcA can act as activator (green) or repressor (red) depending on the position of its binding site within each promoter.
Numbers below indicate the position of the symmetry axis with respect to the tsp and are followed by the name of the corresponding gene and organism. From (Luque and Forchhammer, 2008)

I.6.2. Post-transcriptional regulation

Translation initiation

Cyanobacterial ribosomes are similar tobacterial 70S ribosomes; they show many structural similarities to the*E. coli* ribosome (Lindahl and Zengel, 1986; Sugiura et al., 1998). As in other bacteria, translation starts by the formation of a 30S-mRNA complex. The 30S-binding affinity is thought to increase when a Shine-Dalgarno (SD)

sequence is present. SDis an AG-rich sequence (GAGG, AGGA and GGAG) located 5 to 8 nucleotides upstream from the initiator codon;itis complementary to the 3'-end of the 16S rRNA that is part of the 30S-ribosomal subunit. Most mRNAs in *Synechocystis* possess a SD-likesequence, located at 5 to 19 nucleotides upstream from the initiator codon(Sazuka and Ohara, 1996). Fargo et al. showed that translation could also initiate in the absence of a SD sequencewhen the initiation site is A/U rich (Fargo et al., 1998; Kozak, 2005). Binding of the 30S subunit to theinitiator-factors (IF1, IF2 and IF3) and to fMet-tRNA^{fMet} allows theformation of the30S-initiation complex, which screensfor a favorable translation-initiation region (TIR). IF2 and fMet-tRNA^{fMet} provide a large interaction surface for the 50S-subunitbinding, resultingin the formation of the 70S ribosomal complex, which then initiates translation(Julián et al., 2011).

Orthologous of the 21 genes encoding the small ribosomal subunit have been identified in *Synechocystis*, while 3out of 35 genes (encoding L7, L8 and L30 subunits)have been reported missingfor the large subunit (Sato et al., 1998; Nakao et al., 2010).

Stability of the transcript

mRNA stability is crucial for its expression. Since transcription and translation occur concomitantly in bacteria,changes affecting one of them will affect the other. Ribosomesbindingto the mRNA,as soon as it is transcribed,has been shown to increase its stability by protecting it from degradation (Iost and Dreyfus, 1995; Kulkarni and Golden, 1997). RNAdegradation is accomplished by endonucleases and exonucleases such as ribonuclease E, enolase and PNPase. Horie et al. showed that the *psbA2* mRNA,encoding the D1 subunit ofPSII, is stabilized by the ribosomes under light conditions. Under dark conditions an endoribonuclease (RNase E/G-type) is involved in the mRNA cleavage at an AU-box and at the SD sequence present in the 5'UTR (Horie et al., 2007).

Small-noncoding RNA

Small-noncoding RNA (sRNA) are important gene-regulating factors that are involved in the regulation of many physiological processes (Modi et al., 2011). These sRNA are usually 50 to 400-nucleotides long and do not code for proteins. sRNA includeantisense RNA, transcribed from the complementary DNA strand; sRNA,

transcribed from other loci and the protein-binding sRNA that affect enzyme activity (Gottesman and Storz, 2011).

About 320 sRNA were identified in *E. coli*among which more than 100 have been experimentally confirmed (Vogel and Sharma, 2005; Shinhara et al., 2011). On the other hand,about 314 sRNA were identified in *Synechocystis*(Georg et al., 2009; Voss et al., 2009; Mitschke et al., 2010) and more than 1000 sRNA were identified in the cyanobacterium*Anabaena* sp. PCC 7120(Mitschke et al., 2011).

Bacterial sRNA frequently base pair with the 5'-end of the mRNA. The base pairing generally involves 6 to 8 contiguous bases(Gottesman and Storz, 2011). Some sRNA bind to the coding region of the mRNA and trigger their degradation;this was reported for the *isi*A mRNA in *Synechocystis*, the *ompD* mRNA in *Salmonella* and the *iscRSUA* mRNA in *E. coli*(Dühring et al., 2006; Desnoyers et al., 2009; Pfeiffer et al., 2009). Many sRNA bind to the TIR of the mRNA thus preventingribosome binding. However, sRNA can also activate translation by binding to the mRNA and preventing the formation of secondary structures that mask the TIR. In this case sRNA remodel the mRNA structure in a way exposing the TIR to the ribosome and allowing translation (Prévost et al., 2007).

An example of this regulation in *E. coli* involves the 90-nucleotides RyhB sRNA (induced under iron starvation) and the *shiA* mRNA which encodes a permease for shikimate (an aromatic compound participating in siderophore biosynthesis). The *shiA* mRNA is poorly translated because of a secondary structure that masks the ribosome-binding site (**Figure I.17**); when RyhB is expressed, it interacts with the*shiA* mRNA 5’UTR preventing the formation of the inhibitory structure and allowing its translation (**Figure I.17**) (Prévost et al., 2007).

In many Gram-negative bacteria, an RNA-chaperon protein called Hfq (for **h**ost **f**actor required for phage **Q**β RNA replication) is required for the function and/or stability of sRNA-mRNA interaction. It has been shown that Hfq stabilizes RyhB(Massé and Gottesman, 2002). Hfq homologues were found in a variety of cyanobacteria including *Synechocystis*(Dienst et al., 2008). Although Hfq capacity to regulate gene expression by binding to sRNA was not confirmed in cyanobacteria, it has been shown that it affects mobility in *Synechocystis*(Dienst et al., 2008) as well

asnitrate (and nitrite)transport (and use) in *Anabaena* sp. PCC 7120 (Puerta-Fernández and Vioque, 2011).

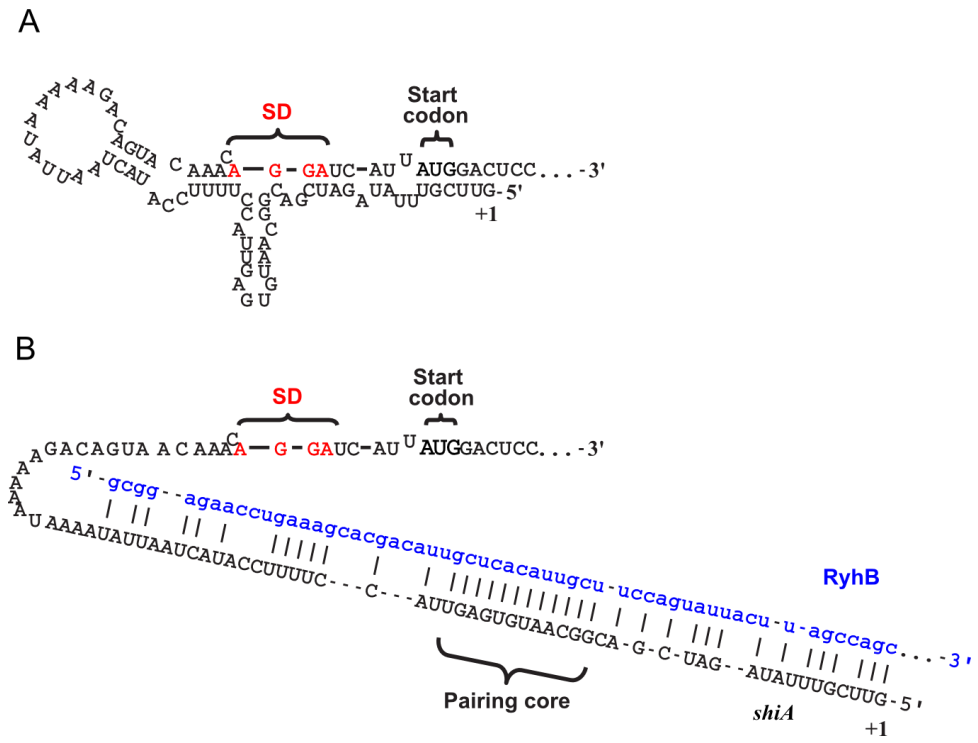

Figure I.17 The *shiA* 5′-UTR potentially forms a structure that blocks translation initiation.
A. Potential secondary structure of *shiA* mRNA from nucleotide +1 to +86. The represented sequence includes the Shine-Dalgarno (SD) and the translation initiator codon (AUG) of *shiA*.
B. RyhB *s*RNA (blue) potentially pairs at the 5′-UTR of *shiA*. The core represents 12-nucleotides consecutive pairing between RyhB and *shiA* mRNA. From (Prévost et al., 2007) with modifications.

Riboswitches

RNA can also exhibit structural changes without the involvement of sRNA or proteins.Theymay directly sense a physiological state by interacting with molecules (cofactors, amino acids, nucleotides or metal ions) or by responding directly to temperature shifts; such RNA are called riboswitches.

Metabolite-dependent riboswitches typically involve two components: a metabolite-binding aptamer and an expression platform (Regulski and Breaker, 2008). Aptamer is a three-dimensional RNA structure that interacts with the metabolite. Aptamers size ranges between 35 to 200 nucleotides. Metabolite binding to an aptamer induces structural changes in the aptamer and in itsneighboring, which affects the expression platform resulting in its inhibition, orits induction, of gene expression.

Riboswitches may control gene expression through transcription attenuation or *via*translation initiation (**Figure I.18**).

In the case of transcription attenuation, the mRNA contains an intrinsic transcriptional terminator. Metabolite binding to the mRNA determines whether the RNA polymerase will terminate or continue transcription through the transcript terminator sequence, allowing the expression of downstream genes (**Figure I.18-A**).

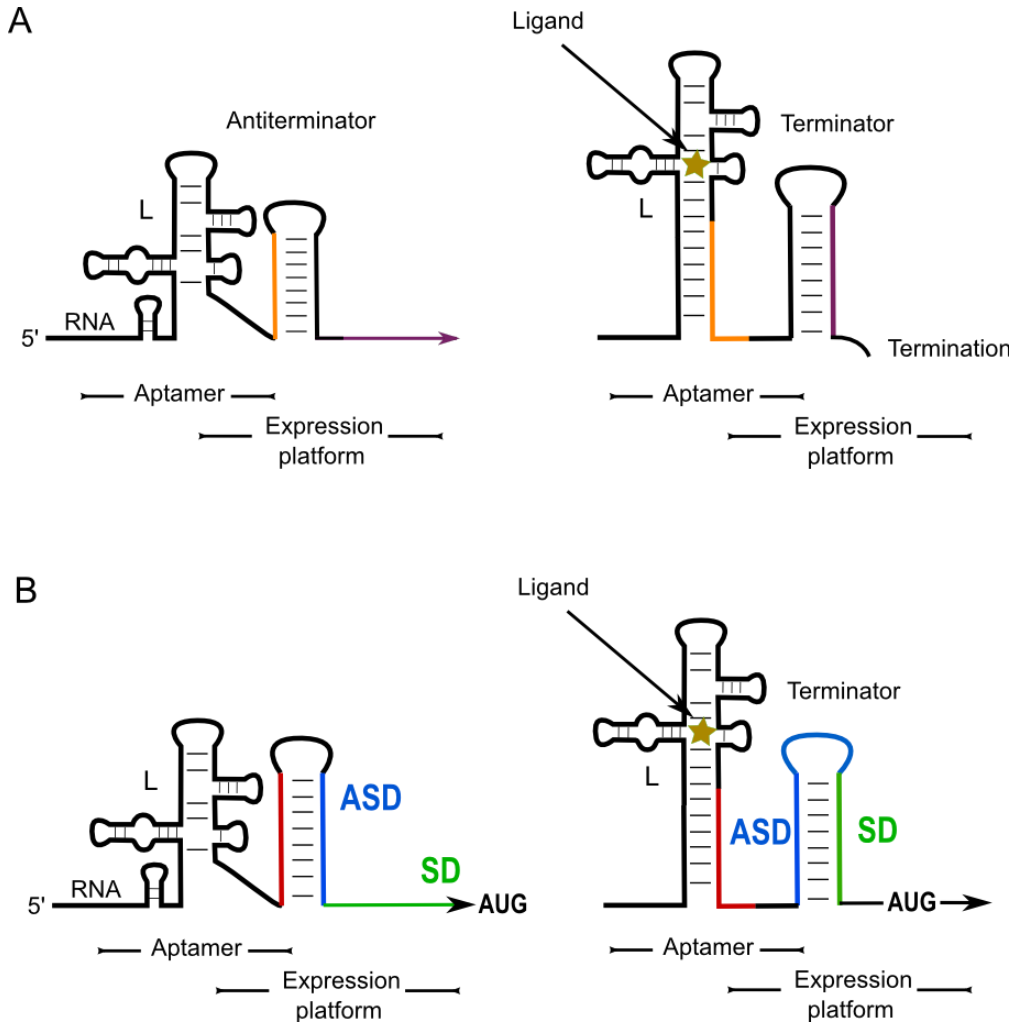

Figure I.18 Basic models for metabolite-binding riboswitches.
(**A** and **B**). In the absence of the ligand (left), the ligand-binding domain (L) is unoccupied, and the RNA adopts a conformation that allows the expression of downstream sequences, either through formation of an antiterminator, which prevents formation of the terminator and therefore allows transcription to proceed (top), or through the capture of the ASD, which liberates the SD and allows translation initiation (bottom).
(**A** and **B**). In the presence of the ligand (star on the right), the ligand-binding domain is occupied, resulting in a structural shift. An inhibitory structure is adopted, which results in a premature transcription termination (top) or a sequestration of the SD sequence in an ASD–SD helix that prevents translation initiation (bottom). Inspired from (Henkin, 2008).

A similar aspect of such a regulation is the *trp* operon in *E. coli*. In the presence of tryptophan, the transcribed *trp* mRNA folds in a way that creates a premature transcriptional terminator resulting in the operon repression. When the tryptophan level is low ($tRNA^{Trp}$level is low) the ribosome stalls temporarily when it encounters*trp* codons. This stalling results in a different folding of the *trp* mRNA, which allowsfor the transcription of the full *trp* operon(Yanofsky, 1987).

In the case of translation regulation, the mRNA is constitutively transcribed. The leader includes a region able to sequester the ribosome-binding site(ASD), usually by pairing with the Shine-Dalgarno (SD) sequence as a function of metabolite availability (**Figure I.18-B**).

Riboswitches are not well studied in cyanobacteria. However it has been shown that some cyanobacteria, like *Synechococcus elongatus*, possess a RNA-motif capable of binding the amino acid glutamine. This motif is named*glnA*-motif since it was founding*glnA*, coding for type I Glutamine synthetase.The *gln*A-motif is frequently positioned upstream from genes involved in nitrogen metabolism, including glutamate synthase and ammonium transporters(Weinberg et al., 2010; Ames and Breaker, 2011). Nevertheless no confirmation of gene regulation (for genes possessing the *glnA* motif) has been assessed experimentally.

Thermosensors. RNA thermosensors do not require metabolites. These are RNA-structural elements that inhibit translation initiation by creating an ASD-SD helix, which prevents ribosome access to the TIR. In most cases, the RNA is inactive (sequestered SD) under normal-growth conditions. An increase in temperature results in the melting of the ASD-SD helix and the release of the SD into a single-stranded state to which ribosome can bind (**Figure I.19**) (Henkin, 2008).

The *rpoH* mRNA, encoding σ^{32} heat-shock transcription factorin *E. coli*(Morita et al., 1999) and the *hsp17* mRNA encoding a heat shock protein in *Synechocystis*(Kortmann et al., 2011) aretwo examples of RNAthermosensors that activate translation at high temperature (**Figure I.19**).

Although the last examples constitute the dominant type of thermosensors, it was recently shown that translation of the *cspA* mRNA, encoding a cold-shock protein in *E. coli*, is activated at low temperature (Giuliodori et al., 2010). In fact, at 37 °C the *cspA* mRNA adopts a structure where the SD and the initiator codon are involved in a

double-stranded structure, resulting in a week translation of the mRNA. At low temperature (20 °C) the mRNA adopts a different structure by exposing the SD and the initiator codon, allowing a better translation efficiency.

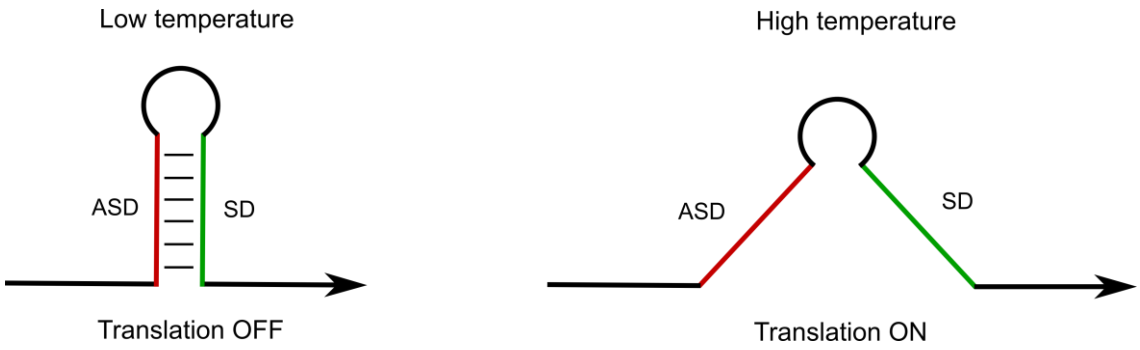

Figure I.19 RNA thermosensors.
At low temperature (Left), the helical structure is stable, resulting in the sequestration of the SD sequence by pairing with the ASD sequence (SD); this results in translation initiation inhibition. At higher temperature (Right), the ASD–SD helix is disrupted and the SD sequence is available for translation initiation. From (Henkin, 2008) with some modifications.

II. Resultsand discussion

FNR_S(produced from a translation-initiation site located within the FNR_L orf) accumulates in *Synechocystis* upon chemoheterotrophic growthand starvation conditions. A common feature to these conditions is that anabolism is disfavored because of the lack of substrates.

The aim of this work is to understand the genetic regulation of FNR isoforms synthesis.

II.1. Effect of nitrogen starvation on *Synechocystis*physiology and FNR accumulation

During this work nitrogen starvation conditions were used to induce FNR_S accumulation because these conditions were the easiest to achieve and gave us the most reproducible results.

In order to better understand the conditions under which FNR_S accumulates, cell growth,pigment content,and therelative amounts of the twoFNR isoforms werestudied in the WT, MI6 and FS1strains during nitrogen starvation.

Liquid cultures, grown under standard conditions (described in section IV.1.1), were transferred to a medium lacking combined nitrogen and incubated for up to 120 hours, under otherwise identical conditions. Aliquots representing different starvation times were collected and analyzed for the above-mentioned properties.

II.1.1. Culture turbidity and chlorophyll content

Optical densitiesat 580 nm (OD_{580nm}) of the cultures during nitrogen starvation show about a two-fold increase after 48 hours (h), consistent with cell growth continuing in these conditions. Then OD_{580nm} increases slightly up to 96 h and subsequently starts to decrease(**Figure II.1**).

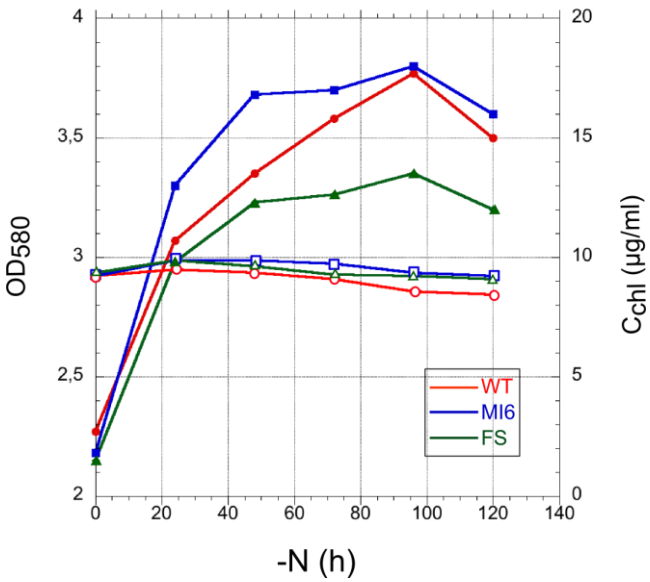

Figure II.1The effect of nitrogen starvation on cell growth and chlorophyll concentration. Empty symbols correspond to the variation of chlorophyll concentration, full symbols to the variation in culture optical density. Circles, squares and triangles represent respectively the WT, MI6 (a mutant unable to produce FNR_S) and FS1 (a mutant unable to produce FNR_L). –N (h) corresponds to the hours under nitrogen starvation.

In parallel, chlorophyll concentration was monitored in the cultures. Figure II.1 indicates that total chlorophyll concentration is nearly constant during nitrogen starvation. After 120 h of nitrogen starvation, the chlorophyll content in the WT and MI6 decreased to 92% of the initial concentration, while in FS1 it reached 85% of the initial concentration.

II.1.2. Evolution of photosynthetic pigments

Absorption spectra of whole cells, collected at different time-points of nitrogen starvation, depict the evolution of different photosynthetic pigments in WT, MI6 and FS1.

The spectra in figures II.2-A, B and C show that PBP absorption (620 nm) decreased, due to a well-known phenomenon called bleaching (Section I.4.2), where PBP degradation provides amino acids for cell survival in the absence of external nitrogen (Allen and Smith, 1969). The bleaching rate was clearly different in the different strains.On the other hand carotenoidabsorptionincreases(350 nm to 500 nm), carotenoid accumulation being a typical response to stress, while chlorophyll *a* (440 nm, 620 nm and 680 nm) does not seem to be greatly affected, in agreement with the results described in the last section (**Figure II.1**).

The spectra show that the rate of PBPdecrease during nitrogen starvation is different between the WT and the mutants. Compared to WT, the remaining level of PBP at 48 h is higher in MI6 and lower in FS1 (dark blue trace in figure II.2 B and C, respectively).

The intensity of PBP-complexes absorption at 620 nm (A_{620nm}) provides an indication of the concentration of biliproteins in the cells. However, the bilins are not the only pigments that absorb at 620 nm. Chlorophyll*a*absorbs at the same wavelength and this is demonstrated,in figure II.2-D, in the absorption spectrum of PAL - a mutant totally devoid of PBP (Ajlani and Vernotte, 1998).

In PAL, A_{620nm} is about 20% of the absorption at 680 nm (A_{680nm}), indicating that about 20% of A_{680nm} contributes to the A_{620nm}in a PBP-containing strain.

In order to better characterize PBP degradation rate, curves that represented the variation of A_{620nm}/A_{680nm} during nitrogenstarvation were plotted (**Figure II.2-E**).

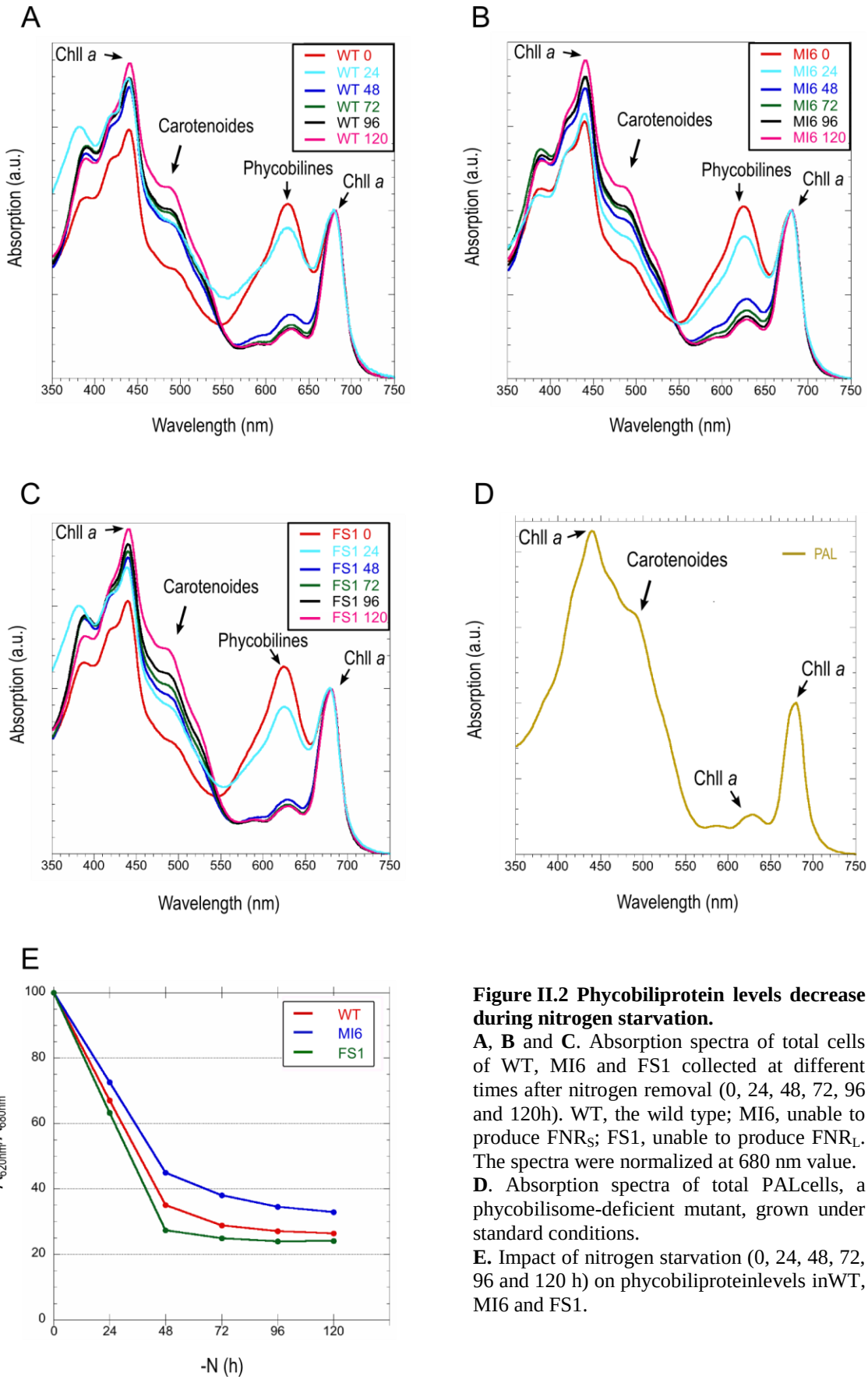

Figure II.2 Phycobiliprotein levels decrease during nitrogen starvation.
A, **B** and **C**. Absorption spectra of total cells of WT, MI6 and FS1 collected at different times after nitrogen removal (0, 24, 48, 72, 96 and 120h). WT, the wild type; MI6, unable to produce FNR_S; FS1, unable to produce FNR_L. The spectra were normalized at 680 nm value.
D. Absorption spectra of total PALcells, a phycobilisome-deficient mutant, grown under standard conditions.
E. Impact of nitrogen starvation (0, 24, 48, 72, 96 and 120 h) on phycobiliproteinlevels inWT, MI6 and FS1.

Figure II.2-E confirms that PBP are degraded rapidly after nitrogen step downup to48 h,and thenthe rate of decrease is slowed down such that at 120 h A_{620nm} approaches 20% of A_{680nm} (*i.e.* all PBP has been degraded).

Figure II.2-Ealso confirms that PBP degradation is slower in MI6 and faster in FS1 when compared to the WT. Although the level of PBP in all strains approaches 0 (20% of A_{680nm})after 120 h of nitrogen starvation, MI6 still contains more PBP than FS1 and the WT.

These results were verified by repeating the experiment three times. Since the only difference between these mutants and the WT is the absence of FNR_S (or FNR_L), $FNR_S$was suggested to play a role in PBP degradation.

II.1.3. Total-proteinand FNR-accumulationpattern

Total protein patterns as well as the accumulation of FNR isoforms were monitored upon separation on a denaturing polyacrylamide gel. The Coomassie-stained gel, infigure II.3-A, shows that when the samples were loaded at equivalent chlorophylllevel, the amounts of total proteins in the different samples were similar.On the other hand, decrease in PBP was clearly visible in all strains during nitrogen starvation(**Figure II.3-A**, 15-20 kDa). Compared to the WT,the gel also shows that PBP decrease was slower in MI6 and faster in FS1. These results are coherent with those drawn from the previous sections.

In addition, FNR immunobloting was performedon the same samples. In the WT, the amount of FNR_L decreases while FNR_S accumulates, upon nitrogen starvation; in MI6, only FNR_L is detected and its level decreased during nitrogen starvation; while in FS1, only FNR_S is detected but its levelclearly increasedupon nitrogen starvation(**Figure II.3-B**).Note that small amounts of FNR_S are detected in the WT under standard conditions and that FNR_S accumulation reaches a maximum after 48 h of nitrogen starvation. At the same time a decrease in FNR_L is observed (clearly seen after 72 h in figure II.3).

Taking into account the observations described here, FNR accumulationwas monitored, for a maximum duration of 72 h after nitrogen step down in the following experiments and chlorophyll content was used to standardize the sample loading.

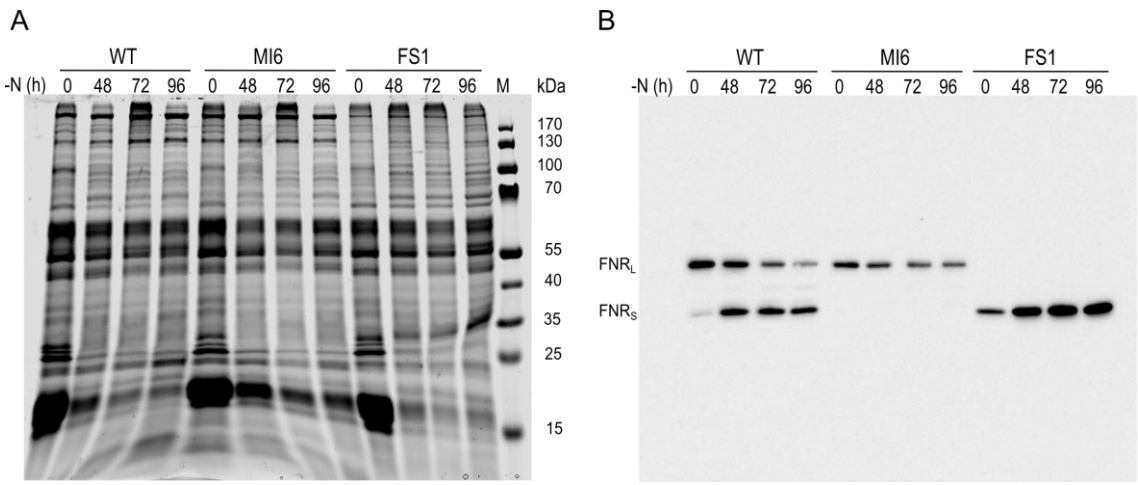

Figure II.3 Impact of nitrogen starvation on production of FNR isoforms in total protein extracts.
A. Coomassie-stained SDS-PAGE of total protein extracts from the WT, MI6 and FS1 mutants starved for 48, 72 and 96 hours (0.5 µg chlorophyll per well).
B. Western blot analysis of the FNR in the same cell extracts, separated on an identical gel but loaded with 10 times less chlorophyll (0.05 µg chlorophyll per well).
WT, the wild type; MI6, unable to produce FNR_S; FS1, unable to produce FNR_L. (M) indicates the protein ladder with the corresponding molecular mass of each protein.

II.2. Ectopic expression of the FNR_L orf

Translation control often occurs at the level of initiation, thus implicating the mRNA 5'UTRas a major site for translational regulation (Pickering and Willis, 2005).Translation regulation is affected by the 5′UTR characteristics, including its length and structure.

The *petH* mRNA of *Synechocystis* was described as having a 5'UTR consisting of 523 bases (van Thor et al., 1998). To examine the *petH* 5'UTR role in *petH* translation regulation,the FNR_L orf was expressed ectopically under the control of the *psbA2* promoter or under the control of its own promoter.Since *petH* is an essential gene under all known growth conditions, we modified an ectopic allele placed at the *psbA2* locus and monitored its ability to produce FNR_S. It has been shown previously that *psbA3* supports photoautotrophic growth in the absence of *psbA2*(Mohamed and Jansson, 1989); so this insertion is neutral to *Synechocystis*. Nitrogen starvation was used to induce FNR_S accumulation.

II.2.1. *petH* 5'UTR is required for FNR_S accumulation

Two cargo plasmids were created: pLC, in which the *petH*orf was fused to the 5'-noncoding region of *psbA2*, and pLC5', where the *psbA2* promoter region was replaced by that of *petH*(**Figure II.4-A**). In each construct, upstream and downstream *psbA2* sequences and a Cm-resistance cassette (*cat*) allowed chromosomal integration by double recombination and positive selection, respectively. FNR_S accumulation from the constructs was monitored in MI6, a mutant in which *petH*is unable to produce FNR_S. Thus, the resulting strains, denoted MLC and MLC5', carried a native allele unable to produce FNR_S, and an ectopic one harboring a wild-type orf that was under the control of two different 5'-noncoding regions. PCR, restriction analysis and DNA sequencing confirmed the genotypes of the mutants (not shown).

FNR accumulation was probed in cell extracts from the wild type, MI6, MLC and MLC5' strains, grown under standard and nitrogen starvation conditions. When nitrogen is present, FNR_L is the major isoform in the WT (0 in **Figure II.4-B**), while FNR_S is dominant after 72 hours of nitrogen starvation (72 in **Figure II.4-B**). In MI6, besides the

absence of FNR_S, the FNR_L decrease during nitrogen starvation is slowed down, compared to the wild type. In MLC, FNR_S was also absent, while MLC5' recovered the ability to accumulate FNR_S upon nitrogen starvation. This demonstrates that ectopic expression of *petH* can lead to FNR_S translation only when the ectopic allele contains the *petH* 5'UTR (MLC5'), while with the *psbA2* 5'UTR it cannot (MLC). Residual amounts of FNR_S are detected in MLC, at both time points. This suggests that when the second-initiating methionine is intact, as it was in the ectopic orf; FNR_S translation initiation occurs, in the absence of the appropriate 5'UTR, albeit at a very low efficiency.

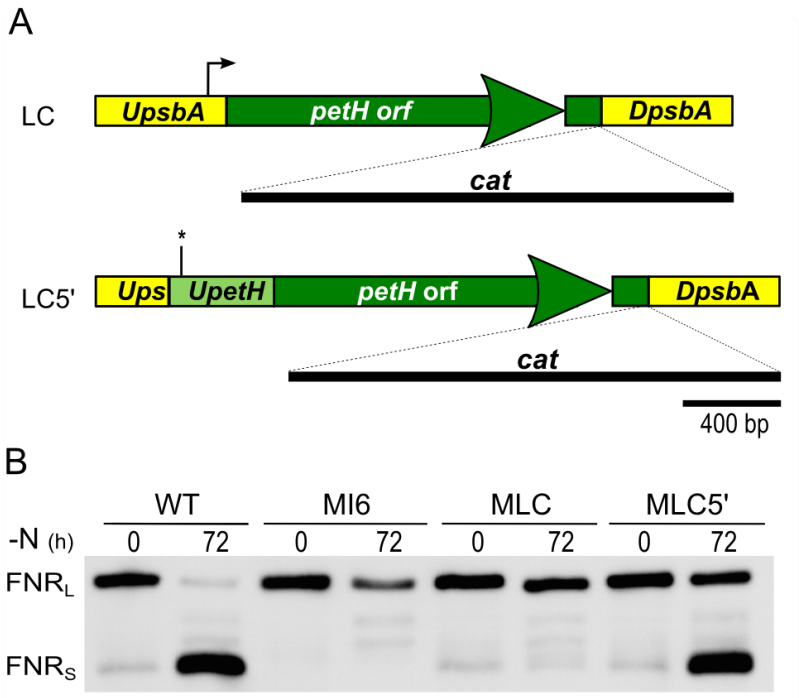

Figure II.4*petH* 5'UTR regulates FNR_S translation.
A. Structure of two ectopic alleles placed at the *psbA2* locus in MI6. In LC, FNR_L orf was under the control of the *psbA2* 5'-noncoding region, while in LC5' the same orf was under the control of the *petH* 5'-noncoding region. A bent arrow indicates the position of *psbA2* tsp and an asterisk indicates the position of *petH* tsp as previously mapped in (van Thor et al., 1998), yellow boxes represent *psbA2* related sequences and green boxes represent those of *petH*, U and D designate upstream and downstream regions, respectively.
B. Impact of nitrogen starvation (for 0 and 72 h) on FNR accumulation in total protein extracts analyzed by western blot. WT, the wild type; MI6, a mutant where the native *petH* is unable to produce FNR_S. MLC and MLC5', ectopically expressed the LC and LC5' alleles, respectively, in MI6.

II.2.2. Ectopic expression resulted in a gene dosage effect

A relatively higher amount of FNR_L was detected in extracts from MLC and MLC5', compared to WT and MI6. This might be a gene dosage effect, due to the expression of two *petH* alleles in these strains. In order to confirm this hypothesis, FNR_L amount was quantified in MI6 (containing only the native *petH*) and MLC (containing both native and ectopic *petH*).

Since chemiluminescence detection is often not quantitative,FNR_L amount was quantified on coomassie-stained SDS-PAGE containing different amounts of purified PBS,to which FNR_L binds. Quantification was performed as mentioned in the experimental procedures chapter. FNR_L amount was estimated in MI6 and MLC. Loading errors were rectified by normalizing to the band containing L_{CM}; this linker strongly binds to the PBS and its amount is known to be constant (see details in section IV.7.2.).

Indeed, PBS from MLC contained twice the amount of FNR_Lcompared to thatin MI6 PBS (**Figure II.5**). This demonstrates that the expression of two *petH* alleles results in the accumulation of more FNR_L in MLC, which is formally designated as a gene dosage effect.

It has been shown that an average of 2 FNR/PBS exists in the wild type *Synechocystis*; the fact that extra FNR_L molecules were bound to the PBS in MLC shows that extra FNR-binding sites are available on the PBS.

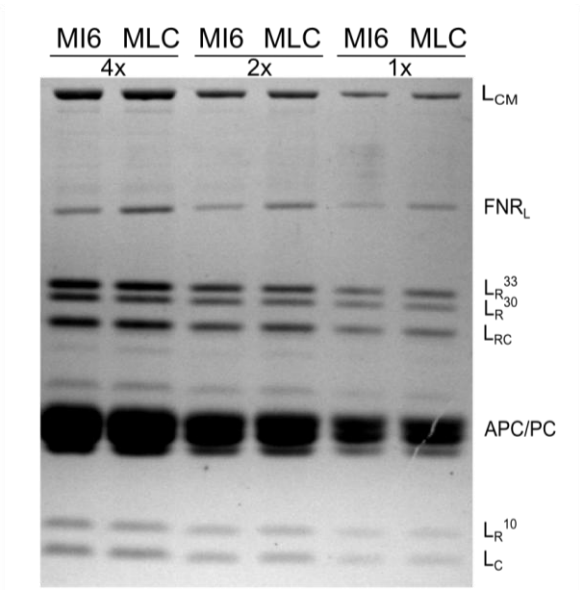

Figure II.5 Phycobilisomes from MLC show higher FNR_L amounts. Different amounts of purified PBS were loaded on an SDS-PAGE and stained with Coomassie blue. The identities of the PBS subunits are labeled on the right. L_{CM}, core-membrane linker; L_R, rod Linkers (33, 30 and 10 designate respectively the mass of each L_R); L_{RC}, rod-core linker; L_C, core linker; APC/PC, allophycocyanin/phycocyanin.

II.3. A promoter responsible for FNR_S accumulation

In an attempt to further elucidate a putative signal responsible for FNR_S translation, deletions within the*petH* 5'-noncoding regionwere constructed. The accumulation of both FNR isoforms was monitored in each deletion mutant.

II.3.1. Deletions within the *petH* 5'-noncoding region

Restriction fragments were deleted from the aforementioned pLC5' (**Figure II.6**), creating two vectors: pBB lacks 370 bases (from 477 to 105 bases upstream to ATG-1), while pHH is missing 345 bases (from 490 to 145 bases upstream to ATG-1). Both deletions preserved the *petH* promoter previously mapped by van Thor et al.(van Thor et al., 1998) (**Figure II.6-A**). In order to monitor the ability of these constructs to express each of the FNR isoforms, the mutated alleles were expressed ectopically in MI6 (unable to produce FNR_S) and in FS1, a mutant unable to produce FNR_L. FNR isoforms were immunodetected in total extracts from mutants grown in the presence of nitrogen (0 h in **Figure II.6-B** and **C**) or nitrogen-starved for only 24h – where FNR_S is already detected (24 h in **Figure II.6-B** and **C**).

Ectopic expression of the above constructs in MI6 resulted in mutants MHH and MBB, where the origin of FNR_L is indistinguishable, due to the expression of the ectopic and/or the native allele, while that of FNR_S results exclusively from the ectopic one –since the native allele is unable to produce FNR_S. Figure II.6-B clearly shows that FNR_S accumulation was abolished by both deletions, since neither MHH nor MBB produced FNR_S under nitrogen starvation. On the other hand, ectopic expression of the same alleles in FS1 resulted in mutants FHH and FBB, where accumulation of FNR_S is indistinguishable due to the expression of the ectopic and/or the native allele, while that of FNR_L results from the ectopic one (the native allele is unable to produce FNR_L). Figure II.6-C shows that neither of the deletions altered FNR_L expression. This result suggests that the deleted fragments were dispensable for FNR_L expression, but contained a promoter or another regulating element responsible for FNR_S expression.

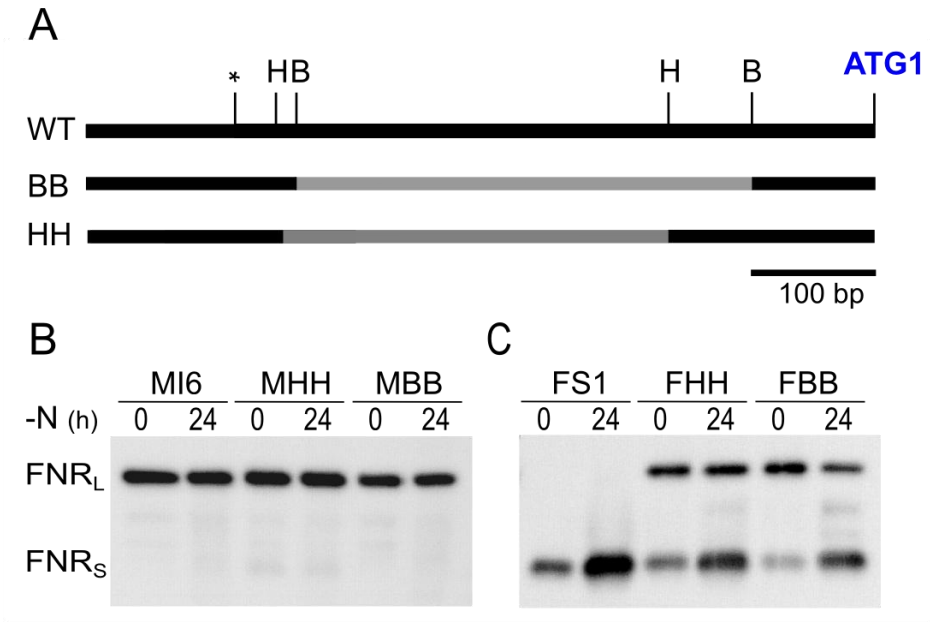

Figure II.6 Deletions within the *petH* 5'-noncoding region.
A. Structure of the 5'-noncoding region in the wild type (upper map) and in two ectopic alleles (BB and HH) lacking internal restriction fragments of 370 and 345 bases, respectively (gray lines). Asterisk indicates the position of the *petH* tsp (at 523 bases upstream from AUG-1) as previously mapped in (van Thor et al., 1998); B, BseRI; H, HpaI.
B. Immunoblot analysis of FNR accumulation, in total protein extracts from nitrogen-starved cells (for 0 and 24 h) shows that the above alleles expressed in MI6 (MHH and MBB) failed to accumulate FNR_S.
C. Expression of the same alleles in FS1, which is unable to produce FNR_L, results in FNR_L accumulation (FHH and FBB).

II.3.2. Genetic mapping of *petH* promoters

In order to further investigate the existence of different promoters, three nested deletions including the previously mappedpromoter (van Thor et al., 1998)were constructed. The deletions were extended up to 105 bases upstream from ATG-1 (NG, NP and NB in **Figure II.7-A**). These constructs were expressed ectopically in MI6 (MNG, MNP and MNB) and the mutants were then nitrogen-starved to monitor their ability to accumulate FNR_S. Figure II.7-B shows that the NG and NP alleles, carrying 378 and 213 bases upstream from ATG-1, respectively, still produced FNR_S (MNG and MNP). Conversely the NB allele, carrying only 105 bases upstream from ATG-1, did not produce FNR_S (MNB).

This confirms that a specific promoter for an FNR_S-specific transcript is located within a fragment extending from 213 (P) to 105 (B) bases upstream from ATG-1. On the other hand, the NB allele was also expressed in FS1 (mutant FNB), and

surprisingly, this allele clearly produces FNR_L in the absence of the promoter previously mapped byvan Thor et al. (**Figure II.7-C**).

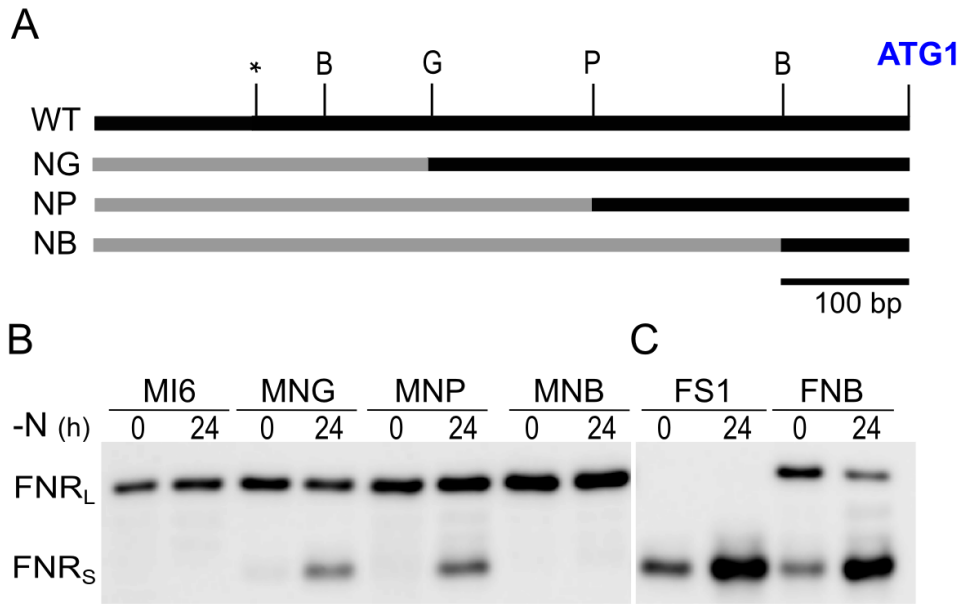

Figure II.7 Genetic mapping of the *petH* promoter.
A. Structure of the 5'-noncoding region in the wild type (upper map) and in three ectopic alleles (NG, NP and NB) bearing nested deletions (gray lines). Asterisk indicates the position of the transcription start as previously mapped in (van Thor et al., 1998); B, BseRI; G, BglII; P, SpeI.
B. Immunoblot analysis of total-protein extracts from cells starved for nitrogen (for 0 and 24 h) to induce FNR_S translation. Expression of the above alleles in MI6 (unable to produce FNR_S) resulted in MNG and MNP, where FNR_S accumulates, and MNB, where it did not.
C. When the NB allele was expressed in FS1 (unable to produce FNR_L), the resulting strain, FNB, accumulates FNR_L.

These results strongly suggest that a promoter, responsible for FNR_L expression, is located within 105 bases upstream from ATG-1.This promoter was not described by van Thor et al.(van Thor et al., 1998).

In addition the results presented is this work suggest that a signal (or promoter) responsible for FNR_S accumulation is located between 213 and 105 bases upstream from ATG-1. Subsequently, it was deemed that a more in-depth investigation of the *petH* promoter was warranted; the results are described in the next section.

II.4. A specific promoter for each FNR isoform

The 5'UTR described by van Thor, (532 bases)did not match our deletion study and seemed unusually long compared to *Synechocystis* 5'UTR(Mitschke et al., 2010). Therefore, the 5'-ends of the *petH* mRNA under conditions that induced FNR_L or FNR_Ssynthesisweremapped. Three tsp were determined andgeneticallyconfirmed.

II.4.1. *petH* transcription-start sites

In order to locate the 5'-ends of the *petH* mRNAs, under standard conditions and conditions under which nitrogen-induced genes are expressed, we have used differential TAP (Tobacco Acid Pyrophosphatase) 5'-RLM-RACE (RNA-Ligase-Mediated Rapid Amplification of cDNA ends). The reactions were carried out with RNA samples extracted from the wild type grown in nitrogen-containing medium (+N) or nitrogen-starved for 8 h (-N). Figure III.1 (in experimental procedures, section III.8) represents the DNA fragments, issued from the differential 5'-RLM-RACE. Sequencing of the differentially amplified products from +N RNA, showed two adjacent tsp, 52 (C) and 34 (A) bases upstream from ATG-1 (**Figure II.8**). The -52 tsp is 8 bases downstream from an extended -10 box (TGgTAggcT). Such elements were found to function without an obvious -35 box in *E. coli*(Barne et al., 1997) and were described in several cyanobacterial promoters (Mazouni et al., 1998; Valladares et al., 2004). It is striking that the upstream element of this promoter is considerably GC rich (75%) when compared to the *Synechocystis* genome (47.7%). The -34 tsp starts on an A that is located 6 bases downstream from a putative -10 Pribnow-like box (TAaAtT) separated by an 18-bases AT-rich spacer from a putative -35 box (aTGgtA). On the other hand, in -N RNA, a tsp was mapped 126 (A) bases upstream from ATG-1; again an extended -10 box (TGtTAgggT) is found with a spacing of 6 bases upstream from the tsp for this promoter. The location of these tsp, summarized in **Figure II.8**, is in excellent agreement with the promoters genetically identified in the previous section (downstream -105 for +N and -213 to -105 for -N).

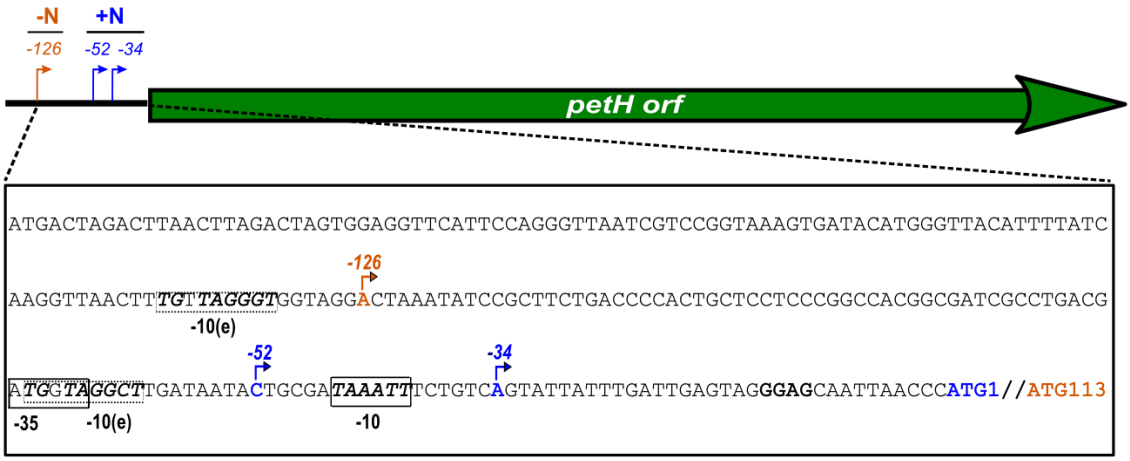

Figure II.8 Location of the *petH* tsps mapped in this work.
Bent arrows indicate the positions of the tsps, -52 and -34 (standard conditions) and -126 (nitrogen starvation conditions), the numbers are relative to the first translation-initiator codon of *petH*. The sequence of the 5'-noncoding region is represented bellow, with the tsps (colored under bent arrows); the promoters elements -10 and -35 (boxed) for tsp -34; extended (e) -10 for tsp -52 and -126 (dotted-line boxes). The start codons are colored in blue and orange and the Shine-Dalgarno (SD) is represented in bold.

These results are consistent with a recent workthat established a genome-wide map of 3527 tsp of *Synechocystis*by differential RNA sequencing and where the -52 *petH*tsp was described(Mitschke et al., 2010). We found that the P_{52}promoter contained a surprisingly G-C rich sequence and that the -10 box resembled the extended -10 element described in many bacteria, including cyanobacteria (Mazouni et al., 1998; Valladares et al., 2004).

Although the second constitutive tsp (-34), mapped here, was not described in (Mitschke et al., 2010), the presence of adequate-10 and -35 promoter elements together with the fact that it starts with an A (according to Mitschke et al., 68% of *Synechocystis* transcripts starts on an A) argues for its validity. It was also noticed that our growth conditions differed slightly from those used in the Mitschke et al. work, where*Synechocystis* was grown at 30°C without CO_2, while it was grown at 33°C in a CO_2 enriched incubator in our laboratory.

It is remarkable, that the -10 box element of P_{52} overlaps with the -35 box element of P_{34} (**Figure II.8**) and that both promoters function simultaneously under our laboratory growth conditions; their functioning might involve different sigma factors (Asayama and Imamura, 2008).

II.4.2. Genetic confirmation of promoters locations

In order to ascertain the location of the newly discovered promoters, the omega-*aadA* cassette, flanked by T4 transcriptional-termination sequences (Prentki and Krisch, 1984), was inserted in the native *petH*gene noncoding region at sites located -240, -195, -145 and -79 bases upstream from ATG-1 (**Figure II.9-A**). Transformation of the wild type resulted in mutants BX, VX, HX and SX, respectively. Total segregation and location of the insertion was confirmed by PCR (**Figure II.9-B**). FNR was immunodetected in total cell extracts from the wild type and each of the mutants, in the presence of nitrogen and after 24 h and 72 h of nitrogen starvation. The FNR isoform patterns in BX and VX were similar to those of the wild type, while HX and SX failed to accumulate FNR_S (**Figure II.9-C**). This result confirms that the distal promoter is responsible for FNR_S accumulation, while the proximal promoters are responsible for the accumulation of FNR_L.

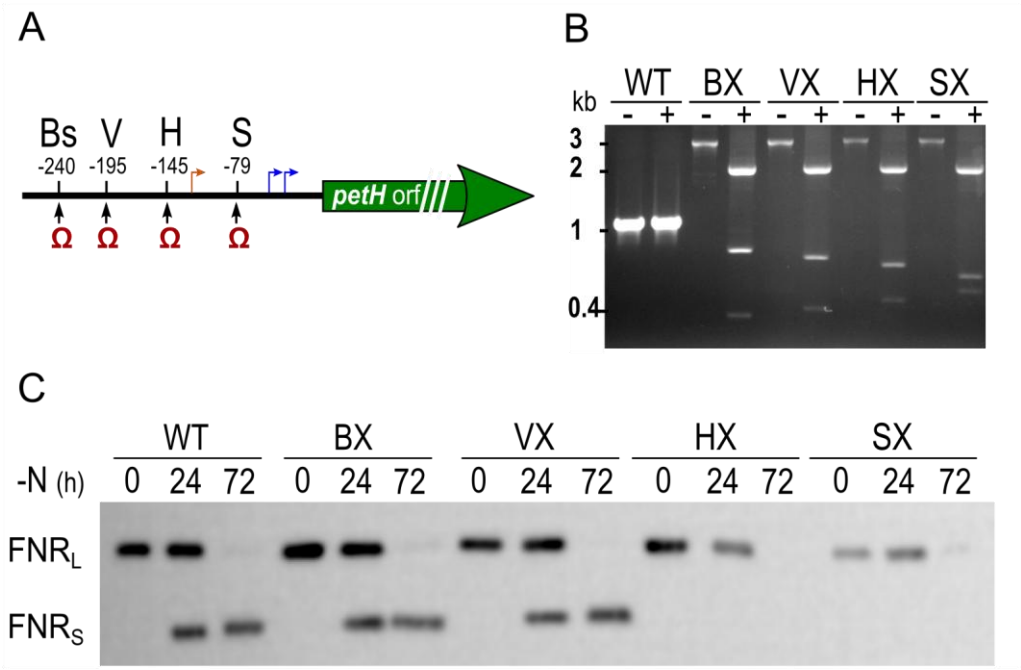

Figure II.9 Omega insertions in the *petH* 5'-noncoding region.
A. Representation of the Ω- cassette insertion sites, a solid line represents the 5' non-coding region and the green arrow represents the *petH* orf. Blue and orange bent arrows indicate the -34, -52 and -126 tsp, respectively. Letters represent the sites name and the numbers below their position relative to ATG-1; Bs, BssHII; V, AvrII; H, HpaI; S, AsiSI;
B. PCR and restriction analysis of the mutants DNA. (-) PCR produced a 1-kb fragment from the wild type (WT) and 3-kb fragments from the insertion mutants (BX, VX, HX and SX). (+) Digestion of the PCR products with HindIII, an enzyme that bracketed the cassette, produced a 2-kb fragment containing the cassette and two fragments representing downstream and upstream regions.
C. Immunodetection of the FNR isoforms in the wild type (WT) and the insertion mutants under standard conditions (0) and upon nitrogen starvation for 24 and 72 hours (24 and 72).

The insertion of an omega cassette 27 bases upstream from the -52 tsp, in SX, seems to result in lower FNR_L amounts than a mutant bearing the same insertion 65 bases farther upstream (HX, in **Figure II.9**); transcription from the -52 tsp could be disturbed in SX due to the absence of its associated UP elements. This result suggests that combined expression from both promoters participate in FNR_L homeostasis in *Synechocystis* under standard growth conditions.

Finally, neither Mitschke et al., nor our work identified the -523 tsp described by van Thor et al., (van Thor et al., 1998; Mitschke et al., 2010). Note that this tsp does not contain promoter consensus sequences. In addition, none of the 3527 genomic 5'-endsdescribed in Mitschke's study was longer than 278 bases. Mitschke et al. proposed that this 5'-end could belong to an antisense RNA that is transcribed in the adjacent *prk* gene.Therefore, the tsp mapped by van Thor et al. does not correspond to an mRNA related to *petH*.

II.4.3. Transcriptionalregulation of the large mRNA

The *petH* transcription organization in *Synechocystis*was found to be very similar to the one found by Valadares et al.in the cyanobacterium *Anabaena* sp. PCC7120.Two transcripts were found for the *AnabaenapetH*, the shorter is constitutive, while the longer is induced in the absence of combined nitrogen and controlled by the global transcriptional regulator NtcA (Valladares et al., 1999).

Two putative NtcA-binding sites, located about 45 bases upstream from the distal *petH* tsp,were detected in*Synechocystis*. Both diverged from the currently accepted consensus GTA(N8)TAC.One site diverged in the number of nucleotides located between the palindromic triplets (N6), while the other possessed a GATinstead of the typical GTA as in the first triplet of the palindromicconsensus sequence (**Figure II.10-WT**).

NtcA binding *in vitro*

In order to analyze whether NtcA binds to the *petH* promoter, electrophoretic-mobility-shift assays (EMSA), using purified *Synechocystis* NtcA, were performed. These experiment were performed in collaboration with C. Galmozzi and M.I.

Muro-Pastor at the "Institute of Plant Biochemistry and Photosynthesis (IBVF)", Sevilla, Spain.

Binding assays were performed with a 229-bases SpeI-SnaBI DNA fragment, which spans positions -85 to +144 with respect to the distal tsp. Fragments with modified versions of the putative binding sites were also tested; N6 where a GTA triplet was changed to CAT and an A into a T, creating an NdeI restriction site, and N8 where the GAT triplet was changed to TAG and a GT into a TC, creating an XbaI restriction site (**Figure II.10**). NtcA was incubated with the WT as well as with the modified labeled probes. An NtcA-DNA complex was detected with theWT and with the N6-modified probes(**Figure II.10**, WT and N6); however, when the N8-modified probe was used, no NtcA-DNA complex was detected (**Figure II.10**, N8). These results indicate that NtcA binds *in vitro* to the N8 site.

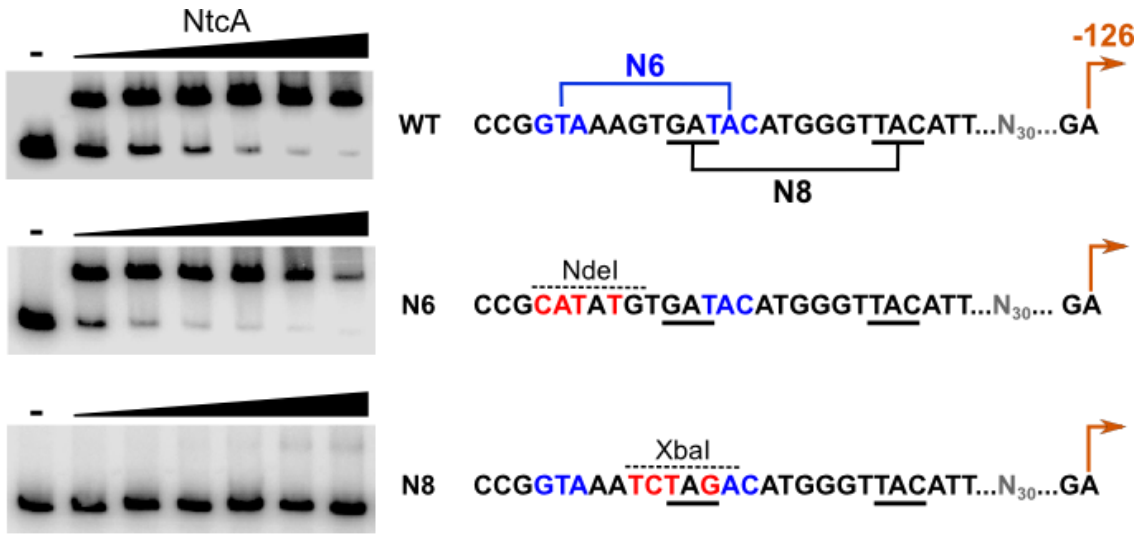

Figure II.10 NtcA binds to the *petH* promoter *in vitro*.
DNA electrophoretic mobility shift assay performed with a 229-bases SpeI-SnaBI fragment, encompassing the distal and the proximal *petH* promoters. The wild-type fragment,WT and fragments where the hypothetical NtcA binding sites (N6 blue and N8 underlined) were modified to the bases shown in red. Mutation of N6 and N8 sites create NdeI and XbaI restriction sites, respectively. Probes were end labeled and incubated in the absence (-) and the presence of different amount of purified NtcA (0.5 to 3 μM).

NtcA regulates *petH* expression

To determine whether the discovered NtcA-binding site operates *in vivo*, the N8-mutation was linked to the omega cassette in a cargo plasmid denoted pNBX and introduced into the *Synechocystis*pet*H* locus by double recombination yielding mutant

NBX (**Figure II.11-A**). Total segregation of the chromosomes was confirmed by PCR and restriction analysis.The presence of the XbaI restriction site confirmed the integration of the modified NtcA-binding site in the segregated chromosome (**Figure II.11-B**). FNR isoforms accumulation upon nitrogen starvation was examined in total-protein extracts from the WT; BX, a strain carrying the omega cassette 115-bases upstream from the distal tsp (described in section II.4.2); and NBX that carried the N8-mutation plus the omega cassette at the same site as BX did. Figure II.11-C shows that, unlike the WT and BX, NBX was unable to accumulate FNR_S.

Since FNR_S translation was shown to depend on the mRNA transcribed from the distal promoter, this result shows that NtcA-binding is required for *petH* transcription from the distal promoter. At the same time, it confirms the requirement of the longer transcript for the synthesis of FNR_S.

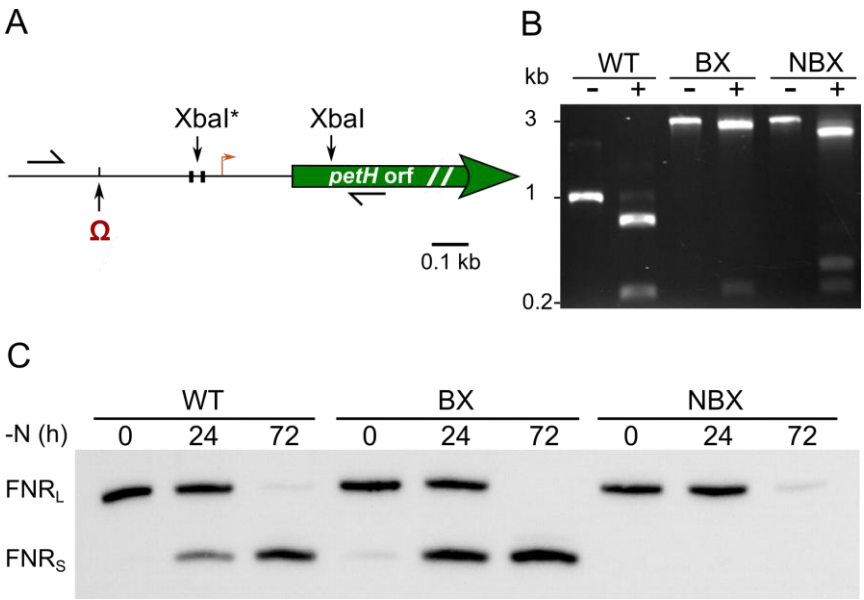

Figure II.11 The NtcA-binding site is required for FNR_S expression.
A. Structure of the mutagenized *petH* gene; a solid line represents the 5'-noncoding region where the N8 mutation, which abolished the NtcA-binding site (two black boxes) and created an XbaI restriction site (XbaI*), is linked to the Ω-cassette. A green arrow represents the *petH* orf; two half arrows indicate the location of PCR primers and an orange arrow indicate the -126 tsp.
B. PCR and restriction analysis of genomic DNA. (–) PCR produced a 1-kb fragment from the WT and 3-kb fragments from BX and NBX, due to the presence of the Ω-cassette. (+) XbaI digestion of the PCR products, the presence of an additional XbaI site, in NBX, results in a supplementary 0.4-kb fragment.
C. FNR immunodetection in cell extracts from the WT, BX and NBX under standard conditions and upon nitrogen starvation for 24 and 72 hours shows that the NtcA-regulated transcript is required for FNR_S translation.

These results also indicate that the transcription organization of *petH* in *Synechocystis*is comparable to that of*Anabaena*;although*petH* translation in *Anabaena*

was not studied. It is likely that the situation in *Anabaena* and *Synechocystis*is very similar.*Anabaena* is a filamentous cyanobacterium capable of nitrogen fixation due to the presence of specialized and differentiated cells called heterocysts. Heterocysts do not perform photosynthesis and drag their need of reductant and organic carbon from the vegetative cells (cells capable of photosynthesis). Heterocysts may therefore be considered as heterotrophic cells.

In *Anabaena*, the longer transcriptwas shown to be expressed in the heterocystswhile the shorterone is expressed in vegetative cells (Valladares et al., 1999); therefore the hypothesis is that FNR_S is present in the heterocysts,while FNR_L probably accumulates in vegetative cells. These findings support the postulate that FNR_S is better adapted to sustain heterotrophic growth while FNR_L is better adapted for photoautotrophic growth.

II.5. Translation regulation retained in *E. coli*

The regulation of FNR_S translation might be due only to the transcript 5'UTR, or alternatively could involve another trans-acting element specifically present in *Synechocystis*. We therefore mimicked the translation regulation in *E. coli*. To do so, *petH* was expressed so as to be transcribed from the *lac* promoter (P*lac*), with either the long or the short 5'UTR, expression in DH5α, resulted in LKm and LKp strains, respectively (**Figure II.12-A**). As shown in **Figure II.12**-B, the shorter 5'UTR produced FNR_L(LKp), while the longer one essentially produced FNR_S(LKm). It was considered that the residual FNR_Lin LKm could be due to the activity of the *Synechocystis* proximal promoters resulting in the transcription of an mRNA with a shorter 5'UTR. This was confirmed by the insertion of the omega cassette 12 bases downstream from the long transcript initiation point in LKm, yielding strain LKo, where the*petH* transcription driven by P_{lac} was abolished. LKo produced FNR_Lonly (**Figure II.12-B**), demonstrating that the presence of FNR_Lin LKm is due to transcription, in *E.coli*, of an mRNA containing a shorter 5'UTR.

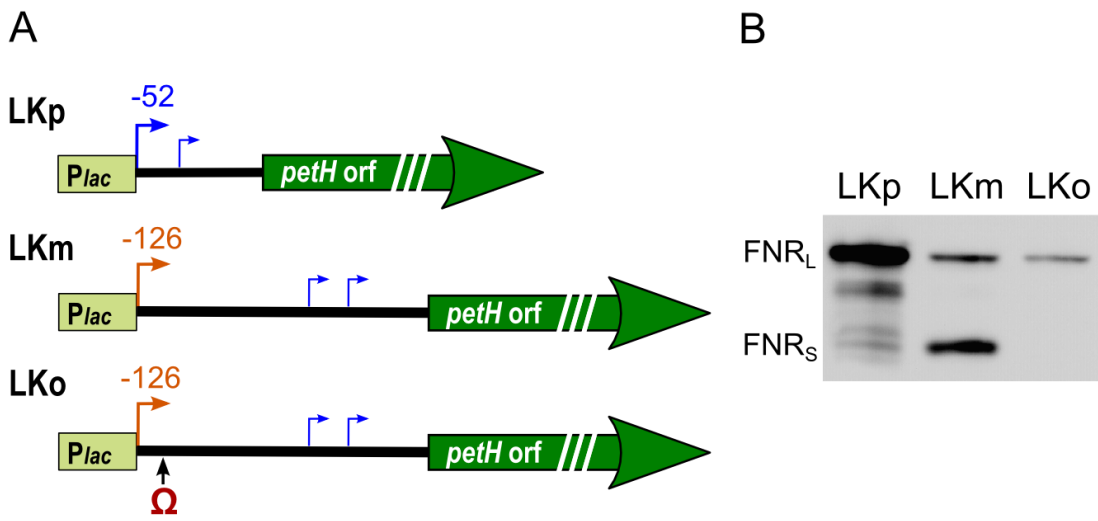

Figure II.12 Similar translation regulation occurs in *E. coli*.
A. Structure of the constructs used for *petH* expression in *E. coli*. The *lac* promoter (P_{lac}) precedes the short 5'UTR (52 bases) in LKp and the long 5'UTR (126 bases) in LKm. LKo derived from LKm in which the Ω cassette was inserted 12 bases downstream from the tsp controlled by P_{lac}.
B. FNR_L and FNR_S accumulation in *E. coli* total extracts determined by immunoblotting. Bent arrows represent the tsp controlled by P_{lac} and smaller bent arrows represent the tsp controlled by the *Synechocystis* constitutive promoters.

This similarity in *petH* translation regulation between *E. coli* and *Synechocystis* suggests that translation regulation is mediated by secondary structures that involve the 5'UTR of the mRNA. It also implies that the translation regulation does not require any trans-acting factor specifically present only in *Synechocystis*.

II.6. Involvement of RNA secondary structures

The results obtained in *E. coli*suggested that secondary structures are involved in translation regulation of FNR isoforms. Therefore mRNA secondary structures were predicted *insilico* and genetically tested by mutagenizing the *petH* 5'-end.

II.6.1. *petH* mRNA 5'-end secondary structure prediction

We looked for possible secondary structures that would explain the translation regulation of FNR isoforms. Secondary structures were predicted using the web-based RNA-folding application "mfold"(Zuker, 2003). It has been shown that the accuracy of a predicted structure is inversely proportional to the length of the sequence and thatthe algorithm, for prediction programs, is significantly more reliable for known base-pairs when the sequencesare broken into smaller fragments (Mathews et al., 1999). For these reasons, the secondary structure of *petH* mRNA was predictedfor a fragment of146-bases instead of the whole transcript. The fragment included the 5'UTR of the long transcript; it started at -126 tsp and ended at +20 from AUG-1. Five possible secondary structures were proposed with a calculated free energy of about -30 kcal.mole^{-1} at 34 °C;fourof these are presented in **Figure II.13**.

All of the predicted structures shared the stem loops I, II and III (**Figure II.13**). The most interesting feature is that all structures had thefirst TIR, and more specifically the SD, base paring with the nucleotides that are specific to the large transcript. Such pairing would block the ribosome binding to AUG-1 and inhibits FNR_L translation.

II.6.2. Deletions within the *petH* 5'UTR encoding sequence

In order to identify the most reliable model of the predicted structures, deletions were constructed within the region encoding the 5'-end of the long transcript. The effect of these deletions was tested in *E. coli* and in *Synechocystis*.

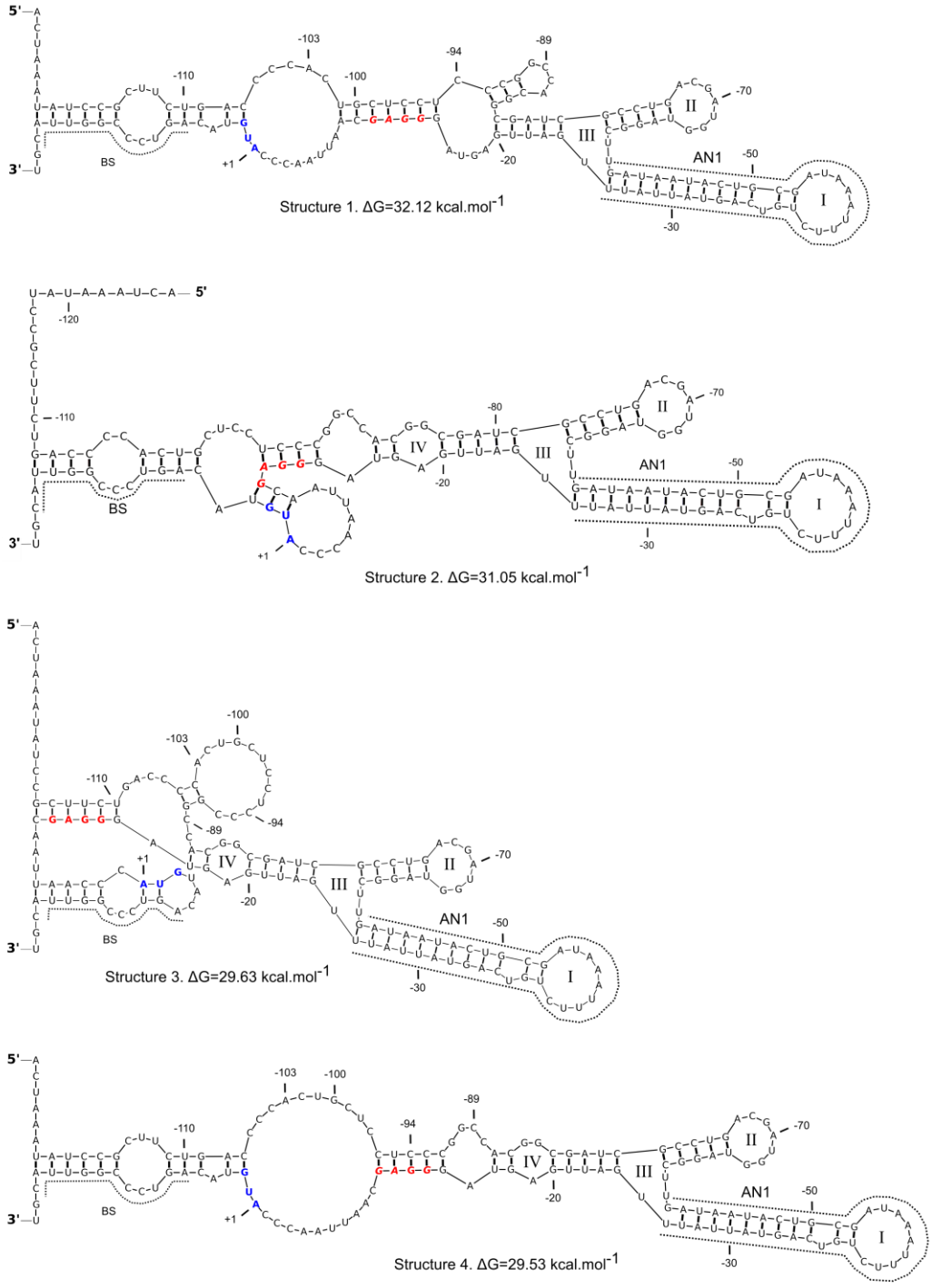

Figure II.13 Secondary structure models for *petH* long 5'UTR.
Four different models predicted by the mRNA folding online program mfold (version2.3; Zucker, 2003). Numbers indicate nucleotide positions relative to the first nucleotide of AUG-1. The ribosome-binding site (SD) is red. The AUG-1 is blue. Dotted lines indicate sequences deleted in AN1 and BS. Latin digits indicate loops that are present in almost all structures.

5'-enddeletions in *E. coli*

The effect of each deletion was first tested in *E. coli*, as outlined in **Figure II.14**.

a. *Deletion of stem loop I*

First, a 34 bases encoding stem-loop I (G-59/U-26), which was present in all the models predicted by mfold, were deleted from pLKm. The plasmid(pLAN1) was expressed in *E. coli* (DH5α) resulting in strain KAN1. Both FNR isoforms accumulated in KAN1 (**Figure II.14-B**). On one hand, the AN1 deletion didn't seem to affect FNR_S accumulation from the larger transcript, while on the other hand, less FNR_Laccumulated from AN1 compared to LKm.

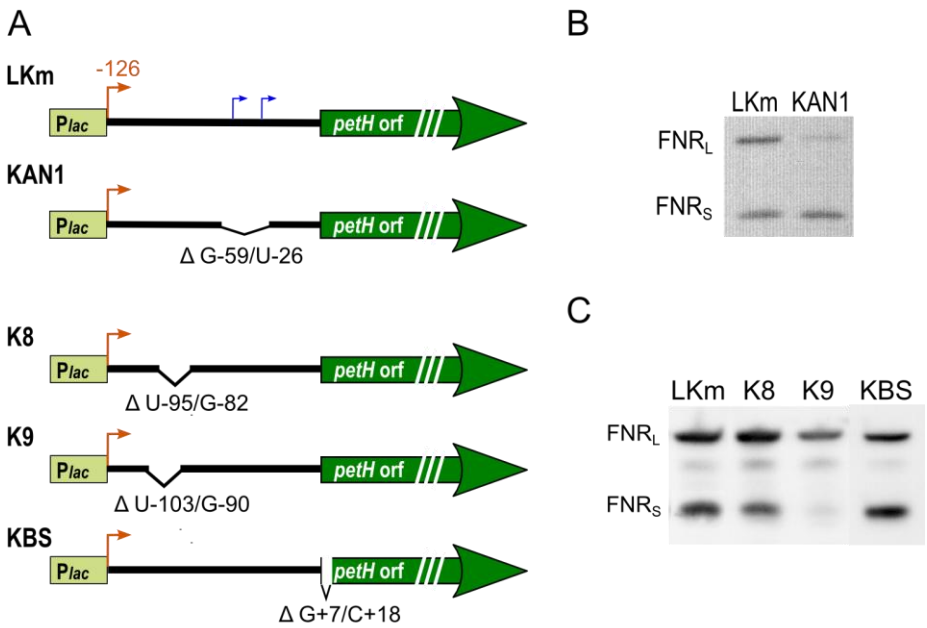

Figure II.14 Effect of deletions constructed to identify a probable secondary structure, adopted by the longer transcript, on FNR accumulation in *E. coli*.
A. Structure of the constructs used for the *petH* expression in *E. coli*. The *lac* promoter (P_{lac}) precedes the long 5'UTR (126 bases) in LKm and the four deletion mutants KAN1, K8, K9 and KBS. Orange bent arrows represent the tsp controlled by P_{lac} and blue bent arrows represent the tsps controlled by the *Synechocystis* constitutive promoters.
B. FNR accumulation in *E. coli* for LKm and AN1 total extracts determined by immunoblotting.
C. FNR accumulation in *E. coli* for LKm, K8, K9 and KBS total extracts determined by immunoblotting.

Since the *Synechocystis*shorter transcripts' promoters were absent in KAN1, a small FNR_Lamountis probably produced from the large transcript in this mutant (remember that these promoters were responsible for FNR_Saccumulation in LKm, section II.5).

FNR_L accumulation could be explained by thedestabilization of the large transcript secondary structures,due to the absence of stem loop I, allowing translation initiation from AUG-1 and FNR_L synthesis.

b. ***Deletions in the region base paring to the TIR***

Subsequently, three deletions were made in the region encoding the first part of the long 5'UTR; K8 (U-95/G-82) and K9 (A-103/G-90) that carried overlapping 14-bases deletions and KBS (A+7/C+18) that carried an in-frame deletion eliminating four codons (Ser99-Tyr103) from the FNR_Lorf (**Figure II.14-A**). FNR isoforms were immunodetected in *E. coli* cell extracts as shown in Figure II.14-C. The mutants accumulated different amounts of FNR_S. Accordingly, the role of the deleted regions in FNR_S accumulation was classified as essential in K9, where FNR_S was not detected, and nonessential in the K8 and KBS, where the amount of FNR_Sdid not seem to begreatly affected (**Figure II.14-C**).

5’-end deletions in *Synechocystis*

In order to confirm the results obtained in *E. coli*, the same deletions were expressed in*Synechocystis*. FNR isoforms were immunodetected in each mutant under standard and nitrogen starvation conditions.

a. ***Deletion of the stem loop I***

The fragment encoding stem loop I contains the constitutive transcripts promoters;its deletion is expected to be lethal for *Synechocystis*, under standard conditions. Therefore, the deleted allele denoted AN1 (**Figure II.15-A**) was expressed ectopically in MI6 (yielding MAN1) and in FS1 (yielding FAN1). FNR isoforms were immunodetected in total extracts from mutants grown under standard conditions or nitrogen-starved for 24 h to trigger the long transcript synthesis (**Figure II.15-C**). As the native allele in MAN1 is unable to produce FNR_S, accumulation of FNR_S results exclusively from the ectopic allele, while that of $FNR_L$is indistinguishably due to the expression of both alleles. Accordingly, Figure II.15-B(MAN1) shows that the deletion carried by AN1 did not abolish *petH* ability to produce FNR_S. Conversely, accumulation of FNR_Lin FAN1 would result only from the ectopic AN1 allele. Figure II.15-C(FAN1) shows that FAN1 failed to accumulate FNR_Lunder standard conditions, which confirms that the constitutive short transcripts, required for

FNR_Lexpression, were missing in AN1. However, traces of $FNR_L$are detected in FAN1 upon nitrogen starvation. This suggests that the "long"AN1 transcript allows some FNR_Ltranslation in *Synechocystis*. These results are consistent with those obtained in *E. coli*KAN1, where small amounts of FNR_Lwere detected from the large transcript.

The similar behavior observed here between *Synechocystis* and *E. coli*,validates the fact that *petH* regulation is retained in *E. coli*.

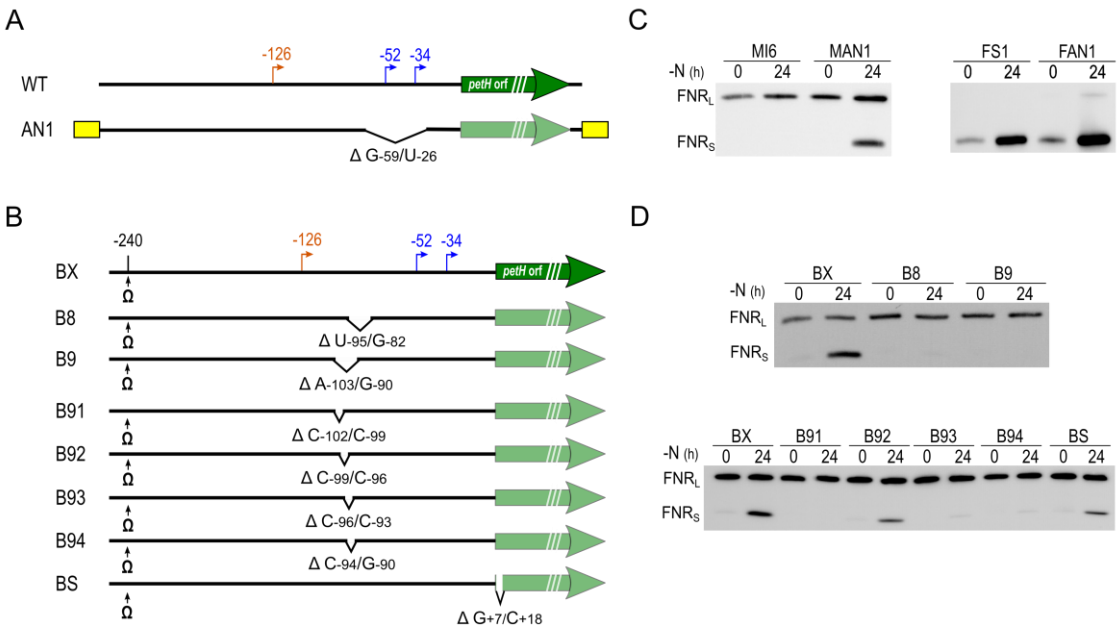

Figure II.15 Effect of deletions constructed to identify a probable secondary structure, adopted by the longer transcript, on FNR accumulation in *Synechocystis*.
A. Structure of the wild-type *petH* and that of the AN1 ectopic allele placed in the *psbA2* locus of MI6 and FS1. The yellow boxes represent sequences belonging to the *psbA2* locus.
B. Structure of the native *petH* in BX, the control strain carrying a wild-type gene and in seven mutants where deletions were introduced together with the omega cassette (Ω). Solid lines represent the *petH* 5'-noncoding region; green arrows represent *petH* orf and bent arrows represent *petH* tsps. The positions of the deleted fragments are shown with nucleotide numbers relative to the first nucleotide of ATG-1.
C. Impact of nitrogen starvation (0 and 24h) on FNR accumulation analyzed by western blot on total protein extracts. MI6, unable to produce FNR_S; MAN1, ectopically expressing the AN1 allele in MI6; FS1, unable to produce FNR_L; FAN1, ectopically expressing AN1 in FS1.
D. Impact of nitrogen starvation (0 and 24h) on FNR accumulation, analyzed by western blot, in total protein extracts of BX and mutants bearing the deletions represented in B.

b. *Deletions in the region base paring to the TIR*

Next, the K8, K9 and KBS deletions wereexpressedin *Synechocystis* resulting in mutants B8, B9 and BS, respectively. Since the above deletions were not expected to affect the constitutive transcripts (the constitutive promoter is present),they were introduced in the native *petH* yielding mutants that were viable and grew normally

under standard conditions. FNR was immunodetected in total cell extracts from each of the constructed mutants and, as a control, from BX that carried the omega cassette, upstream from *petH*, at the same site as the mutants did (**Figure II.15-B**). When compared to BX,the mutants accumulated different FNR_S amounts upon nitrogen starvation.

Surprisingly, the deletions affected differently FNR_S accumulation in B8 and BS compared to K8 and KBS in *E. coli*. B8 abolished FNR_S accumulation while BS affected partially FNR_S production. In *E. coli*, FNR_S accumulated in K8 and in KBS. Accordingly, the effect of the deleted regions on FNR_S accumulation was classified differently in *Synechocystis*; essential in B9and in B8 where FNR_S was not detected; and significant in BS, which accumulate FNR_S but in lesser amounts than BX (**Figure II.15-D;** upper for B8 and B9 and last line of the lower blot for BS).

These results are in disagreement with the previous hypothesis suggesting that translation regulation proceeds similarly in *Synechocystis* and in *E. coli*. It rather shows that the translation regulation of the FNR isoforms is achieved, at least in some deletion mutants, in a different way. This difference was mainly observed in B8 where FNR_S accumulation was abolished in *Synechocystis* and retained in *E. coli*.

These results suggest that the sequences in the B8 and B9 deletions might be involved in important secondary structures that are required for FNR_S translation initiation in *Synechocystis*.

The difference between *Synechocystis* and *E. coli*behavior, towards the B8 deletion,might be due to differences in the translation machinery between these two organisms. Alternatively, the deletion in*E. coli*K8could be causing a different folding of *petH* mRNA than in *Synechocystis*B8. The K8 secondary structure allows FNR_S translation initiation while the ones in B8 do not. As a consequencetranslation initiation from AUG-113 occurs in K8 only.

These results preclude the use of*E. coli* as an alternative for studying *petH* translation regulation.

II.6.3. Additional characterization of the mRNA fold

Smaller deletions were constructed in *Synechocystis*,to allow a better characterization of the secondary structure. Three of the four deletions affected the

overlapping region of B8 and B9.The deletions were B91, B92 and B93 carrying overlapping deletions of 4 bases each (C-102/C-99, C-99/C-96 and C-96/C-93, respectively) that were within the 14 bases deletion of B9 and B94 lacking 5 bases (C-92/C-88) that overlapped completely B9 and B8 (**Figure II.15-B**)

These deletions were introduced in the native *petH* gene yielding mutants that were viable and grew normally under standard conditions. FNR was immunodetected in total cell extracts from each of the constructed mutants and from BX, acting as a control. FNR_S accumulation was different in each deletion. It was totally absent in B91, slightly affected in B92 and considerably disturbed in B93 and B94 (**Figure II.15-D**)

Among the models predicted by mfold, only one secondary structure (**Figure II.13**)was validated by all the deletions results. This secondary structure is represented infigure II.16. The model contains three stem-loops (I, II and III) that were found in all the predicted models, one (IV) that was found in only four of the predicted models and one (VI) that was specific to the model presented infigure II.16. The 5'-end contains a single-stranded region comprising nucleotides A-126 through U-109, followed by paired nucleotides (G-108 to C-105/G+13toU+16), (A-102 to G-89/C+6to U+9).This pairing suggests that interaction between the long 5'UTR and regions within the *petH*orfoccurs; this is confirmed by the fact that deletions B91 and BS affected FNR_S accumulation (**Figure II.15-D**).

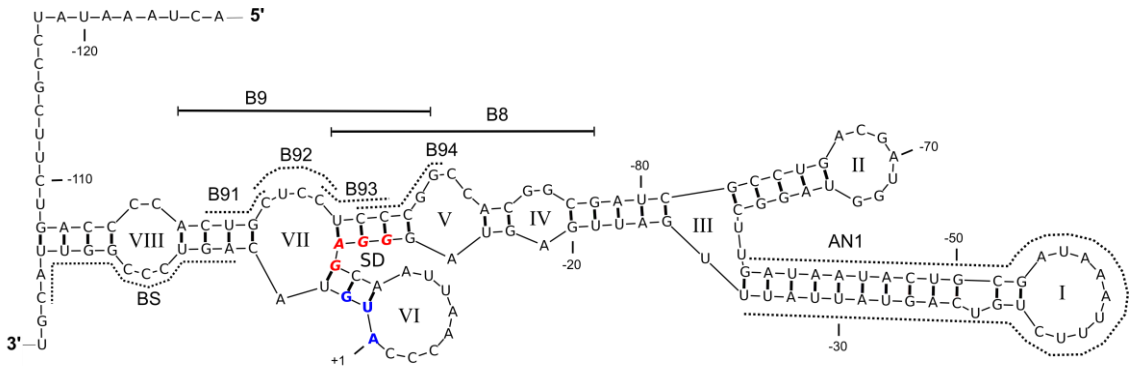

Figure II.16A secondary-structure model for the *petH* long 5'-end that fits mutagenesis results.
This model, predicted by the online RNA folding program mfold (version 2.3) (Zuker, 2003), was chosen among several proposed folds (represented in FigureII.13). This structure contained base pairings that were disrupted by the deletions analyzed in Figure II.15. Solid lines indicate the deleted sequences in B8 and B9 and dotted lines indicate those deleted in B91-94, BS and AN1. The ribosome-binding site (SD) is red and AUG-1 is blue. Numbers indicate nucleotide positions relative to the first nucleotide of AUG-1. Latin digits indicate loops numbers.

Together with stem loop VI, base pairing in (U-95 to C-92/G-15to A-12) makes the ribosome-binding site and AUG-1 unavailable for translation initiation; mutant B93 and to a lesser extend B94 confirm the possibility of such base pairings. The significant effect observed in B92 could be due to steric constraint imposed by the absence of loop VII.

Additional point mutations in stem loop II (GG-68/CC-69 and C-72/G-72) did not affect FNR_Lor FNR_S accumulation confirming that these nucleotides are not involved in base pairing(data not shown).

Based on these results, we hypothesized that RNA structures created in the longer 5'UTR are involved in FNR_S translation initiation. Such structures would inhibit FNR_Ltranslation by preventing its initiation as proposed in **Figure II.17**. However, it cannotbe excluded that such structures could be involved in eliminating the FNR_LTIR through a targeted mRNA-degradation process (Obana et al., 2010). Such a mechanism, if occurring, will leave the *petH* mRNA with only the second TIRthat initiates FNR_S translation.

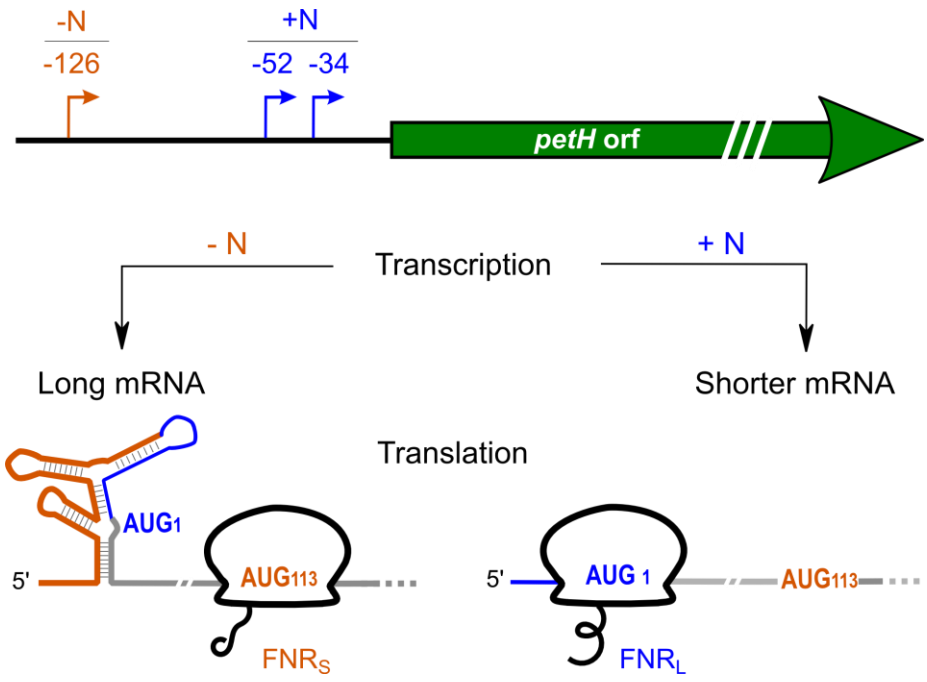

Figure II.17 A model for the 5'UTR-mediated regulation of FNR translation.
Transcripts starting at -126 contain a leader sequence that folds up into a stable secondary structure impeding ribosome binding at AUG-1, either by preventing ribosome binding or by creating an RNA-processing site, which results in translation initiation at AUG-113 and FNR_S translation. Transcripts starting at -52 or -34 allow ribosome binding at AUG-1 and FNR_L translation.

II.7. 5'UTR affects ribosome binding *in vitro*

The results presented in this work strongly suggest that mRNA secondary structures are involved in FNR_S translation initiation. It isproposed that the additional 5'-end fragment in the FNR_S mRNA inhibits FNR_Ltranslation initiation and directs the ribosome toward the FNR_S TIR (**Figure II.17-A**). We therefore tested translation initiation of the long and the short mRNA *in vitro*by toeprinting in collaboration with S. Marzi and P. Romby at the "Institue de Biologie Moléculaire (IBMC)", Strasbourg, France.

The experiment consists of using *in vitro* transcribed mRNA to which the $tRNA^{fMet}$and the 30S ribosomal subunit are added. The formation of a ternary initiation complex (mRNA-tRNA-30S) is observed by primer-extension inhibition (Hartz et al., 1988). Since the translation regulation of the native *petH*in *E. coli* was similar to the one observed in *Synechocystis*(*cf.* section II.5),we used the 30S-ribosomal subunit of *E. coli*(Fechter et al., 2009).

For each mRNA, three different amounts of the 30S-ribosomalsubunit were tested. A control, without the 30S subunit, was included to observe the primer-extensioninhibitions that are inherent to the reverse transcriptase and to the RNA template properties. Aprimer(toe-*petH*) located 36 and 372 nucleotides downstream from AUG-113 and AUG-1, respectively, was used for the reverse transcription. In order to localize the position of primer extension inhibition on each mRNA, a sequencing ladder was migrated beside the toeprinting samples(**Figure II.18-A**).

When the 30S subunit was added to the long mRNA, an initiation complex was spotted at nucleotide +16 from AUG-113. Such a signal position is considered as an optimal toeprinting signal (Fechter et al., 2009). Regardless of the presence of the 30S subunit, strong reverse-transcriptase inhibitions were observed at several positions around AUG-1 and 32 nucleotides upstream from AUG-113 (**Figure II.18-A**).

When the 30S subunit was added to the short mRNA,an initiation complex was observed only around AUG-1 and no initiation complex was observed around

AUG-113. No inhibition was detected in the absence of the 30S subunit, which suggest that the short mRNA contains no strong secondary structures.

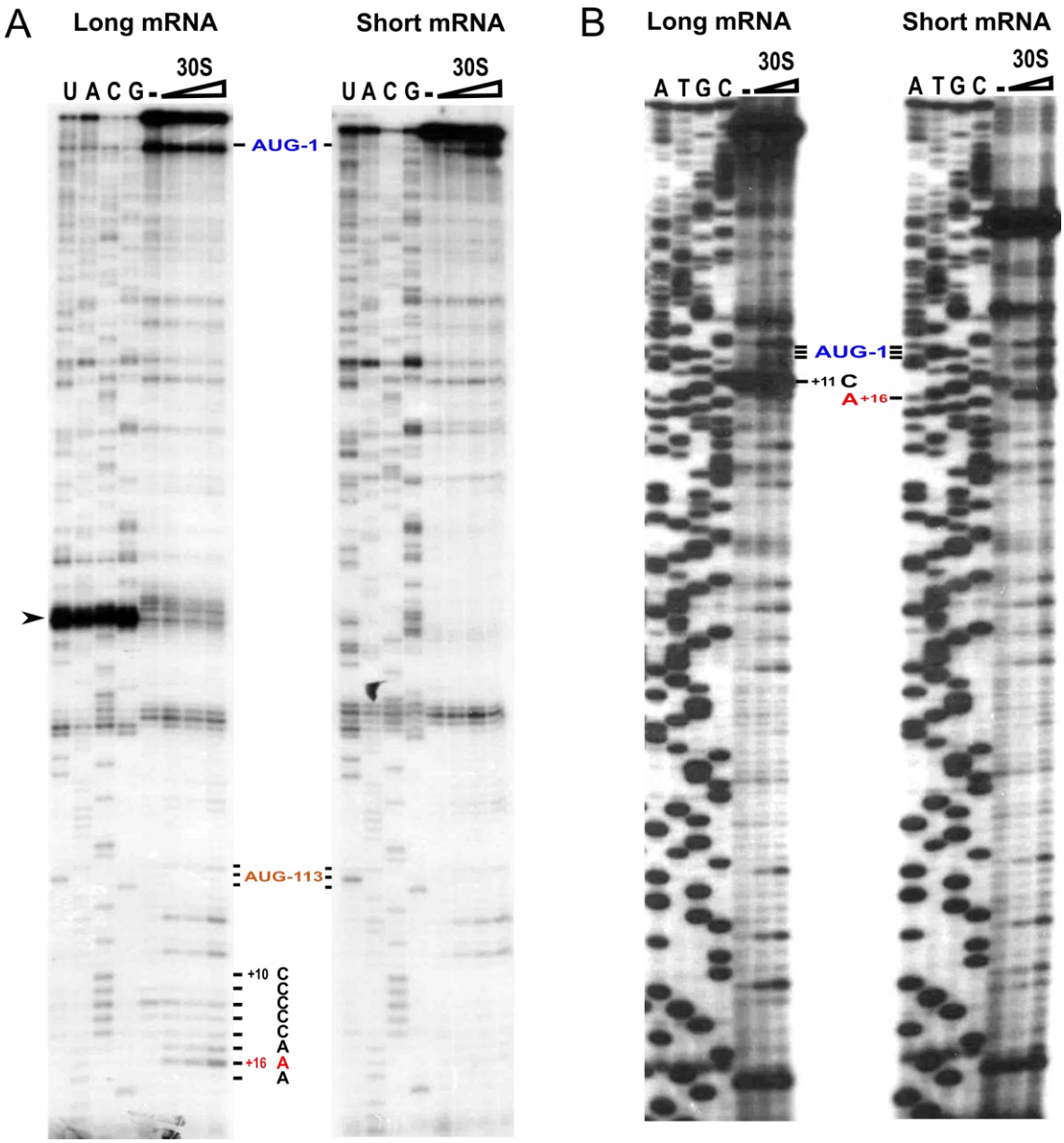

Figure II.18 Toeprinting assays performed with "long" or "short" *petH* transcripts.
A.Toeprinting using primer "toe-*petH"*. In the long mRNA a signal for an active ribosomal initiation complex is observed at position +16 from AUG-113, no such signal was observed, at the same position, in the short mRNA. A black arrow indicates the position of a strong reverse-transcriptase inhibition in the long mRNA. In the short mRNA (right) a signal for an active, mRNA-tRNA-30S, initiation complex is observed around AUG-1. A signal at the same position is detected in the long mRNA (left); this corresponds to a secondary structure since it was observed in the absence of the initiation complex.
B. Toeprint assay using primer FSH. In the short mRNA (right) a signal for an active mRNA-tRNA-30S initiation complex is observed at position +16 from AUG-1. The structure around AUG-1, in the long mRNA (left), is located at +11 from AUG-1.
Triangles indicate increasing concentrations of 30S subunit (4x, 8x and 16x; x is the equivalent of 1 pmole of mRNA); (-) are the controls (no 30S); AUG-1 and AUG-113 correspond to the initiator codons that were shown to function *in vivo* for the short and the long mRNA, respectively; position of the active initiation complex (+16) was determined by counting from the U of the AUG; T, U, A, C and G represent the sequencing ladders. These results are representative experiments of three assays for each toeprinting that gave the same results.

In order to localize the position of the initiation complex observed in the short mRNA,primer extension was carried out using FSH. This primer binds closer to AUG-1 (130 nucleotides downstream from AUG-1).When the initiation complex was formed in the short mRNA, reverse transcriptase inhibition was spotted at position +16 downstream from AUG-1, which again is an optimal toeprint signal(**Figure II.18-B**).

In the long mRNA, the strong reverse-transcriptase inhibition detected close to AUG-1,with toe-*petH*,was detected and localized with FSH at nucleotide +11 downstream from AUG-1.

Strong 30S-independent reverse-transcriptase inhibitionswere specific to the long mRNA, they are most probably due to stable mRNA secondary structures. The structure around AUG-1 might be the one hindering the formation of the initiation complex, while the one observed 32 nucleotides upstream from AUG-113 might promote translation initiation at AUG-113.

In order to check whether the secondary structures observed 32 bases upstream from AUG-113, is involved in FNR_S regulation, a mutant that was constructed in our laboratory to purify FNR_L(Korn et al., 2009) was used. This mutant, called HIFI,carried an 18-bases insertion, 42 nucleotides upstream from ATG-113 (**Figure II.19-A**). Such an insertion should destabilize the putative structure located by reverse transcriptase inhibition.

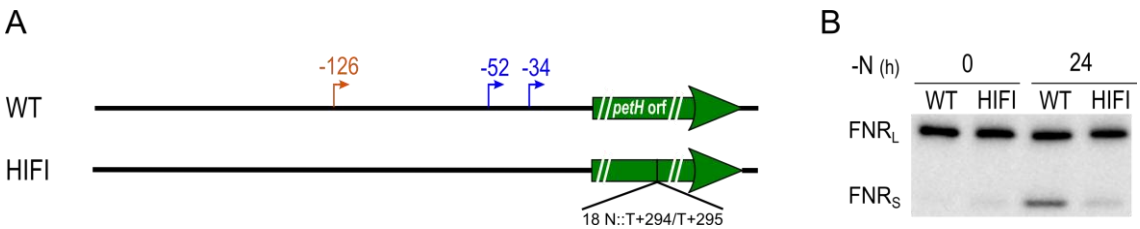

Figure II.19 Effect of an insertion in a probable secondary structure upstream from AUG-113.
A. Structure of the native *petH* in WT and HIFI mutant carrying an insertion, 42 nucleotides upstream from AUG-113. Solid lines represent the *petH* 5'-noncoding region; green arrows represent *petH* orf and bent arrows represent *petH* tsps. (Orange: -126; blue: -52).
B. Impact of nitrogen starvation (0 h and 24h) on FNR accumulation, analyzed by western blot, in total protein extracts from WT and HIFI.

FNR isoforms were immunodetected in total cell extracts from WT and HIFI. Interestingly, the insertionaltered FNR_S accumulation in HIFI while FNR_L seemed to

accumulate as in the WT (**Figure II.19-B**). This result confirms that a structure, close to AUG-113, is involved in FNR_S translation initiation.

The presence of the last mentioned structure seems to depend on the 5'-end of the large transcript since it exists only in the large transcript. This implies that the 5'-end of the long mRNA and the region upstream from AUG-113 might be interacting.

The toeprint findings disfavor the mRNA-processing hypothesis and support our model, suggesting that secondary structuresin the long mRNA inhibit the first TIRand direct the ribosome toward the second TIR. In addition, the insertion in HIFI suggests that FNR_S translation regulation might be more sophisticated since aninteraction between the 5'UTR and a region that is more then 400 bases further (32 nucleotides upstream from ATG-113) is involved.

Such interaction could involve simple base pairing or pseudoknots formed by independent-secondary structures.

RNA structural probing followed by analytical mutations will help us determining the exact structures that are implicated in FNR isoforms translation regulation.

III. Conclusions and perspectives

III.1. Conclusions

During this work, we have characterized a newly discovered phenomenon in which a single gene is translated from two different translation-initiator codons depending on physiological conditions. The gene in question,*petH*, encodes the ferredoxin:NADP oxidoreductase inthe cyanobacterium *Synechocystis* sp. PCC6803 (Thomas et al., 2006).

We showed that, after nitrogen step-down, the chlorophyll content was constant up to 120 hours, while phycobiliprotein levels decreased to approach zero after 72 hours. At the same time, FNR_Llevels decreased while those of FNR_S increased, reaching respectively theirminimal and maximal levels 72 hours after nitrogen step-down.

We discovered that the *petH* mRNA 5'UTR is responsible for FNR_S accumulation. Under standard conditions,two tsp were mapped,52 and 34 bases upstream from the FNR_L initiator codon (ATG-1). Under nitrogen-starvation conditions (where FNR_S accumulates), a tsp was mapped 126 bases upstream from ATG-1. Thus, we concluded that the long mRNA (-126 tsp) is responsible for FNR_S accumulation, while the shorter mRNA (-52 and -34) are responsible for FNR_L accumulation. We also found that the longer transcript requires NtcA, a global-transcriptional regulator. An NtcA-binding site was located 42 nucleotides upstream from the *petH*-126 tsp.

We demonstrated that, in *E. coli*, *petH*translation may also initiate, as in *Synechocystis*, at AUG-1 or AUG-113, depending on the transcript's 5'UTR. Thissimilarity in*petH* translation between the two organisms suggests that translation regulation is mediated by secondary structures present in the mRNA, rather than through *Synechocystis*-specific factors.

Secondary structures, for the long transcript, were modeled and only one out of the five predicted secondary structures was validated by mutagenesis experiments.

Toeprinting assays, performed with the short and long transcripts, located an initiation complex around AUG-1 in the short transcript and around AUG-113 in the long transcript. At the same time, strong-secondary structures were detected, 11-nucleotides downstream from AUG-1 and 30 nucleotides upstream from AUG-113,in the long transcript. An 18-base insertion (42 nucleotides upstream from AUG-113) resulted in loss of FNR_S accumulation from the long transcript. This confirms the involvement of this region in RNA secondary structures that modulate*petH* translation-initiation.

We suggest that long-distance interactions between the long mRNA 5'-end and a region located about 30 nucleotides upstream from AUG-113prevent FNR_L translation initiationand enhance that of FNR_S.

III.2. Perspectives

Determining the mRNA secondary structures will help us understanding *petH* translation regulation. *In vitro* structural-probing experiments of both mRNA were performed and analysis of the results is underway. Mutagenesis will be used to confirm the role of the modeled structures in the regulatory mechanism.

The mRNA secondary structure would also help understanding some subtle variations in translation regulation observed between *E. coli* and *Synechocystis*.

Our results also showed that *petH* transcription in *Synechocystis* was similar to that of *Anabaena* sp. PCC 7102 where two transcripts were found, the shorter being constitutive and located in vegetative cells, while the longer one iscontrolled by NtcA and locatedin heterocysts (specialized cells that differentiate when combined nitrogen is lacking)(Valladares et al., 1999). Similar *petH* translation regulation occurs in *Anabaena*, since we detected two FNR isoforms. This suggests that the same*petH* regulation might be occurring in all cyanobacteria able to produce two FNR isoforms, and that this mechanism might be evolutionarily conserved.

Due to the time limitation, Ihave only studied the genetic regulation of FNR translation. However, the function of each isoform is another important issue. Previous studies proposed that FNR_S is better adapted to sustain heterotrophic growth (NADPH oxidation) while $FNR_L$is better adapted to autotrophic growth (NADP+ reduction). *In vivo*characterization of NADPH reduction in mutants such as FS1 and MI6 are under investigation in our laboratory.

Anabaena can also be used to define a function for each isoform. Wepropose that $FNR_L$is located in vegetative cells (photoautotrophic) while FNR_S accumulates in heterocysts (nitrogen fixing and heterotrophic). Monitoring the accumulation ofFNR isoforms in each of the *Anabaena* cell types willprovide an additional means of testing our hypothesis aboutFNR_L and FNR_S function.

IV. Experimental procedures

IV.1. Strains and growth conditions

IV.1.1. *Synechocystis* sp. PCC 6803

Wild type and mutants *Synechocystis* strains were grown photoautotrophically in an illuminated incubator at 33 °C, in a CO_2 enriched atmosphere (~5%) and under continuous light (50 $\mu E.m^{-2}.s^{-1}$). The growth medium (MM) was based on Allen's medium (Allen, 1968), with some modifications, as described in(Ughy and Ajlani, 2004). For nitrogen starvation, cells were harvested by centrifugation and resuspended in a medium where NaCl replaced $NaNO_3$.

For growth on plates, the medium was supplemented with 1.5% Difco agar and 5 mM sodium thiosulfate.

When appropriate, media were supplemented with 5 $\mu g.mL^{-1}$ streptomycin, 50 $\mu g.mL^{-1}$ spectinomycin, 50 $\mu g.mL^{-1}$ kanamycin or 20 $\mu g.mL^{-1}$ chloramphenicol.

IV.1.2. *Escherichia coli*

Escherichia coli strain, DH5α, was used for molecular cloning, plasmid maintenance and *petH* expression. *E.coli* was grown at 37 °C in LB medium supplemented, when needed, with the required antibiotic (50-100 $\mu g.ml^{-1}$ampicillin, 50 $\mu g.ml^{-1}$ spectinomycinand streptomycin and 20 $\mu g.ml^{-1}$ chloramphenicol). For growth on plates, Difco LB agar was used.

IV.2. Genetic transformation of *Synechocystis* sp.PCC 6803

5 mL of an exponentially growing culture were harvested by centrifugation (4000 g for 5 min at room temperature), the pellet is resuspended in 100 µL of MM and 2 µg of

plasmid DNA are added to the cells. The mixture is shacked for 5 h under continuous light (50 μE.m^{-2}.s^{-1}), and then spread on MM plates. Plates were incubated under dim light and the selecting agent was added underneath the agar 12 h later(Shestakov and Khyen, 1970).

IV.3. DNA isolation from *Synechocystis* sp. PCC 6803

Genomic DNA was isolated as described in(Cai and Wolk, 1990)with some modifications. Cells were harvested, from a 10 mL culture, by centrifugation (4000 g for 2 min at room temperature). The pellet was resuspended in 750 μL of TE buffer (10 mM Tris-HCl pH 8; 0.1 mM EDTA pH 8.4) containing 2% (w/v) SDS. 750 μl of phenol were added and the mixture was vortexed during 5 min. The phenol was separated from the aqueous phases by centrifugation (21000 g for 5 min at room temperature). The aqueous phase was transferred to a new ependorf tube, and the DNA was precipitated by the addition of 0.1 volume of 3 M sodium acetate and 0.7 volume of isopropanol, and by centrifugation (21000 g for 30 min at 4 °C). The pellet was washed with 1 ml of 70% ethanol, dried and then resuspended in 20 to 50 μL of water.

IV.4. Cloning, mutagenesis and plasmid constructions

IV.4.1. Construction of the cargo plasmids

A 1281-bases fragment (from *petH* ATG-1 to 40 bases downstream from the stop codon) was amplified from genomic DNA using primers HLN and HRB (primers used in this study are listed in **Table IV.2**). This fragment was digested with NdeI and BamHI and cloned between the same sites in pPSBA2 (Lagarde et al., 2000) creating pLB. A 2074-bases BamHI fragment containing the *cat* gene (C.C1, (Elhai and Wolk, 1988)) was inserted in the unique BamHI site of pLB yielding pLC.

In pLC5', a 190 bases NcoI-SnaBI fragment of pLC, containing the *psbA2* promoter, was replaced by a 724 bases NcoI-SnaBI fragment containing *petH* 5'-region (from 706 bases upstream to 18 bases downstream from the first *petH* start codon).

Different restriction fragments were deleted from the 5'-noncoding region of pLC5' by a combination of restriction-endonuclease digestion. Each digest was treated with the Klenow fragment of DNA polymerase and self-ligated yielding plasmids pBB, pHH, pNG, pNP and pNB (Table IV.3).

IV.4.2. Insertions in the petH 5'-noncoding region

A 1323-bases fragment containing 716 bases upstream and 607 bases downstream from ATG-1 was amplified using primers, NBE and HSR. The PCR product was cloned in the EcoRV site of pBluescript yielding pNX6. A 2.2 kb fragment containing the omega-*aadA* cassette (Prentki and Krisch, 1984), which confers resistance to streptomycin and spectinomycin and bracketed by transcription terminators, was inserted in specific sites within the *SynechocystispetH* 5'-noncoding sequence carried by pNX6. The plasmid was interrupted by the omega cassette using the following restriction sites BseRI, AvrII, HpaI and AsiSI, resulting in plasmids pBX, pVX, pHX and pSX, respectively (Table IV.3). The resulting constructs were introduced into the wild type by genetic transformation. The structure of the recombinant chromosomes was confirmed by PCR and restriction digestion with HindIII.

Plasmids constructed by PCR were sequenced to verify the fidelity of the PCR amplification. Complete segregation of the mutant alleles was confirmed by PCR and in some cases the PCR products were subjected to restriction analysis and sequencing to ascertain the identity of the amplified fragments.

IV.4.3. Point mutation in the long transcript's 5'-end

A mutagenic PCR was performed on pNX6, using primers LPR and LPF to modify the stem loop II, yielding plasmid pLII. A 231-bases SpeI-SnaBI fragment from pLII was used to replace the same SpeI-SnaBI fragment in pBX yielding the cargo plasmid pLPII.

IV.4.4. Deletions in the long transcript's 5'-end

Except for BS and KBS, which were generated by BsrG1-SnaBI restriction digestion, on pBX and pLKm, respectively, followed by Klenow DNA polymerase treatment and self-ligation yielding plasmid pBS and pKBS; pB8, pB9, pB91, pB92, pB93 and pB94, were constructed by PCR, on pBX as a template, using primers, 8F and 8R; 9F and 9R; 91F and 91R; 92F and 92R; 93F and 93R; 94F and 94R, respectively (Table IV.3). pK8 and pK9 were constructed by PCR, on pLKm as a template, using primers 8F and 8R; 9F and 9R, respectively.

For AN1 the mutagenic PCR was performed on pNX6 using primers ANF and ANR yielding plasmid pNAN. A 694-bases NcoI-SnaBI fragments from pNAN was used to replace a 728-bases NcoI-SnaBI fragment in pLC5' yielding the cargo plasmid pAN1. While a 691-bases AsiSI-MfeI fragment from pNAN was used to replace a 725-bases AsiSI-MfeI fragment in pLKm, yielding pKAN1.

IV.4.5. NtcA-binding site mutagenesis

Mutagenic PCR were performed on pNX6 using primers (NCF1 and NCR1) to modify the N6 site and (NCF2 and NCR2) to modify the N8 site, yielding plasmids pCA1 and pCA2, respectively. The 232-bases SpeI-SnaBI fragments from pCA2 were used to replace the same length SpeI-SnaBI fragment in pBX yielding the cargo plasmid pNBX (Table IV.3).

IV.5. Expression of *petH* in *E. coli*

A 1.9 kb HincII-NheI fragment carrying *petH* (145 bases upstream and 500 bases downstream from the orf) was cloned into pBluescript resulting in pHNS were *petH* transcription was in the same direction as that of P_{lac}. To make a precise transcriptional fusion of the *lac* promoter to the +1 of each *petH* transcript, a fragment was deleted (from the *lac* tsp to the *petH* -126 tsp) by PCR using primers RN and FM, the resulting plasmid was denoted pLKm. A fragment from the *lac* operon tsp to the *petH* -52 tsp was deleted the same way using primers RN and FN resulting in plasmid pLKp. pLKo

consists of pLKm in which a 2062-bases XbaI fragment, containing the omega-*aadA* cassette (Prentki and Krisch, 1984), was inserted 12 nucleotides downstream the *lac*/*petH* tsp. *E. coli* DH5α was used to analyze FNR accumulation from the above constructs.

IV.6. Total-cell extracts and western blots

IV.6.1. Cell extracts preparation

For *Synechocystis*, 10 mL of cells at OD_{580nm} = 2 were collected and resuspended in 1 mL of 50 mM Tricine pH 8 containing complete protease inhibitor (Roche), then broken by vortexing 5 to 10 min with glass beads. Unbroken cells and glass beads were removed by centrifugation, at 4 °C, at 5000 g for 2 min. The supernatant was used as total cell extract.

For *E. coli* 1 mL of cells, at OD_{600nm}= 1, were collected and resuspended in 100 µL of loading buffer and heated at 95 °C for 5 min. 5 to 10 µL of the extracts were loaded per well.

IV.6.2. Chlorophyll *a*quantification

10 to 50 µL of the total cell extracts were added to 1 mL 100% methanol. Once in methanol, excess light should be avoided in order to avoid chlorophyll to pheophytin conversion. The solution was vortexed for few seconds to extract chlorophylls, followed by one minute of centrifugation at 21000 g at room temperature to remove insoluble materials. The supernatant was transferred into cuvettes and the absorbance measured at 666 nm. The absorbance was divided by the chlorophyll extinction coefficient in methanol (76 mL mg^{-1} cm^{-1}) to obtain the chlorophyll concentration (mg/mL). 0.02 or 0.04 µg chlorophyll were loaded in 2.9 or 4.8 mm well, respectively

IV.6.3. Gel electrophoresis and immunoblotting

Proteins were separated using denaturing 10% Tris-Tricine PAGE as described in (Schägger and von Jagow, 1987) with some modifications. For immunoblot analysis,

proteins were transferred to PVDF membranes. Blots were blocked with TBS buffer (20 mM Tris-HCl pH 7.6; 136 mM NaCl) supplemented with 0.1% Tween and 5% dry skimmed milk, and incubated with the primary antibody (1:10,000 dilution). After washing with TBS-tween 0.1% buffer, blots were incubated with a 1:15,000 dilution of peroxidase-conjugated anti-rabbit IgG (Promega). The signal was visualized using RapidStep ECL chemiluminescent substrate (Merck). Images were generated using a cooled CCD camera (Chemi Smart 5000, Vilber Lourmat) and analyzed using ImageJ software.

IV.7. Phycobilisomes analysis

PBS from the WT and mutants were purified as described in (Elmorjani et al., 1986; Ajlani et al., 1995)with some modifications. All steps were carried out at room temperature.

IV.7.1. PBS purification

50 mL of cyanobacterial culture at OD_{580} = 2 were harvested by centrifugation at 6500 g for 5 min. Cells were resuspended in 1 mL of 0.8 M potassium phosphate buffer pH 8.0 (KKP) and then centrifuged again at 6500 g for 5 min. The pellet is frozen at -20 °C. Cells were thawed and resuspended in 1 mL KKP containing complete protease inhibitor (Roche). 500 µL of glass beads were added. The mixture was vortexed for 5 min to break the cells. The solution was centrifuged for 2 min, at 1500 g to remove glass beads and unbroken cells. The supernatant was transferred into a 2 mL tube. Glass beads and unbroken cells were washed with 0.5 mL of 0.9 M KKP, than centrifuged again at 1500 g for 2 min, this supernatant was added to the earlier one. Triton X-100 was added to the supernatant to a final concentration of 2% (v/v). After 20 min incubation in the dark and under continuous agitation, debris were removed by centrifugation at 21000 g for 20 min. The supernatant was removed carefully from underneath the floating chlorophyll-containing triton layer. Up to 2 mL of the supernatant samples were loaded onto sucrose step-gradients prepared in a Beckman

ultra-clear^{TM} tubes 14x89 mm, with the following sucrose molarities: 1 M (3 mL); 0.75 M (3 mL); 0.5 M (3 mL); 0.25 M (1 mL).

Gradients were spun for 12 to 16 h in a Beckman SW41 rotor at 37000 rpm and 17 °C. The blue-colored band containing the PBS complex was collected from the 0.75 M zone.

IV.7.2. SDS-PAGE and FNR_L quantification

To analyze the PBS composition, 10 to 12% Tris-Tricine PAGE were used.

30 µL of PBS sample at OD_{620} = 10 was precipitated by adding an equal volume of 20% (v/v) TCA and incubating for 1 min on ice. After 2 min centrifugation at 21000 g and 4 °C, the supernatant was removed and the pellet was resuspended in the loading buffer.

Different amounts of each sample were loaded on a gel (**Figure IV.1**). After sample separation, the gel wasstained (Invitrogen SimplyBlue)and scanned (Epson V750 Pro). The scanned file was analyzed with ImageJ to measure bands intensity (I).The ratio (FNR_L-MLC)/(FNR_L-MI6), denoted I_1, was calculated; it indicates the ratio of FNR_L in MLC compared to that of MI6. The ratio (L_{CM}-MLC)/(L_{CM}-MI6), denoted I_2, was also calculated. $L_{CM}$is a linker that strongly binds to the PBS and which amount is known to be constant.The FNR_Lratio was normalizedto that of the L_{CM} resulting in I_1/I_2(**Table IV.1**).I_1/I_2indicates that there is an average of 2.2 times more FNR_L in MLC compared to MI6.

Table IV.1 FNR_L quantification

Samples	FNR_Lintensity(a.u.)	I_1 (FNR_L-MLC/MI6)	L_{CM} intensity (a.u.)	I_2(L_{CM}-MLC/MI6)	I_1/I_2
MI6 8x	10.86	2	18.82	1.01	1.98
MLC 8x	22.24		19.39		
MI6 4x	5.23	2.2	9.48	1.07	2.05
MLC 4x	11.67		9.99		
MI6 2x	2.31	2.3	5.31	0.96	2.39
MLC 2x	5.45		5.11		
MI6 1x	0.67	3.5	2.01	1.2	2.91
MLC 1x	2.37		2.48		

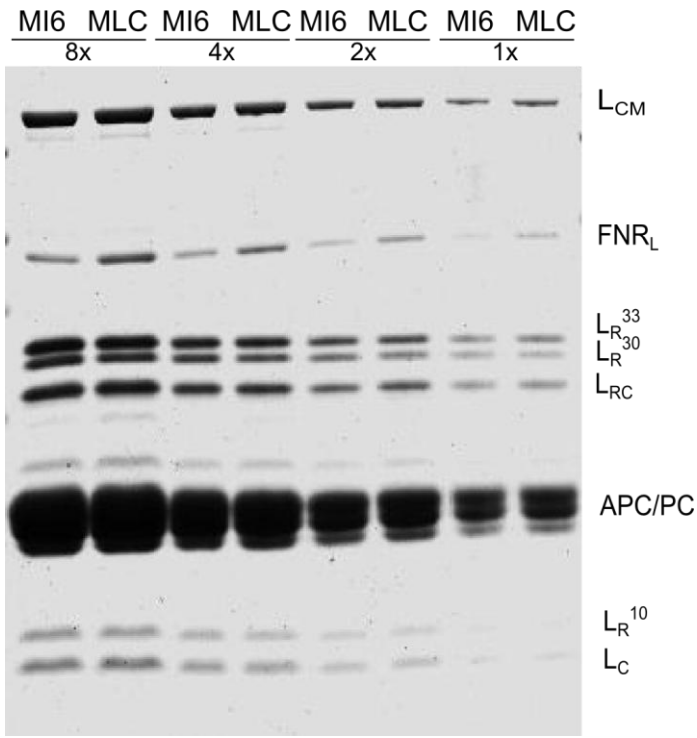

Figure IV.1Phycobilisomes from MLC show higher FNR_L amounts.
Four different amounts of purified PBS were loaded on an SDS-PAGE and stained with Coomassie blue. The identities of the PBS subunits are labeled on the right. L_{CM}, core-membrane linker; L_R, rod Linkers (33, 30 and 10 designate respectively the mass of each L_R); L_{RC}, rod-core linker; L_C, core linker; APC/PC, allophycocyanin/phycocyanin.

IV.8. Transcriptional-start sites mapping

Total RNA, from wild-type *Synechocystis* grown in nitrogen-containing medium or nitrogen-starved for 8 h, was extracted according to (Aiba et al., 1981). 5'-RACE (rapid amplification of cDNA ends) was carried out using Ambion's FirstChoise RLM-RACE kit. Two reactions were set up for each RNA sample. One of them included treatment with tobacco acid pyrophosphatase (TAP); 5 µg of total RNA was treated with TAP for 1 h at 37 °C in a volume of 10 µL. 10 pmole of 5'-RACE RNA adaptor (provided in the kit) was added to the RNA sample, and ligation was performed in the presence of T4-RNA ligase for 1 h at 37 °C. Retrotranscriptions were carried out with 0.5 µg of RNA ligated to the adaptor and gene-specific primer (EGR) using M-MLV reverse transcriptase. 2 µL portions of the reverse transcription reaction were used as templates for subsequent PCRs with a gene-specific primer (RAS) and a primer corresponding to

sequences from the RNA adaptor. PCR products of about 200 bases (present only in the TAP treated samples) were isolated from agarose gels and cloned into the EcoRV site of the pBluescript vector (Stratagene) for sequencing. The first nucleotide following the adaptor sequence was taken as the tsp (**Figure IV.2**).

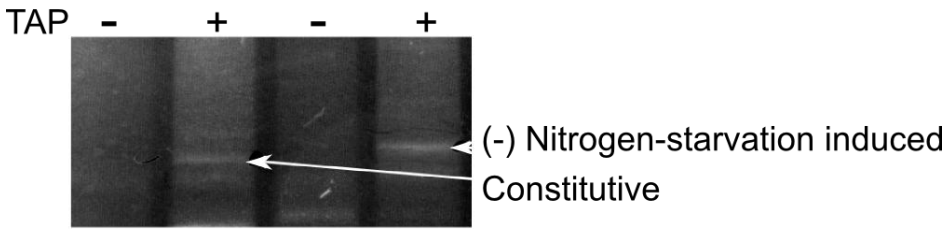

Figure IV.2 RACE mapping of petH 5'-ends at the two growth conditions indicated on the right. The PCR products present in the TAP treated samples were considered to originate from primary transcript. Cloning and sequencing of these products resulted in the tsp described in the results section.

IV.9. *In vitro* probingof the translation initiation complex

IV.9.1. Plasmid preparation

753 bases and 679 bases fragments encoding the long and the short mRNA,were amplified from pLC5', respectively. T7S and HSR primers were used for the long RNA and T7L and HSR for the short RNA. The amplified fragments include the 5'UTR of each mRNA and the first 607 bases of the orf. Fragments were cloned in the EcoRV site of the pBluescript yielding pT7L and pT7S. The plasmids were sequenced to verify the fidelity of the PCR amplification.

IV.9.2. *In vitro*transcription

RNA were transcribed *in vitro* with T7-RNA polymerase. Transcription yielded a product including 3 additional G at the 5'-end. The DNA templates were prepared as follows, pT7S and pT7L were digested by SmaI; the SmaI fragments (704 bases for pT7S and 630 bases for pT7L) were purified from agarose gels, using NucleoSpin Extract II kit (Machrey-Nagel). RNAs were transcribed *in vitro*, using 50 µg of the

template DNA in a final volume of 500 µL and T7 RNA polymerase. The buffer was T7 buffer (40 mM Tris-HCl pH 8, 15 mM $MgCl_2$, 50 mM NaCl), complemented with 5 mM DTE, 100 µg BSA, 4 mM of each NTP, 5 mM GMP, 1 mM spermidine and 20 units RNasin (Promega). The transcription reaction was performed for 2 h and 30 min at 37 °C. the template DNA was eliminated by 75 units of DNase I for 1 h at 37 °C. The reaction was stopped by adding 50 mM EDTA. Mixtures were submitted to phenol/chloroform (v/v) extraction and RNAs were ethanol precipitated. RNA were purified by 6% polyacrylamide-8M urea gel electrophoresis. The band corresponding to the length of the expected RNA was excised and the RNA eluted over night at 4 °C in a buffer containing 0.5 M NH_4Ac, 1 mM EDTA and 20% (v) acidic phenol. After phenol/chloroform extraction, RNAs were ethanol precipitated and suspended in water for direct use.

IV.9.3. Toeprinting assays

The translation initiation complex formation and primer extension inhibition were performed as described in (Moine et al., 1990) with some modifications.

1 pmole of mRNA were annealed to 100,000 counts per minute (cpm) of 5'-end labeled toe-*petH* primer in 5 µL of toe-buffer (+) (20 mM Tris-HCl pH 7.5, 10 mM $MgCl_2$, 60 mM KCl, 1 mM DTT). The mixture was heated at 90 °C for 1 min, cooled down on ice then incubated at room temperature for 5 min. The 30S-ribosomal subunit was activated by incubation for 30 min at 37 °C. 4 µM of activated 30S and toe-buffer (–) (20 mM Tris-HCl pH 7.5, 60 mM KCl, 1 mM DTT) were added to the annealing mixture. The $MgCl_2$ concentration was adjusted in each tube to a finale concentration of 8 mM. The mixture was incubated 15 min at 37 °C. 4 mM of uncharged $tRNA_f^{Met}$ were added and the mixture was incubated for 5 min at 37 °C. Primer extension was performed by adding 20 units of the MMLV reverse transcriptase (New England Biolabs) and 2.5 mM of dNTPs mixture and incubating 30 min at 37 °C. The mixtures were ethanol precipitated, after adding 1 µg of carrier tRNA, and resuspended in formamide loading buffer (95% formamide, 1% XC, 1% BB). 5,000 to 10,000 cpm of each sample were separated on 8% polyacrylamide-8 M urea gel. Signals were visualized using autoradiography. Images were scanned and analyzed using ImageJ software.

IV.9.4. Sequenceladders

For each **RNA** ladder, 4 pmoles of RNA were mixed with 100,000 cpm of 5'-end labeled primers in a finale volume of 4 µL. The mixtures were heated at 90 °C for 1 min then cooled down on ice. Hybridization of the primer to the mRNA was performed, in a finale volume of 5 µL, at room temperature for 10 min after the addition of the AMV reverse transcriptase buffer (Qbiogen). Extension was performed at 37 °C for 30 min after the addition of 2 units of AMV reverse transcriptase, 10 mM dNTP and 1.5 mM of the ddNTP specific to each ladder were added. The template RNA was destroyed, after the extension, using alkaline treatment by adding 20 µL of a buffer containing 50 mM Tris-HCl pH 7.5, 7.5 mM EDTA, 0.5% SDS and 3 µL of 3 M KOH. After 3 min at 90 °C, followed by 1 h at 37 °C, 3 µL of 3 M acetic acid were added to neutralize the KOH. cDNA were ethanol precipitated and the pellets resuspended in formamide loading buffer (95% formamide, 1% XC, 1% BB). 5,000 to 10,000 cpm were loaded per lane.

DNA Sequence ladders were prepared with SequiTherm EXCEL™ II DNA Sequencing Kit (Epicentre). For these preparations, the 704-bases SmaI DNA fragment from pT7S, was used as a template.

Table IV.2Primers used in this work.

Primer	**Sequence** (5' - 3')
8F	ATCGCCTGACGATGGTAG
8R	GGAGCAGTGGGGTCAGAAG
91F	TCCTCCCGGCCACGGCGAT
91R	TGGGGTCAGAAGCGGATATTTAG
92F	TCCCGGCCACGGCGATCG
92R	CAGTGGGGTCAGAAGCGG
93F	CGGCCACGGCGATCGCCTG
93R	GAGCAGTGGGGTCAGAAGC
94F	ACGGCGATCGCCTGACGATG
94R	GGAGGAGCAGTGGGGTCAG
9F	CCACGGCGATCGCCTGACG
9R	GGGGTCAGAAGCGGATATTTAG
ANF	TGATTGAGTAGGGAGCAATTAAC
ANR	AAGCCTACCATCGTCAGGC
EGR	CCACTTCCCTCGGATTGAC
FM	ACTAAATATCCGCTTCTGACCC
FN	CTGCGATAAATTTCTGTCAG
FSH	GTGATGAACGTGCTGCCACTA
HLN	CCCATATGAAACAACCC
HRB	CTCCCCTTCAGGATCCAAAC
HSR	CACCGTGTCTGGTGGAAGC
LPF	GATCGCCTGAGGATCCTAGGCTTG
LPR	CAAGCCTAGGATCCTCAGGCGATC
NBE	CTCTGGGATCCATGGGCGGTG
NCF1	GTTAATCGTCCGCATATGTGATACATGG
NCF2	CCGGTAAATCTAGACATGGGTTAC
NCR1	CCATGTATCACATATGCGGACGATTAAC
NCR2	GTAACCCATGTCTAGATTTACCGG
RAS	GATTACCGGCATCGCTCTG
RHI	CCAGCGGAGAGGTCAAACGTGAGGT
RN	CCACACAACATACGAGCC
T7L	TAATACGACTCACTATAGGGCTGCGATAAATTTCTGTCAG
T7S	TAATACGACTCACTATAGGGACTAAATATCCGCTTCTGACC
Toe-*petH*	CGATAAATATTGACGGG

Table IV.3Plasmids used in this study.

plasmids	Properties	Source
pPSBA2	*Synechocystis* suicide vector, deriving from pSL1180 and containing upstream and downstream from the *psbAII* orf separated by a multiple cloning site (Amp^r)	(Lagarde et al., 2000)
pLC	*petH* orf and the *cat* gene cassette inserted in the multiple cloning site of pS1 (Amp^r, Cm^r)	This study
pLC5'	165 bases containing P_{psbAII} in pLC was replaced by 706 bases of *petH* 5'-noncoding region (Amp^r, Cm^r)	This study
pBB	370-bases BseRI-BseRI fragment deleted from pLC5' (Amp^r, Cm^r)	This study
pHH	344-bases HpaI-HpaI fragment deleted from pLC5' (Amp^r, Cm^r)	This study
pNG	214-bases NcoI-BglII fragment deleted from pLC5' (Amp^r, Cm^r)	This study
pNP	488-bases NcoI-SpeI, fragment deleted from pLC5' (Amp^r, Cm^r)	This study
pNB	608-bases NcoI-BseRI fragment deleted from pLC5' (Amp^r, Cm^r)	This study
pAN1	Δ G59/T26 upstream from ATG-1 deleted from pLC5' (Amp^r, Cm^r)	This study
pDW9	Origin of the Ω fragment containing *aadA* plus strong translation-transcription terminators on both sides (Amp^r, Sm^r/Sp^r)	(Golden and Wiest, 1988)
pNX6	1323-bases fragment of *petH* amplified with NBE and HSR cloned in the EcoRV site of pBluescript (Amp^r)	This study
pNXA	Derivative of pNX6 with an AvrII restriction site created 197 bases upstream from *petH* ATG-1 (Amp^r)	This study
pBX	pNX6 with Ω inserted in the BssHII site (Amp^r, Sp^r, Sm^r)	This study
pB8	pBX –Δ T-95/G-92 upstream from ATG-1 (Amp^r)	This study
pB9	pBX –Δ A-103/G-90 upstream from ATG-1 (Amp^r)	This study
pB91	pBX –Δ C-102/C-99 upstream from ATG-1 (Amp^r)	This study
pB92	pBX –Δ C-99/C-96 upstream from ATG-1 (Amp^r)	This study
pB93	pBX –Δ C-96/C-93 upstream from ATG-1 (Amp^r)	This study
pB94	pBX –Δ C-92/C-88 upstream from ATG-1 (Amp^r)	This study
pBS	pBX –Δ A+7/C+18downstream from ATG-1 (Amp^r)	This study
pVX	pNXA with Ω inserted at AvrII site (Amp^r, Sp^r, Sm^r)	This study
pHX	pNX6 with Ω inserted at HpaI site (Amp^r, Sp^r, Sm^r)	This study
pSX	pNX6 with Ω inserted at AsiSI site (Amp^r, Sp^r, Sm^r)	This study
pHNS	1905-bases HincII-NheI fragment containing *petH* cloned in pBt (Amp^r)	This study
pLKp	Deletion, from pHNS, of a 212-bases fragment from the *lacZ* tsp to the –52 tsp of *petH* (Amp^r)	This study
pLKm	Deletion, from pHNS, of a 138- bases fragment from the *lacZ* tsp to the –52 tsp of *petH* (Amp^r)	This study
pLKo	Ω cassette inserted 12 bases downstream the +1 of *lac* in pLKm (Amp^r, Sp^r, Sm^r)	This study
pLPII	pBX with GG-68/-69CC and C-72/G-72 upstream form *petH* ATG-1	This study
pCA1	pNX6 – GTAAA-181/CATAT-177 upstream form ATG1	This study
pCA2	pNX6 – GATAC-174/TAGAC-170 upstream form ATG1	This study
pNBX	pBX with GATAC174/TAGAC170 upstream form *petH*	This study

	ATG1	
pT7L	679-bases fragment of *petH* amplified with T7L and HSR cloned in the EcoRV site of pBluescript (Amp^r)	This study
pT7S	753-bases fragment of *petH* amplified with T7L and HSR cloned in the EcoRV site of pBluescript (Amp^r)	This study
pLKAN1	Δ G59/T26 upstream from ATG-1 deleted from pLKm	This study
pLK8	pLKm –Δ T95/G92 upstream from ATG-1 (Amp^r)	This study
pLK9	pLKm –Δ A103/G90 upstream from ATG-1 (Amp^r)	This study
pKBS	pLKm –Δ A7/C18 downstream from ATG-1 (Amp^r)	This study

Table IV.4Bacterial strains used in this study.

Strains	Properties	Source
Synechocystis		
WT	Wild-type strain of *Synechocystis* sp. strain PCC 6803	PCC
MI6	Missense mutation in *petH* where ATG-113 was changed to ATC (Sp^r, Sm^r)	(Thomas et al., 2006)
FS1	Frame shift mutation creating an early stop codon in *petH* upstream from ATG-113(Sp^r, Sm^r)	(Thomas et al., 2006)
MLC	MI6 –Δ*psbAII*::*petH, cat* (Cm^r)	This study
MLC5'	MLC –165-bases, containing P_{psbAII}, replaced by 706-bases of *petH* 5'-noncoding region (Cm^r)	This study
MBB	MLC5' –Δ G-477/C-105 upstream from ATG-1 in the ectopic *petH*	This study
MHH	MLC5' –Δ A-490/A-145 upstream from ATG-1 in the ectopic *petH*	This study
MNG	MLC5' –Δ G-702/A-379 upstream from ATG-1 in the ectopic *petH*	This study
MNP	MLC5' - Δ G-702/A-215 upstream from ATG-1 in the ectopic *petH*	This study
MNB	MLC5' –Δ G-702/A-108 upstream from ATG-1 in the ectopic *petH*	This study
BX	*petH*::Ω-*aadA* –insertion 240 bases upstream from ATG-1	This study
VX	*petH*::Ω-*aadA* –insertion 195 bases upstream from ATG-1	This study
HX	*petH*::Ω-*aadA* –insertion 145 bases upstream from ATG-1	This study
SX	*petH*::Ω-*aadA* –insertion 79 bases upstream from ATG-1	This study
LPII	BX - GG-68/CC-69 and C-72/G-72 upstream form ATG1 (stem loop II mutation)	This study
NBX	BX - GATAC-174/TAGAC-170 upstream form ATG-1	This study
HIFI	WT – 18 bases::T+294/T+295 downstream from ATG-1	Korn et al., 2010
E. coli		
DH5α	*E. coli* host for cloning and expression	Life technologies
LKp	DH5α containing pLKp	This study
LKm	DH5α containing pLKm	This study
LKo	DH5α containing pLKo	This study
KAN1	DH5α containing pKAN1	This study
K8	DH5α containing pK8	This study
K9	DH5α containing pK9	This study
KBS	DH5α containing pKBS	This study

V. References

Aiba, H., Adhya, S., and de Crombrugghe, B. (1981). Evidence for two functional gal promoters in intact Escherichia coli cells. J. Biol. Chem *256*, 11905–11910.

Ajlani, G., Vernotte, C., DiMagno, L., and Haselkorn, R. (1995). Phycobilisome core mutants of Synechocystis PCC 6803. Biochim. Biophys. Acta *1231*, 189–196.

Ajlani, G., and Vernotte, C. (1998). Construction and characterization of a phycobiliprotein-less mutant of Synechocystis sp. PCC 6803. Plant Mol. Biol *37*, 577–580.

Allen, M., and Smith, A. (1969). Nitrogen Chlorosis in blue-green algae. Archiv Fur Mikrobiologie *69*, 114-&.

Allen, M.M. (1968). Simple conditions for growth of unicellular blue-green algae on plates. J. Phycol. *4*, 1–4.

Ames, T.D., and Breaker, R.R. (2011). Bacterial aptamers that selectively bind glutamine. RNA Biol *8*, 82–89.

Arteni, A.A., Ajlani, G., and Boekema, E.J. (2009). Structural organisation of phycobilisomes from Synechocystis sp. strain PCC6803 and their interaction with the membrane. Biochim. Biophys. Acta *1787*, 272–279.

Asayama, M., Imamura, S., Yoshihara, S., Miyazaki, A., Yoshida, N., Sazuka, T., Kaneko, T., Ohara, O., Tabata, S., Osanai, T., et al. (2004). SigC, the group 2 sigma factor of RNA polymerase, contributes to the late-stage gene expression and nitrogen promoter recognition in the cyanobacterium Synechocystis sp. strain PCC 6803. Biosci. Biotechnol. Biochem. *68*, 477–487.

Asayama, M., and Imamura, S. (2008). Stringent promoter recognition and autoregulation by the group 3 σ-factor SigF in the cyanobacterium Synechocystis sp. strain PCC 6803. Nucleic Acids Research *36*, 5297–5305.

Barber, J., Chapman, D., and Telfer, A. (1987). Characterisation of a PS II reaction centre isolated from the chloroplasts of Pisum sativum. FEBS Letters *220*, 67–73.

Barne, K.A., Bown, J.A., Busby, S.J., and Minchin, S.D. (1997). Region 2.5 of the Escherichia coli RNA polymerase sigma70 subunit is responsible for the recognition of the "extended-10" motif at promoters. Embo J. *16*, 4034–4040.

Battchikova, N., and Aro, E.-M. (2007). Cyanobacterial NDH-1 complexes: multiplicity in function and subunit composition. Physiol Plant *131*, 22–32.

Ben-Shem, A., Frolow, F., and Nelson, N. (2003). Crystal structure of plant photosystem I. Nature *426*, 630–635.

Berg, O.G., and von Hippel, P.H. (1988). Selection of DNA binding sites by regulatory proteins: II. The binding specificity of cyclic AMP receptor protein to recognition sites. Journal of Molecular Biology *200*, 709–723.

Blankenship, R.E. (2002). Molecular Mechanisms of Photosynthesis (John Wiley & Sons).

Bryant, D.A., Guglielmi, G., Marsac, N.T., Castets, A.-M., and Cohen-Bazire, G. (1979). The structure of cyanobacterial phycobilisomes: a model. Archives of Microbiology

123, 113–127.

Cai, Y.P., and Wolk, C.P. (1990). Use of a conditionally lethal gene in Anabaena sp. strain PCC 7120 to select for double recombinants and to entrap insertion sequences. J. Bacteriol *172*, 3138–3145.

Collier, J.L., and Grossman, A. (1992). Chlorosis induced by nutrient deprivation in Synechococcus sp. strain PCC 7942: not all bleaching is the same. J. Bacteriol. *174*, 4718–4726.

Collier, J.L., and Grossman, A. (1994). A small polypeptide triggers complete degradation of light-harvesting phycobiliproteins in nutrient-deprived cyanobacteria. Embo J *13*, 1039–1047.

Cox, P.A., Banack, S.A., Murch, S.J., Rasmussen, U., Tien, G., Bidigare, R.R., Metcalf, J.S., Morrison, L.F., Codd, G.A., and Bergman, B. (2005). Diverse taxa of cyanobacteria produce β-N-methylamino-l-alanine, a neurotoxic amino acid. Proceedings of the National Academy of Sciences of the United States of America *102*, 5074–5078.

deHaseth, P.L., Zupancic, M.L., and Record, M.T., Jr (1998). RNA polymerase-promoter interactions: the comings and goings of RNA polymerase. J. Bacteriol. *180*, 3019–3025.

DeRuyter, Y.S., and Fromme, P. (2008). Molecular Structure of the Photosynthetic Apparatus. In The Cyanobacteria: Molecular Biology, Genomics and Evolution, pp. 217–269.

Desnoyers, G., Morissette, A., Prévost, K., and Massé, E. (2009). Small RNA-induced differential degradation of the polycistronic mRNA iscRSUA. Embo J. *28*, 1551–1561.

Dienst, D., Dühring, U., Mollenkopf, H.-J., Vogel, J., Golecki, J., Hess, W.R., and Wilde, A. (2008). The cyanobacterial homologue of the RNA chaperone Hfq is essential for motility of Synechocystis sp. PCC 6803. Microbiology (Reading, Engl.) *154*, 3134–3143.

Dines, M., Sendersky, E., David, L., Schwarz, R., and Adir, N. (2008). Structural, functional, and mutational analysis of the NblA protein provides insight into possible modes of interaction with the phycobilisome. J. Biol. Chem. *283*, 30330–30340.

Dühring, U., Axmann, I.M., Hess, W.R., and Wilde, A. (2006). An internal antisense RNA regulates expression of the photosynthesis gene isiA. Proc. Natl. Acad. Sci. U.S.A. *103*, 7054–7058.

Elhai, J., and Wolk, C.P. (1988). A versatile class of positive-selection vectors based on the nonviability of palindrome-containing plasmids that allows cloning into long polylinkers. Gene *68*, 119–138.

Elmorjani, K., Thomas, J.-C., and Sebban, P. (1986). Phycobilisomes of wild type and pigment mutants of the cyanobacterium Synechocystis PCC 6803. Arch. Microbiol. *146*, 186–191.

Fargo, D.C., Zhang, M., Gillham, N.W., and Boynton, J.E. (1998). Shine-Dalgarno-like sequences are not required for translation of chloroplast mRNAs in Chlamydomonas reinhardtii chloroplasts or in Escherichia coli. Mol. Gen. Genet. *257*, 271–282.

Fechter, P., Chevalier, C., Yusupova, G., Yusupov, M., Romby, P., and Marzi, S. (2009). Ribosomal initiation complexes probed by toeprinting and effect of trans-acting

translational regulators in bacteria. Methods Mol. Biol. *540*, 247–263.

Fillat, M.F., Flores, E., and Gómez-Moreno, C. (1993). Homology of the N-terminal domain of the petH gene product from Anabaena sp. PCC 7119 to the CpcD phycobilisome linker polypeptide. Plant Mol. Biol. *22*, 725–729.

Frias, J.E., Merida, A., Herrero, A., Martin-Nieto, J., and Flores, E. (1993). General distribution of the nitrogen control gene ntcA in cyanobacteria. J. Bacteriol. *175*, 5710–5713.

Galmozzi, C.V., Saelices, L., Florencio, F.J., and Muro-Pastor, M.I. (2010). Posttranscriptional regulation of glutamine synthetase in the filamentous Cyanobacterium Anabaena sp. PCC 7120: differential expression between vegetative cells and heterocysts. J. Bacteriol. *192*, 4701–4711.

García-Domínguez, M., Reyes, J.C., and Florencio, F.J. (2000). NtcA represses transcription of gifA and gifB, genes that encode inhibitors of glutamine synthetase type I from Synechocystis sp. PCC 6803. Mol. Microbiol. *35*, 1192–1201.

Garnier, F., Dubacq, J.P., and Thomas, J.C. (1994). Evidence for a transient association of new proteins with the Spirulina maxima phycobilisome in relation to light Intensity. Plant Physiol *106*, 747–754.

Georg, J., Voss, B., Scholz, I., Mitschke, J., Wilde, A., and Hess, W.R. (2009). Evidence for a major role of antisense RNAs in cyanobacterial gene regulation. Mol. Syst. Biol. *5*, 305.

Giovannoni, S.J., Turner, S., Olsen, G.J., Barns, S., Lane, D.J., and Pace, N.R. (1988). Evolutionary relationships among cyanobacteria and green chloroplasts. Journal of Bacteriology *170*, 3584–3592.

Giuliodori, A.M., Di Pietro, F., Marzi, S., Masquida, B., Wagner, R., Romby, P., Gualerzi, C.O., and Pon, C.L. (2010). The cspA mRNA is a thermosensor that modulates translation of the cold-shock protein CspA. Mol. Cell *37*, 21–33.

Glazer, A.N. (1989). Light guides. Directional energy transfer in a photosynthetic antenna. J. Biol. Chem. *264*, 1–4.

Golbeck, J.H. (1993). Shared thematic elements in photochemical reaction centers. Proc. Natl. Acad. Sci. U.S.A. *90*, 1642–1646.

Gomez-Lojero, C., Perez-Gomez, B., Shen, G., Schluchter, W.M., and Bryant, D.A. (2003). Interaction of ferredoxin:NADP+ oxidoreductase with phycobilisomes and phycobilisome substructures of the cyanobacterium Synechococcus sp. strain PCC 7002. Biochemistry *42*, 13800–13811.

Gottesman, S., and Storz, G. (2011). Bacterial Small RNA Regulators: Versatile Roles and Rapidly Evolving Variations. Cold Spring Harbor Perspectives in Biology *3*,.

Grigorieva, G., and Shestakov, S. (1982). Transformation in the cyanobacterium Synechocystis sp. 6803. FEMS Microbiology Letters *13*, 367–370.

Grossman, A. (1990). Chromatic adaptation and the events involved in phycobilisome biosynthesis. Plant, Cell & Environment *13*, 651–666.

Grossman, A., Schaefer, M.R., Chiang, G.G., and Collier, J.L. (1993). The phycobilisome, a light-harvesting complex responsive to environmental conditions. Microbiol. Rev. *57*, 725–749.

Gummadova, J.O., Fletcher, G.J., Moolna, A., Hanke, G.T., Hase, T., and Bowsher, C.G. (2007). Expression of multiple forms of ferredoxin NADP+ oxidoreductase in wheat leaves. J. Exp. Bot. *58*, 3971–3985.

Hackenberg, C., Engelhardt, A., Matthijs, H.C.P., Wittink, F., Bauwe, H., Kaplan, A., and Hagemann, M. (2009). Photorespiratory 2-phosphoglycolate metabolism and photoreduction of O2 cooperate in high-light acclimation of Synechocystis sp. strain PCC 6803. Planta *230*, 625–637.

Hankamer, B., Barber, J., and Boekema, E.J. (1997). Structure and membrane organization of photosystem II in green plants. Annual Review of Plant Physiology and Plant Molecular Biology *48*, 641–671.

Hartz, D., McPheeters, D.S., Traut, R., and Gold, L. (1988). Extension inhibition analysis of translation initiation complexes. Meth. Enzymol. *164*, 419–425.

Henkin, T.M. (2008). Riboswitch RNAs: using RNA to sense cellular metabolism. Genes & Development *22*, 3383–3390.

Herrero, A., Muro-Pastor, A.M., and Flores, E. (2001). Nitrogen Control in Cyanobacteria. Journal of Bacteriology *183*, 411–425.

Horie, Y., Ito, Y., Ono, M., Moriwaki, N., Kato, H., Hamakubo, Y., Amano, T., Wachi, M., Shirai, M., and Asayama, M. (2007). Dark-induced mRNA instability involves RNase E/G-type endoribonuclease cleavage at the AU-box and SD sequences in cyanobacteria. Mol. Genet. Genomics *278*, 331–346.

Ikeuchi, M., and Tabata, S. (2001). Synechocystis sp. PCC 6803 - a useful tool in the study of the genetics of cyanobacteria. Photosyn. Res. *70*, 73–83.

Imamura, S., Asayama, M., and Shirai, M. (2004). In vitro transcription analysis by reconstituted cyanobacterial RNA polymerase: roles of group 1 and 2 sigma factors and a core subunit, RpoC2. Genes Cells *9*, 1175–1187.

Imamura, S., Yoshihara, S., Nakano, S., Shiozaki, N., Yamada, A., Tanaka, K., Takahashi, H., Asayama, M., and Shirai, M. (2003). Purification, characterization, and gene expression of all sigma factors of RNA polymerase in a cyanobacterium. J. Mol. Biol *325*, 857–872.

Imamura, S., and Asayama, M. (2009). Sigma Factors for Cyanobacterial Transcription. Gene Regul Syst Bio *3*, 65–87.

Iost, I., and Dreyfus, M. (1995). The stability of Escherichia coli lacZ mRNA depends upon the simultaneity of its synthesis and translation. Embo J. *14*, 3252–3261.

Jiang, F., Wisén, S., Widersten, M., Bergman, B., and Mannervik, B. (2000). Examination of the transcription factor NtcA-binding motif by in vitro selection of DNA sequences from a random library. J. Mol. Biol *301*, 783–793.

Julián, P., Milon, P., Agirrezabala, X., Lasso, G., Gil, D., Rodnina, M.V., and Valle, M. (2011). The Cryo-EM Structure of a Complete 30S Translation Initiation Complex from Escherichia coli. PLoS Biol *9*, e1001095.

Kammerer, W., Deuschle, U., Gentz, R., and Bujard, H. (1986). Functional dissection of Escherichia coli promoters: information in the transcribed region is involved in late steps of the overall process. Embo J. *5*, 2995–3000.

Kaneko, T., Sato, S., Kotani, H., Tanaka, A., Asamizu, E., Nakamura, Y., Miyajima, N.,

Hirosawa, M., Sugiura, M., Sasamoto, S., et al. (1996). Sequence analysis of the genome of the unicellular cyanobacterium Synechocystis sp. strain PCC6803. II. Sequence determination of the entire genome and assignment of potential protein-coding regions. DNA Res. *3*, 109–136.

Karplus, P.A., and Faber, H.R. (2004). Structural Aspects of Plant Ferredoxin : NADP(+) Oxidoreductases. Photosyn. Res. *81*, 303–315.

Karradt, A., Sobanski, J., Mattow, J., Lockau, W., and Baier, K. (2008). NblA, a Key Protein of Phycobilisome Degradation, Interacts with ClpC, a HSP100 Chaperone Partner of a Cyanobacterial Clp Protease. Journal of Biological Chemistry *283*, 32394–32403.

Kehoe, D.M. (2010). Chromatic adaptation and the evolution of light color sensing in cyanobacteria. Proceedings of the National Academy of Sciences *107*, 9029–9030.

Korn, A., Ajlani, G., Lagoutte, B., Gall, A., and Sétif, P. (2009). Ferredoxin:NADP+ oxidoreductase association with phycocyanin modulates its properties. J. Biol. Chem. *284*, 31789–31797.

Kortmann, J., Sczodrok, S., Rinnenthal, J., Schwalbe, H., and Narberhaus, F. (2011). Translation on demand by a simple RNA-based thermosensor. Nucleic Acids Research *39*, 2855–2868.

Kozak, M. (2005). Regulation of translation via mRNA structure in prokaryotes and eukaryotes. Gene *361*, 13–37.

Krauss, N., Hinrichs, W., Witt, I., Fromme, P., Pritzkow, W., Dauter, Z., Betzel, C., Wilson, K.S., Witt, H.T., and Saenger, W. (1993). Three-dimensional structure of system I of photosynthesis at 6 Å resolution. Nature *361*, 326–331.

Kulkarni, R.D., and Golden, S.S. (1997). mRNA stability is regulated by a coding- region element and the unique 5′ untranslated leader sequences of the three Synechococcus psbA transcripts. Molecular Microbiology *24*, 1131–1142.

Kurisu, G., Kusunoki, M., Katoh, E., Yamazaki, T., Teshima, K., Onda, Y., Kimata-Ariga, Y., and Hase, T. (2001). Structure of the electron transfer complex between ferredoxin and ferredoxin-NADP(+) reductase. Nat. Struct. Biol. *8*, 117–121.

Körner, H., Sofia, H.J., and Zumft, W.G. (2003). Phylogeny of the bacterial superfamily of Crp-Fnr transcription regulators: exploiting the metabolic spectrum by controlling alternative gene programs. FEMS Microbiol. Rev. *27*, 559–592.

Lagarde, D., Beuf, L., and Vermaas, W. (2000). Increased production of zeaxanthin and other pigments by application of genetic engineering techniques to Synechocystis sp. strain PCC 6803. Appl. Environ. Microbiol *66*, 64–72.

Lemeille, S., Geiselmann, J., and Latifi, A. (2005). Crosstalk regulation among group 2-sigma factors in Synechocystis PCC6803. BMC Microbiol. *5*, 18.

Liberton, M., Howard Berg, R., Heuser, J., Roth, R., and Pakrasi, H.B. (2006). Ultrastructure of the membrane systems in the unicellular cyanobacterium Synechocystis sp. strain PCC 6803. Protoplasma *227*, 129–138.

Lindahl, L., and Zengel, J.M. (1986). Ribosomal genes in Escherichia coli. Annu. Rev. Genet. *20*, 297–326.

Llácer, J.L., Espinosa, J., Castells, M.A., Contreras, A., Forchhammer, K., and Rubio, V.

(2010). Structural basis for the regulation of NtcA-dependent transcription by proteins PipX and PII. Proceedings of the National Academy of Sciences *107*, 15397–15402.

de Lorimier, R., Bryant, D.A., and Stevens Jr., S.E. (1990). Genetic analysis of a 9 kDa phycocyanin-associated linker polypeptide. Biochimica Et Biophysica Acta (BBA) - Bioenergetics *1019*, 29–41.

Luque, I., Flores, E., and Herrero, A. (1994). Molecular mechanism for the operation of nitrogen control in cyanobacteria. Embo J *13*, 2862–2869.

Luque, I., Zabulon, G., Contreras, A., and Houmard, J. (2001). Convergence of two global transcriptional regulators on nitrogen induction of the stress-acclimation gene nblA in the cyanobacterium Synechococcus sp. PCC 7942. Mol. Microbiol. *41*, 937–947.

Luque, I., and Forchhammer, K. (2008). Nitrogen Assimilation and C/N Balance Sensing. In The Cyanobacteria: Molecular Biology, Genomics and Evolution, pp. 335–382.

Lönneborg, A., Lind, L.K., Kalla, S.R., Gustafsson, P., and Oquist, G. (1985). Acclimation Processes in the Light-Harvesting System of the Cyanobacterium Anacystis nidulans following a Light Shift from White to Red Light. Plant Physiol. *78*, 110–114.

Madigan, M.T., Martinko, J.M., and Parker, J. (1996). Brock Biology of Microorganisms (Pearson US Imports & PHIPEs).

de Marsac, N.T., and Cohen-bazire, G. (1977). Molecular composition of cyanobacterial phycobilisomes. Proceedings of the National Academy of Sciences *74*, 1635–1639.

Massé, E., and Gottesman, S. (2002). A small RNA regulates the expression of genes involved in iron metabolism in Escherichia coli. Proc. Natl. Acad. Sci. U.S.A. *99*, 4620–4625.

Mathews, D.H., Sabina, J., Zuker, M., and Turner, D.H. (1999). Expanded sequence dependence of thermodynamic parameters improves prediction of RNA secondary structure. Journal of Molecular Biology *288*, 911–940.

Mazouni, K., Bulteau, S., Cassier-Chauvat, C., and Chauvat, F. (1998). Promoter element spacing controls basal expression and light inducibility of the cyanobacterial secA gene. Mol Microbiol *30*, 1113–1122.

McEvoy, J.P., and Brudvig, G.W. (2006). Water-splitting chemistry of photosystem II. Chem. Rev. *106*, 4455–4483.

Mehler, A.H. (1951). Studies on reactions of illuminated chloroplasts. II. Stimulation and inhibition of the reaction with molecular oxygen. Arch. Biochem. Biophys. *34*, 339–351.

Mitschke, J., Georg, J., Scholz, I., Sharma, C.M., Dienst, D., Bantscheff, J., Voß, B., Steglich, C., Wilde, A., Vogel, J., et al. (2010). An experimentally anchored map of transcriptional start sites in the model cyanobacterium Synechocystis sp. PCC6803. Proceedings of the National Academy of Sciences.

Mitschke, J., Vioque, A., Haas, F., Hess, W.R., and Muro-Pastor, A.M. (2011). Dynamics of transcriptional start site selection during nitrogen stress-induced cell differentiation in Anabaena sp. PCC7120. Proc. Natl. Acad. Sci. U.S.A. *108*, 20130–

20135.

Modi, S.R., Camacho, D.M., Kohanski, M.A., Walker, G.C., and Collins, J.J. (2011). Functional characterization of bacterial sRNAs using a network biology approach. Proceedings of the National Academy of Sciences.

Mohamed, A., and Jansson, C. (1989). Influence of light on accumulation of photosynthesis-specific transcripts in the cyanobacterium Synechocystis 6803. Plant Mol. Biol *13*, 693–700.

Moine, H., Romby, P., Springer, M., Grunberg-Manago, M., Ebel, J.-P., Ehresmann, B., and Ehresmann, C. (1990). Escherichia coli threonyl-tRNA synthetase and tRNAThr modulate the binding of the ribosome to the translational initiation site of the ThrS mRNA. Journal of Molecular Biology *216*, 299–310.

Morita, M.T., Tanaka, Y., Kodama, T.S., Kyogoku, Y., Yanagi, H., and Yura, T. (1999). Translational induction of heat shock transcription factor σ32: evidence for a built-in RNA thermosensor. Genes Dev *13*, 655–665.

Morsy, F.M., Nakajima, M., Yoshida, T., Fujiwara, T., Sakamoto, T., and Wada, K. (2008). Subcellular localization of ferredoxin-NADP(+) oxidoreductase in phycobilisome retaining oxygenic photosysnthetic organisms. Photosyn. Res. *95*, 73–85.

Nakao, M., Okamoto, S., Kohara, M., Fujishiro, T., Fujisawa, T., Sato, S., Tabata, S., Kaneko, T., and Nakamura, Y. (2010). CyanoBase: the cyanobacteria genome database update 2010. Nucleic Acids Res. *38*, D379–D381.

Obana, N., Shirahama, Y., Abe, K., and Nakamura, K. (2010). Stabilization of Clostridium perfringens collagenase mRNA by VR-RNA-dependent cleavage in 5' leader sequence. Mol. Microbiol *77*, 1416–1428.

Okutani, S., Hanke, G.T., Satomi, Y., Takao, T., Kurisu, G., Suzuki, A., and Hase, T. (2005). Three maize leaf ferredoxin:NADPH oxidoreductases vary in subchloroplast location, expression, and interaction with ferredoxin. Plant Physiol. *139*, 1451–1459.

Passner, J.M., and Steitz, T.A. (1997). The structure of a CAP–DNA complex having two cAMP molecules bound to each monomer. Proc Natl Acad Sci U S A *94*, 2843–2847.

Pfeiffer, V., Papenfort, K., Lucchini, S., Hinton, J.C.D., and Vogel, J. (2009). Coding sequence targeting by MicC RNA reveals bacterial mRNA silencing downstream of translational initiation. Nat. Struct. Mol. Biol. *16*, 840–846.

Pickering, B.M., and Willis, A.E. (2005). The implications of structured 5' untranslated regions on translation and disease. Seminars in Cell & Developmental Biology *16*, 39–47.

Pils, D., and Schmetterer, G. (2001). Characterization of three bioenergetically active respiratory terminal oxidases in the cyanobacterium Synechocystis sp. strain PCC 6803. FEMS Microbiol. Lett. *203*, 217–222.

Prentki, P., and Krisch, H.M. (1984). In vitro insertional mutagenesis with a selectable DNA fragment. Gene *29*, 303–313.

Prévost, K., Salvail, H., Desnoyers, G., Jacques, J., Phaneuf, É., and Massé, E. (2007). The small RNA RyhB activates the translation of shiA mRNA encoding a permease of shikimate, a compound involved in siderophore synthesis. Molecular Microbiology *64*,

1260–1273.

Puerta-Fernández, E., and Vioque, A. (2011). Hfq is required for optimal nitrate assimilation in the Cyanobacterium Anabaena sp. strain PCC 7120. J. Bacteriol. *193*, 3546–3555.

Raven, P.H. (1970). A multiple origin for plastids and mitochondria. Science *169*, 641–646.

Regulski, E.E., and Breaker, R.R. (2008). In-line probing analysis of riboswitches. Methods Mol. Biol. *419*, 53–67.

Reuter, W., Westermann, M., Brass, S., Ernst, A., Böger, P., and Wehrmeyer, W. (1994). Structure, composition, and assembly of paracrystalline phycobiliproteins in Synechocystis sp. strain BO 8402 and of phycobilisomes in the derivative strain BO 9201. J. Bacteriol. *176*, 896–904.

Reuter, W., Wiegand, G., Huber, R., and Than, M.E. (1999). Structural analysis at 2.2 A of orthorhombic crystals presents the asymmetry of the allophycocyanin-linker complex, AP.LC7.8, from phycobilisomes of Mastigocladus laminosus. Proc Natl Acad Sci U S A *96*, 1363–1368.

Richaud, C., Zabulon, G., Joder, A., and Thomas, J.C. (2001). Nitrogen or sulfur starvation differentially affects phycobilisome degradation and expression of the nblA gene in Synechocystis strain PCC 6803. J. Bacteriol. *183*, 2989–2994.

Rippka, R., Deruelles, J., Waterbury, J.B., Herdman, M., and Stanier, R.Y. (1979). Generic Assignments, Strain Histories and Properties of Pure Cultures of Cyanobacteria. Journal of General Microbiology *111*, 1–61.

Rosinski, J., Hainfeld, J.F., Rigbi, M., and Siegelman, H.W. (1981). Phycobilisome Ultrastructure and Chromatic Adaptation in Fremyella diplosiphon. Annals of Botany *47*, 1–12.

Sato, N., Wada, A., and Tanaka, A. (1998). Ribosomal Proteins in the Cyanobacterium Anabaena variabilis Strain M3: Presence of L25 Protein. Plant and Cell Physiology *39*, 1367–1371.

Sazuka, T., and Ohara, O. (1996). Sequence features surrounding the translation initiation sites assigned on the genome sequence of Synechocystis sp. strain PCC6803 by amino-terminal protein sequencing. DNA Res. *3*, 225–232.

Schluchter, W.M., and Bryant, D.A. (1992). Molecular characterization of ferredoxin-NADP+ oxidoreductase in cyanobacteria: cloning and sequence of the petH gene of Synechococcus sp. PCC 7002 and studies on the gene product. Biochemistry *31*, 3092–3102.

Schopf, J.W. (1993). Microfossils of the Early Archean Apex chert: new evidence of the antiquity of life. Science *260*, 640–646.

Schägger, H., and von Jagow, G. (1987). Tricine-sodium dodecyl sulfate-polyacrylamide gel electrophoresis for the separation of proteins in the range from 1 to 100 kDa. Anal. Biochem. *166*, 368–379.

Shestakov, S.V., and Khyen, N.T. (1970). Evidence for genetic transformation in blue-green alga Anacystis nidulans. Mol. Gen. Genet *107*, 372–375.

Shikanai, T. (2007). Cyclic electron transport around photosystem I: genetic approaches.

Annu Rev Plant Biol *58*, 199–217.

Shimada, T., Fujita, N., Yamamoto, K., and Ishihama, A. (2011). Novel Roles of cAMP Receptor Protein (CRP) in Regulation of Transport and Metabolism of Carbon Sources. PLoS One *6*,.

Shinhara, A., Matsui, M., Hiraoka, K., Nomura, W., Hirano, R., Nakahigashi, K., Tomita, M., Mori, H., and Kanai, A. (2011). Deep sequencing reveals as-yet-undiscovered small RNAs in Escherichia coli. BMC Genomics *12*, 428.

Sidler, W.A. (1994). Phycobilisome and phycobiliprotein structures. In The Molecular Biology of Cyanobacteria, D.A. Bryant, ed. (Dordrecht: Kluwer Acad. Pub.), pp. 139–216.

Stanier, R.Y., Kunisawa, R., Mandel, M., and Cohen-Bazire, G. (1971). Purification and properties of unicellular blue-green algae (order Chroococcales). Bacteriol Rev *35*, 171–205.

Stroebel, D., Choquet, Y., Popot, J.-L., and Picot, D. (2003). An atypical haem in the cytochrome b(6)f complex. Nature *426*, 413–418.

Sugiura, M., Hirose, T., and Sugita, M. (1998). Evolution and mechanism of translation in chloroplasts. Annual Review of Genetics *32*, 437–459.

Thomas, J.C., Ughy, B., Lagoutte, B., and Ajlani, G. (2006). A second isoform of the ferredoxin:NADP oxidoreductase generated by an in-frame initiation of translation. Proc Natl Acad Sci U S A *103*, 18368–18373.

van Thor, J.J., Gruters, O.W., Matthijs, H.C., and Hellingwerf, K.J. (1999). Localization and function of ferredoxin:NADP+ reductase bound to the phycobilisomes of Synechocystis. Embo J *18*, 4128–4136.

van Thor, J.J., Hellingwerf, K.J., and Matthijs, H.C. (1998). Characterization and transcriptional regulation of the Synechocystis PCC 6803 petH gene, encoding ferredoxin-NADP+ oxidoreductase: involvement of a novel type of divergent operator. Plant Mol. Biol *36*, 353–363.

Trumpower, B.L. (1990). The protonmotive Q cycle. Energy transduction by coupling of proton translocation to electron transfer by the cytochrome bc1 complex. J. Biol. Chem. *265*, 11409–11412.

Turner, S., Pryer, K.M., Miao, V.P., and Palmer, J.D. (1999). Investigating deep phylogenetic relationships among cyanobacteria and plastids by small subunit rRNA sequence analysis. J. Eukaryot. Microbiol. *46*, 327–338.

Ughy, B., and Ajlani, G. (2004). Phycobilisome rod mutants in Synechocystis sp. strain PCC6803. Microbiology *150*, 4147–4156.

Valladares, A., Muro-Pastor, A.M., Fillat, M.F., Herrero, A., and Flores, E. (1999). Constitutive and nitrogen-regulated promoters of the petH gene encoding ferredoxin:NADP+ reductase in the heterocyst-forming cyanobacterium Anabaena sp. FEBS Lett *449*, 159–164.

Valladares, A., Muro-Pastor, A.M., Herrero, A., and Flores, E. (2004). The NtcA-dependent P1 promoter is utilized for glnA expression in N2-fixing heterocysts of Anabaena sp. strain PCC 7120. J. Bacteriol. *186*, 7337–7343.

Vega-Palas, M.A., Flores, E., and Herrero, A. (1992). NtcA, a global nitrogen regulator

from the cyanobacterium Synechococcus that belongs to the Crp family of bacterial regulators. Mol. Microbiol. *6*, 1853–1859.

Vermaas, W.F. (2001). Photosynthesis and Respiration in Cyanobacteria. In Encyclopedia of Life Sciences, John Wiley & Sons, Ltd, ed. (Chichester, UK: John Wiley & Sons, Ltd), p.

Vicente, J.B., Gomes, C.M., Wasserfallen, A., and Teixeira, M. (2002). Module fusion in an A-type flavoprotein from the cyanobacterium Synechocystis condenses a multiple-component pathway in a single polypeptide chain. Biochem. Biophys. Res. Commun. *294*, 82–87.

Vogel, J., and Sharma, C.M. (2005). How to find small non-coding RNAs in bacteria. Biol. Chem. *386*, 1219–1238.

Voss, B., Georg, J., Schön, V., Ude, S., and Hess, W.R. (2009). Biocomputational prediction of non-coding RNAs in model cyanobacteria. BMC Genomics *10*, 123.

Vázquez-Bermúdez, M.F., Flores, E., and Herrero, A. (2002). Analysis of binding sites for the nitrogen-control transcription factor NtcA in the promoters of Synechococcus nitrogen-regulated genes. Biochim. Biophys. Acta *1578*, 95–98.

Wehrmeyer, W. (1982). Organization and composition of cyanobacterial and rhodophycean phycobilisomes.

Weinberg, Z., Wang, J.X., Bogue, J., Yang, J., Corbino, K., Moy, R.H., and Breaker, R.R. (2010). Comparative genomics reveals 104 candidate structured RNAs from bacteria, archaea, and their metagenomes. Genome Biol. *11*, R31.

Yanofsky, C. (1987). Tryptophan synthetase: its charmed history. Bioessays *6*, 133–137.

Yu, M.H., and Glazer, A.N. (1982). Cyanobacterial phycobilisomes. Role of the linker polypeptides in the assembly of phycocyanin. J. Biol. Chem. *257*, 3429–3433.

Zanetti, G., and Aliverti, A. (1991). zanetti, g. & aliverti, a. (1991) ferredoxin: nadp+ oxidoreductase, in chemistry and biochemistry of, flavoenzymes (müller, f., ed.) vol. 2, pp. 305–3.

Zuker, M. (2003). Mfold web server for nucleic acid folding and hybridization prediction. Nucleic Acids Research *31*, 3406–3415.

VI. Annexe

Molecular Microbiology (2011) 81(5), 1178–1189
doi:10.1111/j.1365-2958.2011.07739.x
First published online 26 July 2011

A larger transcript is required for the synthesis of the smaller isoform of ferredoxin:NADP oxidoreductase

Amin Omairi-Nasser, Adrienne Gomez de Gracia and Ghada Ajlani*
Institut de Biologie et de Technologie de Saclay, Centre National de la Recherche Scientifique and Commissariat à l'Energie Atomique, 91191 Gif-sur-Yvette.

Summary

Ferredoxin:NADP oxidoreductases (FNRs) constitute a family of flavoenzymes that catalyse the exchange of electrons between ferredoxin and NADP(H). In cyanobacteria FNR provides NADPH for photoautotrophic metabolism, but the enzyme is also capable of oxidizing NADPH providing reduced ferredoxin. In the cyanobacterium *Synechocystis* sp. strain PCC6803, the unique *petH* gene has two translation products depending on growth conditions. As a consequence two isoforms of the FNR accumulate – FNR_L and FNR_S. In the present work, analysis of *petH* expression reveals that different transcriptional start points (tsp) are responsible for this differential translation initiation. Under standard conditions (where FNR_L accumulates), two tsps were found at –52 and –34 relative to the first translation start site. Under nitrogen-starvation conditions (where FNR_S accumulates) a tsp was mapped at –126 relative to the first translation start site. Therefore, the transcript responsible for FNR_S translation is longer than that producing FNR_L. In addition, expression of the short or long transcript in *E. coli* resulted in the accumulation of FNR_L or FNR_S respectively. This result demonstrates that translation can initiate at two different sites, 336-bases apart (ATG-1 to ATG-113), depending only on the 5′UTR structure.

Introduction

In cyanobacteria and chloroplasts ferredoxin:NADP oxidoreductase (FNR) is involved in the last step of oxygenic photosynthesis, providing NADPH for CO_2 assimilation and other anabolic reactions. However, FNR is also implicated in the oxidation of NADPH, produced by catabolism or accumulated due to an imbalance in the photosynthetic reactions (Bowsher *et al.*, 1993; Neuhaus and Emes, 2000; Benz *et al.*, 2010). In most phycobilisome (PBS)-containing cyanobacteria, *petH* encodes an FNR that contains an N-terminal domain whose sequence is similar to PBS-linker polypeptides (Schluchter and Bryant, 1992). This domain is responsible for the attachment of FNR to PBS (van Thor *et al.*, 1999; Thomas *et al.*, 2006). The PBS is a large, abundant pigment-protein complex that harvests light for photosynthetic reactions – for a review see Anderson and Toole (1998). However, when the combined nitrogen level becomes low (nitrogen starvation), non-diazotrophic cyanobacteria respond by slowing down photosynthesis and catabolizing reserves to survive. Nitrogen starvation induces degradation of PBS, supplying amino acids for the synthesis of essential proteins while also reducing photosynthetic light harvesting (Allen and Smith, 1969; Sauer *et al.*, 2001).

Synechocystis sp. strain PCC6803 (hereafter called *Synechocystis*) is a unicellular non-diazotrophic cyanobacterium in which NADPH and ATP, produced by photosynthetic electron transfer, are used for anabolic reactions such as CO_2 fixation. *Synechocystis* is also capable of chemoheterotrophic metabolism, where sugar molecules are catabolized to produce the NADPH and ATP needed for other reactions. It was shown that sugar catabolic genes were directly induced by nitrogen depletion (Osanai *et al.*, 2006), which suggests that amino acids provided by PBS degradation might also be used as a carbon source during nitrogen starvation. This also implies that heterotrophic metabolism participates in *Synechocystis* survival under nitrogen starvation.

The unique *petH* gene of *Synechocystis* was shown to have two translation products: FNR_L (413 amino acids), the large isoform that attaches to PBS, and FNR_S (300 amino acids), a small isoform lacking the PBS-linker domain. FNR_L is present under standard photoautotrophic conditions, while FNR_S is present under nutrient-starvation and heterotrophic conditions (Thomas *et al.*, 2006). About 6 h following nitrogen depletion, the FNR_S/FNR_L ratio increases, such that FNR_S becomes the major isoform after about 60 h.

The *petH* mRNA of *Synechocystis* was described as having a 5′-untranslated region (5′UTR) of 523 bases

Accepted 11 June, 2011. *For correspondence. E-mail gajlani@cea.fr; Tel. (+33) 169 086 569; Fax (+33) 169 084 007.

(van Thor *et al.*, 1998), which is considered to be unusually long in *Synechocystis*. None of the genomic 5′UTR determined in Mitschke *et al.* (2011) was longer than 278 bases. In the work described here, reinvestigation of *petH* transcription in *Synechocystis* shows a new transcription organization, shedding light on the mechanism by which this gene produces two translation products. We localize the *petH* transcription start sites (transcriptional start point, tsp) in *Synechocystis* under conditions known to result in FNR_L or FNR_S translation, and confirm the function of each tsp by the insertion of transcriptional terminators at different sites within the *petH* 5′-non-coding region. Moreover, we show that even *Escherichia coli* is capable of alternative translation initiation provided that the *petH* transcript contains the appropriate 5′UTR. Finally, we introduced deletions in the long 5′UTR, which confirmed its role in the alternative translation initiation leading to the small isoform accumulation.

Results

The petH *5′ UTR is required for* FNR_S *accumulation*

Since *petH* is an essential gene under all known growth conditions, we modified an ectopic allele placed at the *psbA2* locus and monitored its ability to produce FNR_S. It has been shown that *psbA3* supports photoautotrophic growth in the absence of *psbA2* (Mohamed and Jansson, 1989), so this insertion is neutral to *Synechocystis*. Nitrogen starvation was chosen to induce FNR_S accumulation because this method gave the most reproducible results – compared with heterotrophic growth. Two cargo plasmids were created: pLC, in which the *petH* ORF was fused to the 5′-noncoding region of *psbA2*, and pLC5′, where the *psbA2* promoter region was replaced by that of *petH* (Fig. 1A). In each construct, upstream and downstream *psbA2* sequences and a Cm-resistance cassette allowed chromosomal integration by double recombination and positive selection respectively. FNR_S accumulation from the constructs was monitored in MI6, a mutant in which *petH* was unable to produce FNR_S because of a missense mutation (ATG-113/ATC) that changes the second-initiating methionine into an isoleucine (Thomas *et al.*, 2006). Thus, the resulting strains, denoted MLC and MLC5′, carried a native allele unable to produce FNR_S, and an ectopic one harbouring a wild-type ORF that was under the control of two different 5′-noncoding regions. PCR, restriction analysis and DNA sequencing confirmed the genotypes of the mutants (data not shown).

FNR accumulation was probed in cell extracts from the wild type, MI6, MLC and MLC5′, grown under normal and nitrogen-starvation conditions. In the wild type, FNR_L is the major isoform when nitrogen is present (0 in Fig. 1B), while FNR_S is dominant after 72 h of nitrogen starvation (72 in Fig. 1B). In MI6, besides the absence of FNR_S, FNR_L decrease and cell bleaching during nitrogen starvation are slowed down, compared with the wild type (Thomas *et al.*, 2006). In MLC, FNR_S was also absent, while MLC5′ recovered the ability to accumulate FNR_S upon nitrogen starvation. This demonstrates that ectopic expression of *petH* can lead to FNR_S translation only when the ectopic allele contains the *petH* 5′UTR (MLC5′), while with the *psbA2* 5′UTR it cannot (MLC). Residual amounts of FNR_S are detected in MLC, at both time points. This suggests that when the second-initiating methionine is intact, as it was in the ectopic ORFs; FNR_S translation initiation occurs, in the absence of the appropriate 5′UTR, albeit at a very low efficiency.

In addition, extracts from MLC and MLC5′ contained a relatively higher amount of FNR_L, compared with the wild type and MI6, which is due to the expression of two *petH* alleles in these strains (gene dosage effect). Quantification of FNR_L in PBS isolated from MI6 and MLC confirmed this finding. Indeed, PBS from MLC contained at least twice the amount of FNR_L found in MI6 (Fig. S1).

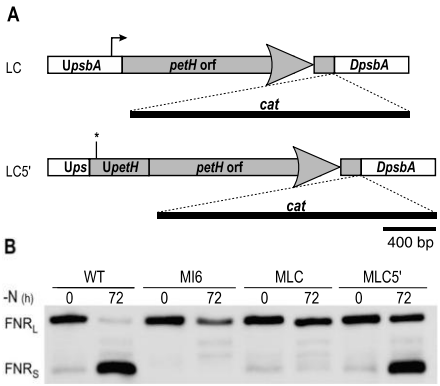

Fig. 1. *petH* 5′UTR regulates FNR_S translation.
A. Structure of two ectopic alleles placed at the *psbA2* locus of MI6, a mutant unable to produce FNR_S. In LC, FNR_L ORF was under the control of the *psbA2* 5′-noncoding region, while in LC5′ the same ORF was under the control of the *petH* 5′-noncoding region. A bent arrow indicates the position of *psbA2* tsp and an asterisk indicates the position of *petH* tsp as previously mapped in van Thor *et al.* (1998), white boxes represent *psbA2* related sequences and gray boxes represent those of *petH*, U and D designate upstream and downstream regions respectively.
B. Impact of nitrogen starvation (for 0 and 72 h) on FNR accumulation in total protein extracts analysed by Western blot. WT, the wild type; MI6, unable to produce FNR_S. MLC and MLC5′, ectopically expressed the LC and LC5′ alleles, respectively, in MI6.

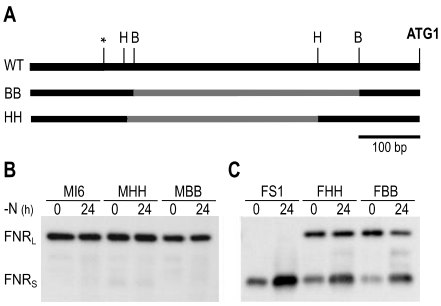

Fig. 2. Deletions within the *petH* 5′-noncoding region.
A. Structure of the 5′-noncoding region in the wild type (upper map) and in two ectopic alleles (BB and HH) lacking internal restriction fragments of 370 and 345 bases respectively (gray lines). Asterisk indicates the position of the *petH* transcription start as previously mapped in van Thor *et al.* (1998); B, BseRI; H, HpaI.
B. Immunoblot analysis of FNR accumulation, in total protein extracts from nitrogen-starved cells (for 0 and 24 h) shows that the above alleles expressed in MI6 (MHH and MBB), failed to accumulate FNR$_S$.
C. Expression of the same alleles in FS1, which is unable to produce FNR$_L$, results in FNR$_L$ accumulation (FHH and FBB).

Locating the region responsible for FNR$_S$ accumulation

To localize a putative signal responsible for FNR$_S$ translation, we deleted restriction fragments from the aforementioned pLC5′, creating two vectors. pBB lacks 370 bases (from 477 to 105 bases upstream to ATG-1), while pHH is missing 345 bases (from 490 to 145 bases upstream to ATG-1). Both deletions preserved the *petH* promoter previously mapped in van Thor *et al.* (1998) (Fig. 2A). In order to monitor the ability of these constructs to express each of the FNR isoforms, the mutated alleles were expressed ectopically in MI6 (unable to produce FNR$_S$, see last section) and in FS1, a mutant unable to produce FNR$_L$ due to the presence of a stop codon upstream from ATG-113 (Thomas *et al.*, 2006). FNR isoforms were immunodetected in total extracts from mutants grown in the presence of nitrogen (0 in Fig. 2B and C) or nitrogen-starved 24 h only since FNR$_S$ was already detected at that time point (24 in Fig. 2B and C). Ectopic expression of the above constructs in MI6 resulted in mutants MHH and MBB, where the origin of FNR$_L$ is indistinguishable due to the expression of the ectopic and/or the native allele, while that of FNR$_S$ results exclusively from the ectopic one – since the native allele is unable to produce FNR$_S$. Figure 2B clearly shows that FNR$_S$ accumulation was abolished by both of the deletions, since neither MHH nor MBB produced FNR$_S$ under nitrogen starvation. On the other hand, ectopic expression of the same alleles in FS1 resulted in mutants FHH and FBB, where accumulation of FNR$_S$ is indistinguishable due to the expression of the ectopic and/or the native allele, while that of FNR$_L$ results from the ectopic one (the native allele is unable to produce FNR$_L$). Figure 2C shows that neither of the deletions altered FNR$_L$ expression. This result suggests that the deleted fragments were dispensable for FNR$_L$ expression, but contained a promoter or other regulating element responsible for FNR$_S$ expression. To test this hypothesis we constructed three nested deletions including the promoter mapped in (van Thor *et al.*, 1998), which were extended up to 105 bases upstream from ATG-1 (NG, NP and NB in Fig. 3A). These constructs were expressed ectopically in MI6 (MNG, MNP and MNB) and the mutants were nitrogen-starved to monitor their ability to accumulate FNR$_S$. Figure 3B shows that the NG and NP alleles, carrying 378 and 213 bases upstream from ATG-1, respectively, still produced FNR$_S$ (MNG and MNP). Conversely the NB allele, carrying only 105 bases upstream from ATG-1, did not produce FNR$_S$ (MNB). This confirms that a specific promoter for an FNR$_S$-specific transcript should be located within a fragment extending from 213 (P) to 105 (B) bases upstream from ATG-1. On the other side, the NB allele was also expressed in FS1 (mutant FNB), and surprisingly, this allele clearly produces FNR$_L$ in the absence of the promoter previously mapped in van Thor *et al.* (1998) (Fig. 3C). These results strongly suggest that a promoter, responsible for FNR$_L$ expression, is located within 105 bases upstream from ATG-1, while a signal (or promoter) responsible for FNR$_S$ accumulation is located between

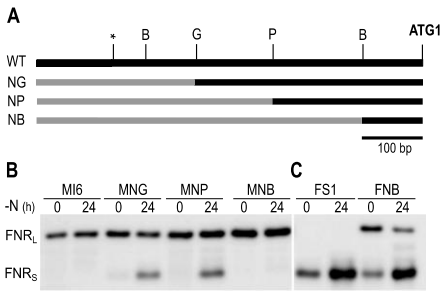

Fig. 3. Genetic mapping of the *petH* promoter.
A. Structure of the 5′-noncoding region in the wild type (upper map) and in three ectopic alleles (NG, NP and NB) bearing nested deletions (gray lines). Asterisk indicates the position of the transcription start as previously mapped in van Thor *et al.* (1998); B, BseRI; G, BglII; P, SpeI.
B. Immunoblot analysis of total protein extracts from cells starved for nitrogen (for 0 and 24 h) to induce FNR$_S$ translation. Expression of the above alleles in MI6 (unable to produce FNR$_S$) resulted in MNG and MNP, where FNR$_S$ accumulates, and MNB, where it did not.
C. When the NB allele was expressed in FS1 (unable to produce FNR$_L$), the resulting strain, FNB, accumulates FNR$_L$.

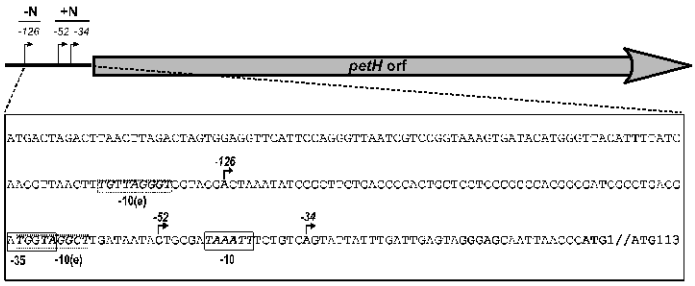

Fig. 4. Representation of the *petH* tsps mapped in this work. Bent arrows indicate the positions of the tsps, -52 and -34 (standard conditions) and -126 (nitrogen-starvation conditions), the numbers are relative to the first translational start site of *petH* (ATG-1). The sequence of the 5′-noncoding region is represented bellow, with the tsps (bold under bent arrows), the promoters -10 boxes and -35 box (boxed) for tsp -34, extended (e) -10 boxes for tsp -52 and -126 (dotted line boxes). The start codons and the ribosome binding site are represented in bold.

213 and 105 bases upstream from ATG-1. We therefore decided to characterize the *petH* promoter further.

petH *transcription start sites*

In order to locate the 5′-ends of the *petH* mRNAs, under standard conditions and conditions under which nitrogen induced genes are expressed, we have used differential TAP (Tobacco Acid Pyrophosphatase) 5′-RLM-RACE (RNA-Ligase-Mediated Rapid Amplification of cDNA ends). The reactions were carried out with RNA samples extracted from the wild type grown in nitrogen-containing medium (+N) or nitrogen-starved for 8 h (-N). Figure S2 represents the DNA fragments, issued from the differential 5′-RLM-RACE described in *Experimental procedures*. Sequencing of the differentially amplified products from +N RNA showed two adjacent tsps, 52 (C) and 34 (A) bases upstream from ATG-1 (Fig. 4). The -52 tsp is 8 bases downstream from an extended -10 box (TGgTAggcT). Such elements were found to function without an obvious -35 box in *E. coli* (Barne *et al.*, 1997) and were described in several cyanobacterial promoters (Mazouni *et al.*, 1998; Valladares *et al.*, 2004). It is striking that the UP element of this promoter is considerably GC rich (75%) compared with the *Synechocystis* genome (47.7%). The -34 tsp starts on an A that is located 6 bases downstream from a putative -10 Pribnow-like box (TAaATT) separated by an 18-bases AT-rich spacer from a putative -35 box (aTGgtA). On the other hand, in -N RNA, a tsp was mapped 126 (A) bases upstream from ATG-1; again an extended -10 box (TGtTAgggT) is found with a spacing of 6 bases upstream from the tsp for this promoter. The location of these tsps, summarized in Fig. 4, is in excellent agreement with the promoters genetically identified in the previous section (downstream -105 for +N and -213 to -105 for -N).

Genetic confirmation of promoter location

In order to ascertain the location of the newly discovered promoters, the omega-*aadA* cassette, flanked by T4 transcriptional termination sequences (Prentki and Krisch, 1984), was inserted in the native *petH*-noncoding region at sites -240, -195, -145 and -79 bp upstream from ATG-1 (Fig. 5A). Transformation of the wild type resulted in mutants BX, VX, HX and SX respectively. Total segre-

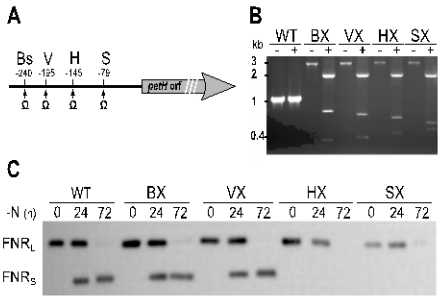

Fig. 5. Insertion of the omega cassette in the 5′-noncoding region.
A. Representation of the Ωcassette insertion sites, a solid line represents the 5′-noncoding region and the gray arrow represents the ORF of *petH*. Letters represent the sites name and the numbers below their position relative to ATG-1; Bs, BssHII; V, AvrII; H, HpaI; S, AsiSI.
B. PCR and restriction analysis of the mutants DNA. (-) PCR produced a 1 kb fragment from the wild type (WT) and 3 kb fragments from the insertion mutants (BX, VX, HX and SX). (+) Digestion of the PCR products with HindIII, an enzyme that bracketed the cassette, produced a 2-kb fragment containing the cassette and two fragments representing downstream and upstream regions.
C. Immunodetection of the FNR isoforms in the wild type (WT) and the insertion mutants under standard conditions (0) and upon nitrogen starvation for 24 and 72 h.

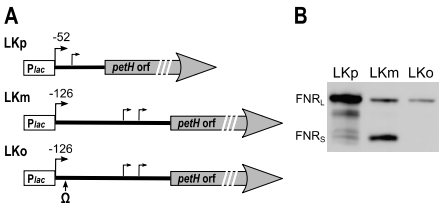

Fig. 6. Similar translation regulation occurs in *E. coli*.
A. Structure of the constructs used for *petH* expression in *E. coli*. The *lac* promoter (P_{lac}) precedes the short 5′UTR (52 bases) in LKp and the long 5′UTR (126 bases) in LKm. LKo derived from LKm in which the Ω cassette was inserted 12 bases downstream from the tsp controlled by P_{lac}.
B. FNR_L and FNR_S accumulation in *E. coli* total extracts determined by immunoblotting. Bent arrows represent the tsp controlled by P_{lac} and smaller bent arrows represent the tsps controlled by the *Synechocystis* constitutive promoters.

gation and location of the insertion was confirmed by PCR (Fig. 5B). FNR was immunodetected in total cell extracts from the wild type and each of the mutants, in the presence of nitrogen and after 24 and 72 h of nitrogen starvation. The FNR isoform patterns in BX and VX were similar to those of the wild type, while HX and SX failed to accumulate FNR_S (Fig. 5C). This result confirms that the distal promoter is responsible for FNR_S accumulation, while the proximal promoters are responsible for the accumulation of FNR_L. It is noteworthy that SX, where the omega cassette is inserted 27 bases from the –52 tsp, repeatedly accumulated less FNR_L than the other strains.

5′ UTR regulation retained in E.coli

The regulation of FNR_S translation may be due to the transcript 5′UTR only, or alternatively could involve another trans-acting element specifically present in *Synechocystis*. We therefore mimicked this translation regulation in *E. coli*. *petH* was expressed so as to be transcribed from the *lac* promoter (P_{lac}), with either the long or the short 5′UTR in LKm and LKp respectively (Fig. 6A). As shown in Fig. 6B, the shorter 5′UTR (52 bases) produced FNR_L in LKp, while the longer one (126 bases) essentially produced FNR_S in LKm. We considered that the residual FNR_L in LKm could be due to the activity of the *Synechocystis* proximal promoters resulting in the transcription of an mRNA with a shorter 5′UTR. This was confirmed by the insertion of the omega cassette 12 bases downstream from the long transcript initiation point in LKm, yielding strain LKo, where *petH* transcription driven by P_{lac} was abolished. LKo produced FNR_L only (Fig. 6B), demonstrating that the presence of FNR_L in LKm is due to transcription, possibly from the *Synechocystis* constitutive promoters, of an mRNA containing a shorter 5′UTR.

Deletions within the long 5′ UTR encoding sequence

Analysis of the long 5′UTR sequence revealed the presence of several dyads of symmetry that could mediate stable RNA secondary structure formation. Possible folding, of an RNA fragment starting at –126 (tsp) and ending at +20 relative to AUG-1, was predicted using the web-based RNA-folding application mfold (Zuker, 2003). Five possible secondary structures were proposed with a calculated free energy of about –30 kcal mol^{-1} at 34°C (Fig. S3).

In order to identify the most probable model, we examined the effect of deletions, constructed within the region encoding the 5′-end of the long transcript, on FNR accumulation. The mutants were constructed in *Synechocystis*, as described in *Experimental procedures* and outlined in Fig. 7A and B.

First, we deleted 34 bases encoding stem-loop structure I (G-59/U-26), which was present in all five models predicted by mfold. Since this fragment also contained the constitutive transcripts' promoter elements, such deletion was expected to be lethal under standard conditions due to the absence of FNR. Therefore, the deleted allele denoted AN1 (Fig. 7A) was expressed ectopically in MI6 (yielding MAN1) and in FS1 (yielding FAN1). FNR isoforms were Immunodetected in total extracts from mutants grown under standard conditions or nitrogen-starved for 24 h (Fig. 7C). As the native allele in MAN1 is unable to produce FNR_S, accumulation of FNR_S results exclusively from the ectopic AN1 allele, while that of FNR_L is indistinguishably due to the expression of both alleles. Accordingly, Fig. 7C (MAN1) proved that the deletion carried by AN1 did not abolish *petH* ability to produce FNR_S. Conversely, accumulation of FNR_L in FAN1 would result only from the ectopic AN1 allele. Figure 7C (FAN1) shows that FAN1 failed to accumulate FNR_L under standard conditions, which confirms that the constitutive transcript, required for FNR_L expression, was missing in AN1. However, traces of FNR_L are detected in FAN1 upon nitrogen starvation. This suggests that the AN1 'longer mRNA' also allows some FNR_L translation.

Next, we constructed deletions that strongly weakened base pairing around AUG-1 according to the secondary structure models (Fig. S3). Six deletions were in the region encoding the first part of the long 5′UTR; B8 (U-95/G-82) and B9 (A-103/G-90) carried overlapping 14-bases deletions; B91, B92 and B93 carried overlapping deletions of 4 bases each (C-102/C-99, C-99/C-96 and C-96/C-93 respectively) that were within the 14 bases deletion of B9; B94 lacked 5 bases (C-94/G-90) that overlapped

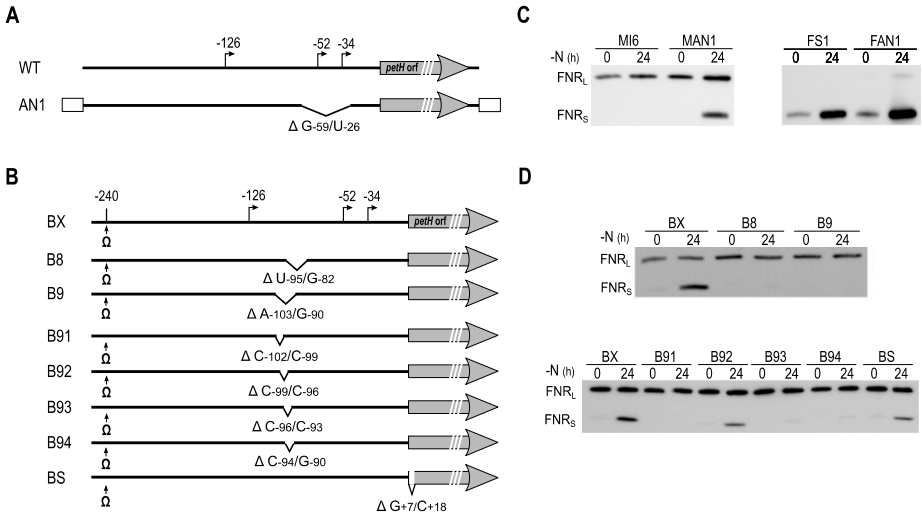

Fig. 7. Effect of the deletions constructed to identify a probable secondary structure adopted by the 5′UTR of the longer transcript.
A. Structure of the wild-type *petH* and that of the AN1 ectopic allele placed in the *psbA2* locus of MI6 and FS1. The white boxes represent sequences belonging to the *psbA2* locus.
B. Structure of the native *petH* in BX, the control strain carrying a wild-type gene and in seven mutants where deletions were introduced together with the omega cassette (Ω). Solid lines represent the *petH* 5′-noncoding region; grey arrows represent *petH* ORF and bent arrows represent *petH* tsps. The positions of the deleted fragments are shown with nucleotide numbers relative to the first nucleotide of ATG-1.
C. Impact of nitrogen starvation (0 and 24 h) on FNR accumulation analysed by Western blot on total protein extracts. MI6, a mutant unable to produce FNR_S; MAN1, a mutant ectopically expressing the AN1 allele in MI6; FS1, a mutant unable to produce FNR_L; FAN1, a mutant ectopically expressing AN1 in FS1.
D. Impact of nitrogen starvation (0 and 24 h) on FNR accumulation analysed by Western blot on total protein extracts of BX and mutants bearing the deletions represented in (B).

B9 and B8. An additional construct, BS (A+7/C+18), carried an in frame deletion that eliminates four codons (3–6) from the FNR_L ORF (Fig. 7B). Since the above deletions were not expected to affect the constitutive transcripts, they were introduced in the native *petH* gene yielding mutants that were viable and grew normally under standard conditions. PCR and DNA sequencing confirmed total segregation and the presence of the mutations respectively (data not shown). FNR was immunodetected in total cell extracts from each of the constructed mutants and, as a control, from BX that carried the omega cassette, upstream from *petH*, at the same site as the mutants did (Fig. 7B). The mutants accumulated different FNR_S amounts upon nitrogen starvation, compared with BX. Accordingly, the role of the deleted regions in FNR_S accumulation was classified as essential in B9, B8 and B91, where FNR_S was not detected; critical in B93 and B94, where traces of FNR_S was detected, and significant in B92 and BS, which accumulate FNR_S but in lesser amounts than BX (Fig. 7D).

Among the five models predicted by mfold (Fig. S3) only one secondary structure was validated by the deletion results. This secondary structure is represented in Fig. 8. The model contains three stem-loops (I, II and III) that were found in all the predicted models, one (IV) that was found in only four of the predicted models and one (VI) that was specific to the model presented in Fig. 8. The 5′-end contains a single-stranded region comprising nucleotides A-126 through U-109, followed by paired nucleotides (G-108 to C-105/G+13 to U+16) (A-102 to G-89/C+6 to U+9) with suggests that base pairing occurs between the long 5′UTR and regions within the *petH* ORF, this was confirmed by the fact that deletions in mutants B91 and BS affected FNR_S accumulation (Fig. 7D). Together with stem-loop VI, base pairing in (U-95 to C-92/G-15 to A-12) makes the ribosome binding site and AUG-1 unavailable for translation initiation; mutant B93 and B94 confirm the possibility of such base pairings. The significant effect observed by the deletion in B92 could be due to steric constraint imposed by the absence of loop VII.

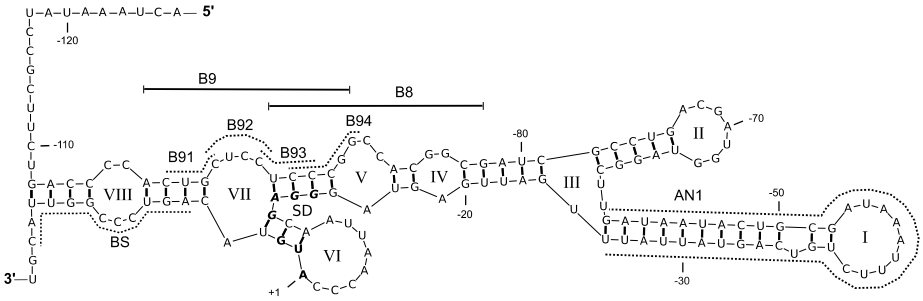

Fig. 8. Secondary structure model for the *petH* long 5′UTR. This model, predicted by the online RNA-folding program mfold (version 2.3) (Zuker, 2003), was chosen among several proposed folds (represented in Fig. S3). This structure contained base pairings that were disrupted by the deletions analysed in Fig. 7. Solid lines indicate the deleted sequences in B8 and B9 and dotted lines indicate those deleted in B91-94, BS and AN1. The ribosome binding site (SD) and AUG-1 are in bold. Numbers indicate nucleotide positions relative to the first nucleotide of AUG-1. Latin digits indicate loops numbers.

Discussion

The attachment of FNR_L to the PBS via its PBS-linker domain clearly confers an evolutionary advantage, given the proliferation of the FNR_L isoform in PBS-containing cyanobacteria. Induction of FNR_S translation is presumably favourable, for *Synechocystis* and some other cyanobacteria, under conditions of nutrient starvation, heterotrophy or high NADPH – where cell reserves are mobilized, photosynthesis is slowed down and NADPH oxidation is required (Sauer *et al*., 2001). The mechanism by which, depending on growth conditions, the unique *petH* gene is capable of differential translation initiation resulting in FNR_L or FNR_S accumulation was unknown.

Here we discovered a novel mechanism involving a specific 5′UTR for the transcript encoding each of the isoforms. Comparison of translation products when the *petH* ORF was placed under the control of its own 5′-noncoding region or under that of *psbA2* proved that FNR_S translation requires the *petH* 5′-noncoding region. Furthermore, mapping of the transcripts 5′-end shows that under standard conditions, two tsps are used (–52 and –34), while under nitrogen-starvation conditions a third upstream tsp (–126) is used.

Our results are consistent with the recent work of Mitschke *et al*. (Mitschke *et al*., 2011) that established a genome-wide map of 3527 tsps of *Synechocystis* by differential RNA sequencing and where the –52 tsp was described. We found that the associated promoter (P_{52}) contained a surprisingly GC rich sequence and that the –10 box resembled the extended –10 element described in many bacteria including cyanobacteria (Mazouni *et al*., 1998; Valladares *et al*., 2004). Although the second constitutive tsp (–34), mapped here, was not described in Mitschke *et al*. (2011), the presence of adequate, –10 and –35, promoter elements together with the fact that it starts with an A (according to Mitschke *et al*., 68% of *Synechocystis* transcripts starts on an A) argues for its validity. We also noticed that our growth conditions differed from those used in the Mitschke *et al*. work, where *Synechocystis* was grown at 30°C without CO_2, while it was grown at 33°C in a CO_2 enriched incubator in our work.

It is remarkable that the –10 box element of P_{52} overlaps with the –35 box element of P_{34} (Fig. 4) and that both promoters function simultaneously under our growth conditions; their functioning might involve different sigma factors (Asayama and Imamura, 2008). The insertion of an omega cassette 27 bases downstream from the –52 tsp seems to result in lower FNR_L amounts than a mutant bearing the same insertion 65 bases farther upstream (SX compared with HX, in Fig. 5); transcription from the –52 tsp could be disturbed in this mutant due to the absence of its associated UP elements. Taken together these results suggest that combined expression from both promoters participate in FNR_L homeostasis in *Synechocystis* under standard growth conditions. Neither Mitschke *et al*. (2011) nor the work described here identified the –523 tsp described by van Thor *et al*. (1998), note that this tsp does not contain promoter consencus sequences. Mitschke *et al*. proposed that this 5′-end could belong to an antisense RNA that is transcribed in the adjacent *prk* gene.

It was also speculated that some internal tsp could produce FNR_S in *Synechocystis*, but our results exclude this assumption and demonstrate that FNR_S is translated from an mRNA having a tsp further upstream (–126), resulting in a longer 5′UTR. This mRNA prevents translation initiation at ATG-1, while promoting translation initiation at ATG-113, leading to FNR_S accumulation. *petH*

expression in *E. coli* resulted in FNR_L or FNR_S accumulation when the coding region was preceded by the shorter or the longer 5′UTR respectively. This suggests that the translation regulation does not require a specific factor present in *Synechocystis* only.

A similar *petH* transcription organization was described for *Anabaena* sp. strain PCC7120, where two tsps were mapped at nucleotides –63 and –188 relative to the first translation-initiation codon. The former is constitutive, while the latter is induced in the absence of combined nitrogen (Valladares *et al.*, 1999). Interestingly prediction of the *Anabaena* longer transcript folding resulted in secondary structures similar to the ones found for *Synechocystis* (data not shown). The similarity of the translation-regulation mechanisms in both cyanobacteria needs to be demonstrated.

We have attempted to further elucidate the role of the long 5′UTR in FNR_S synthesis. A series of 5- to 34-base deletions within the long 5′UTR led us to a hypothetical model for the long 5′UTR secondary structure (Fig. 8). The region from bases –103 to –90 is clearly required for FNR_S induction and is involved in the base pairing that makes AUG-1 and its associated ribosome binding site inaccessible to the translation-initiation complex (Fig. 8). Thus translation can only be initiated at AUG-113, giving FNR_S. Most interesting was the AN1-deletion results; the deleted region contained a stem-loop structure (stem-loop I, $\Delta G = 8$ kcal mol^{-1}) that was present in all five models predicted by mfold (Figs 8 and S3). This deletion did not affect FNR_S accumulation, which suggests that a secondary structure similar to the one occurring in the wild type was still produced in AN1. But the fact that traces of FNR_L were synthesized, upon nitrogen starvation (Fig. 7C), suggests that the secondary structure was slightly destabilized allowing leakage of FNR_L translation initiation.

We speculate that RNA structures created in the longer 5′UTR are involved in FNR_S translation initiation as schematized in Fig. 9. Such structures would inhibit FNR_L translation either by blocking the initiation site or by eliminating it through a targeted mRNA-degradation process (Obana *et al.*, 2010).

The RNA chaperone Hfq is known to stabilize RNA base pairing in bacteria (Waters and Storz, 2009). Dienst *et al.* showed that an Hfq orthologue was functional in *Synechocystis* (Dienst *et al.*, 2008). However, the FNR accumulation pattern was unaffected in an *hfq*-deficient mutant of *Synechocystis* (data not shown). Therefore, Hfq does not seem to be important for a putative RNA pairing that could result in the alternative translation initiation observed here.

Further investigations are in progress to elucidate the RNA structure responsible for this novel form of translation regulation, in which the 5′UTR prevents translation initiation at a proximal site while promoting it at a site located 336 bases further downstream.

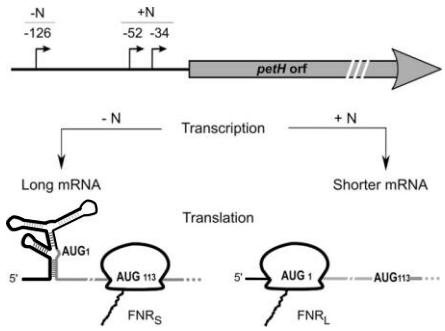

Fig. 9. Schematic representation of the 5′UTR-mediated regulation of FNR translation. Transcripts starting at –126 (long) contain a leader sequence that folds into a stable secondary structure, blocking initiation at AUG-1, either by preventing ribosome binding or by creating an RNA-processing site. Thus translation can only be initiated at AUG-113, giving FNR_S. Transcripts starting at –52 or –34 (shorter) permit ribosome binding at AUG-1, leading to FNR_L translation.

Experimental procedures

Strains and growth conditions

Wild type and mutants of *Synechocystis* were grown photoautotrophically in an illuminated incubator at 33°C in a CO_2 enriched atmosphere and under continuous light (50 μE m^{-2} s^{-1}). The medium composition is described in Ughy and Ajlani (2004). For nitrogen starvation cells were harvested by centrifugation and resuspended in a medium where NaCl replaced $NaNO_3$. When appropriate, media were supplemented with 5 μg ml^{-1} streptomycin, 50 μg ml^{-1} spectinomycin or 20 μg ml^{-1} chloramphenicol.

Construction of the cargo plasmids

A 1281 bp fragment (from the *petH* ATG-1 to 40 bp downstream the stop codon) was amplified from genomic DNA using primers HLN and HRB (the sequences of primers used in this study are listed in Table 1). This fragment was digested with NdeI and BamHI and cloned between the same sites of pPSBA2 (Lagarde *et al.*, 2000) creating pLB. A 2074 bp BamHI fragment containing the cat gene [C.C1 (Elhai and Wolk, 1988)] was inserted in the unique BamHI site of pLB yielding pLC (Fig. 1). In pLC5′, a 190 bp NcoI-SnaBI fragment of pLC, containing the *psbA2* promoter, was replaced by a 724 bp NcoI-SnaBI fragment containing *petH* 5′-region (from 706 bp upstream to 18 bp downstream from the first *petH* start codon). Different restriction fragments were deleted from the 5′-noncoding region of pLC5′ by a combination of restriction-endonuclease digestion. Each digest was treated with the Klenow fragment of DNA polymerase and

Table 1. Oligonucleotide primers used in this work.

Primer	Sequence (5′–3′)
8F	ATCGCCTGACGATGGTAG
8R	GGAGCAGTGGGGTCAGAAG
9F	CCACGGCGATCGCCTGACG
9R	GGGGTCAGAAGCGGATATTTAG
91F	TCCTCCCGGCCACGGCGAT
91R	TGGGGTCAGAAGCGGATATTTAG
92F	TCCCGGCCACGGCGATCG
92R	CAGTGGGGTCAGAAGCGG
93F	CGGCCACGGCGATCGCCTG
93R	GAGCAGTGGGGTCAGAAGC
94F	ACGGCGATCGCCTGACGATG
94R	GGAGGAGCAGTGGGGTCAG
ANF	TGATTGAGTAGGGAGCAATTAAC
ANR	AAGCCTACCATCGTCAGGC
EGR	CCACTTCCCTCGGATTGAC
FHI	GGCAACACCAATAAGAACCACGCGGTC
FM	ACTAAATATCCGCTTCTGACCC
FN	CTGCGATAAATTTCTGTCAG
HLN	CCCATATGAAACAACCC
HRB	CTCCCCTTCAGGATCCAAAC
HRE	CGGAGAAATTCTAACGACG
HSN	CCCATATGTACAGTCCC
HSR	CACCGTGTCTGGTGGAAGC
NBE	CTCTGGGATCCATGGGCGGTG
RAS	GATTACCGGCATCGCTCTG
RHI	CCAGCGGAGAGGTCAAACGTGAGGT
RN	CCACACAACATACGAGCC

self-ligated yielding plasmids pBB, pHH, pNG, pNP and pNB (Table 2).

Insertion mutagenesis in the petH *5′-noncoding region*

A 1323 bp fragment containing 716 bp upstream and 607 bp downstream ATG-1 was amplified using oligos, NBE and HSR, the PCR product was cloned in the EcoRV site of pBluescript yielding pNX. A 2.2 kb fragment containing the omega-*aadA* cassette (Prentki and Krisch, 1984), which confers resistance to streptomycin and spectinomycin and bracketed by transcription terminators was inserted in specific sites within the *Synechocystis petH* 5′-noncoding sequence carried by pNX. The plasmid was interrupted by the omega cassette using the following restriction sites BseRI, AvrII, HpaI and AsiSI, resulting in plasmids pBX, pVX, pHX and pSX respectively (Table 2). The resulting constructs were introduced into the wild type by genetic transformation. The structure of the recombinant chromosomes was confirmed by PCR and restriction digestion with HindIII (Fig. 5B).

Plasmids constructed by PCR were sequenced to verify the fidelity of the PCR amplification. Complete segregation of the mutant alleles was confirmed by PCR and in some cases the PCR products were subjected to restriction analysis and sequencing to ascertain the identity of the amplified fragments (data not shown).

Expression of petH *in* E. coli

A 1.9 kb HincII-NheI fragment carrying *petH* (145 bases upstream and 500 bases downstream from the ORF) was cloned into pBluescript resulting in pHNS where *petH* transcription was in the same direction as that of P_{lac}. To make a precise transcriptional fusion of the *lac* promoter to the +1 of each *petH* transcript, a fragment was deleted (from the *lac* tsp to the *petH* –126 tsp) by PCR using oligos RN and FM, the resulting plasmid was denoted pLKm. A fragment from the *lac* operon tsp to the *petH* –52 tsp was deleted the same way using oligos RN and FN resulting in plasmid pLKp. pLKo consists of pLKm in which a 2062-bases XbaI fragment, containing the omega-*aadA* cassette (Prentki and Krisch, 1984), was inserted 12 nucleotides downstream the *lac*/*petH* tsp. *E. coli.* DH5α was used to analyse FNR accumulation from the above constructs.

Deletions in the long transcript's 5′-end

All the deletions were prepared by PCR except that of BS, which was performed by BsrG1-SnaBI restriction digestion, on pBX, followed by Klenow DNA polymerase treatment and self-ligation yielding plasmid pBS. For the PCR construction of pB8, pB9, pB91, pB92, pB93 and pB94, primers, 8F and 8R; 9F and 9R; 91F and 91R; 92F and 92R; 93F and 93R; 94F and 94R, were used respectively (Table 2). For AN1 the mutagenic PCR was performed on pNX6 using primers ANF and ANR yielding plasmid pNAN, a 694-bases NcoI-SnaBI fragment from pNAN was used to replace a 728-bases NcoI-SnaBI fragment in pLC5′ yielding the cargo plasmid pAN1.

Preparation of cell extracts

For *Synechocystis* 10 ml of cells, at $OD_{580} = 2$, were collected and resuspended in 1 ml of Tricine 50 mM pH 8 containing complete protease inhibitor (Roche), then broken by vortexing 6 min with glass beads. Unbroken cells and glass beads were removed by centrifugation at 5000 *g* for 2 min. The supernatant was used as total cell extract. Chlorophyll concentration was used to ensure equivalent loading of cell extracts, 0.02 or 0.04 μg of chlorophyll was loaded per 2.9 or 4.8 mm well respectively. For *E. coli* 1 ml of cells, at $OD_{600} = 1$, grown in LB with ampicillin (100 μg ml^{-1}), were collected and resuspended in 100 μl of loading buffer and heated at 95°C for 5 min. A total of 5–10 μl of the extracts was loaded per well.

Gel electrophoresis and immunoblotting

Proteins were separated using denaturing Tris-Tricine PAGE. For immunoblot analysis, proteins were transferred to PVDF membranes. Blots were blocked with TBS buffer supplemented with 0.1% Tween and 5% dry skimmed milk, and incubated with the primary antibody (1:10 000 dilution). After washing, blots were incubated with a 1:15 000 dilution of peroxidase-conjugated anti-rabbit IgG (Promega). The signal was visualized using RapidStep ECL chemiluminescent substrate (Merck). Images were generated using a cooled CCD camera (Chemi Smart 5000, Vilber Lourmat) and ImageJ software.

Transcriptional start site mapping

Total RNA was extracted, from wild-type *Synechocystis* grown in nitrogen-containing medium or nitrogen-starved for

Table 2. Bacterial strains and plasmids used in this study.

Strains or plasmids	Properties	Source
Synechocystis		
WT	Wild-type strain of *Synechocystis* sp. strain PCC 6803	PCC
MI6	Missense mutation in *petH* where ATG-113 was changed to ATC (Sp^r, Sm^r)	Thomas *et al.* (2006)
FS1	Frameshift mutation creating an early stop codon in *petH* upstream from ATG-113 (Sp^r, Sm^r)	Thomas *et al.* (2006)
MLC	MI6 – Δ*psbAII*::*petH*, *cat* (Cm^r)	This study
MLC5′	MLC – 165 bp, containing P_{psbAII}, replaced by 706 bp of *petH* 5′-noncoding region (Cm^r)	This study
MBB	MLC5′ – Δ G477/C105 upstream from ATG-1 in the ectopic *petH*	This study
MHH	MLC5′ – Δ A490/A145 upstream from ATG-1 in the ectopic *petH*	This study
MNG	MLC5′ – Δ G702/A379 upstream from ATG-1 in the ectopic *petH*	This study
MNP	MLC5′ – Δ G702/A215 upstream from ATG-1 in the ectopic *petH*	This study
MNB	MLC5′ – Δ G702/A108 upstream from ATG-1 in the ectopic *petH*	This study
MAN1	MLC5′ – ΔG59-T26 upstream from ATG-1 in the ectopic *petH*	This study
FAN1	FS1 – ΔG59-T26 upstream from ATG-1 in the ectopic *petH*	This study
FBB	Same as MBB but in an FS1 background	This study
FHH	Same as MHH but in an FS1 background	This study
FNB	Same as MNB but in an FS1 background	This study
BX	*petH*$^-$::Ω-*aadA* – insertion 240 bp upstream from ATG-1	This study
VX	*petH*$^-$::Ω-*aadA* – insertion 195 pb upstream from ATG-1	This study
HX	*petH*$^-$::Ω-*aadA* – insertion 145 bp upstream from ATG-1	This study
SX	*petH*$^-$::Ω-*aadA* – insertion 79 bp upstream from ATG-1	This study
B8	BX – Δ T95/G92 upstream from ATG-1	This study
B9	BX – Δ A103/G90 upstream from ATG-1	This study
B91	BX – Δ C102/C99 upstream from ATG-1	This study
B92	BX – Δ C99/C96 upstream from ATG-1	This study
B93	BX – Δ C96/C93 upstream from ATG-1	This study
B94	BX – Δ C92/C88 upstream from ATG-1	This study
BS	BX – Δ A7/C18 downstream from ATG-1	This study
Plasmids		
pPSBA2	*Synechocystis* suicide vector, deriving from pSL1180 and containing upstream and downstream from the *psbAII* ORF separated by a multiple cloning site (Amp^r)	Lagarde *et al.* (2000)
pLC	*petH* orf and the *cat* gene cassette inserted in the multiple cloning site of pS1 (Amp^r, Cm^r)	This study
pLC5′	165 bp containing P_{psbAII} in pLC was replaced by 706 bp of *petH* 5′-noncoding region (Amp^r, Cm^r)	This study
pBB	370 bp BseRI-BseRI fragment deleted from pLC5′ (Amp^r, Cm^r)	This study
pHH	344 bp HpaI-HpaI fragment deleted from pLC5′ (Amp^r, Cm^r)	This study
pNG	214 bp NcoI-BglII fragment deleted from pLC5′ (Amp^r, Cm^r)	This study
pNP	488 bp NcoI-SpeI, fragment deleted from pLC5′ (Amp^r, Cm^r)	This study
pNB	608 bp NcoI-BseRI fragment deleted from pLC5′ (Amp^r, Cm^r)	This study
pAN1	G59-T26 upstream from ATG-1 deleted from pLC5′ (Amp^r, Cm^r)	This study
pDW9	Origin of the Ω fragment containing *aadA* plus strong translation-transcription terminators on both sides (Amp^r, Sm^r/Sp^r)	Golden and Wiest (1988)
pNX6	1323 bp fragment of *petH* amplified with NBE and HSR cloned in the EcoRV site of pBluescript (Amp^r)	This study
pNXA	pNX6 derivative with an AvrII restriction site created 197 pb upstream from *petH* orATG-1 (Amp^r)	This study
pNAN	pNX6 derivative with G59-T26 upstream from ATG-1 deleted (Amp^r)	
pBX	pNX6 with Ω inserted in the BssHII site (Amp^r, Sp^r, Sm^r)	This study
pB8	pBX – Δ T95/G92 upstream from ATG-1 (Amp^r)	This study
pB9	pBX – Δ A103/G90 upstream from ATG-1 (Amp^r)	This study
pB91	pBX – Δ C102/C99 upstream from ATG-1 (Amp^r)	This study
pB92	pBX – Δ C99/C96 upstream from ATG-1 (Amp^r)	This study
pB93	pBX – Δ C96/C93 upstream from ATG-1 (Amp^r)	This study
pB94	pBX – Δ C92/C88 upstream from ATG-1 (Amp^r)	This study
pBS	pBX – Δ A7/C18 downstream from ATG-1 (Amp^r)	This study
pVX	pNXA with Ω inserted at AvrII site (Amp^r, Sp^r, Sm^r)	This study
pHX	pNX6 with Ω inserted at HpaI site (Amp^r, Sp^r, Sm^r)	This study
pSX	pNX6 with Ω inserted at AsiSI site (Amp^r, Sp^r, Sm^r)	This study
pHNS	1905 bp HincII-NheI fragment containing *petH* cloned in pBt (Amp^r)	This study
pLKp	Deletion, from pHNS, of a 212 bp fragment from the *lacZ* tsp to the –52 tsp of *petH* (Amp^r)	This study
pLKm	Deletion, from pHNS, of a 138 bp fragment from the *lacZ* tsp to the –52 tsp of *petH* (Amp^r)	This study
pLKo	Ω cassette inserted 12 bp downstream the +1 of *lac* in pLKm (Amp^r Sp^r, Sm^r)	This study
E. coli		
DH5α	*E. coli* host for cloning and expression	Life technologies
LKp	DH5α containing pLKp	This study
LKm	DH5α containing pLKm	This study
LKo	DH5α containing pLKo	This study

8 h, according to Aiba *et al.* (1981) with slight modifications. 5′ RACE (rapid amplification of cDNA ends) was carried out using Ambion's FirstChoise RLM-RACE kit. Two reactions were set up for each RNA sample. One of them included treatment with tobacco acid pyrophosphatase (TAP); 5 μg of total RNA was treated with TAP for 1 h at 37°C in a volume of 10 μl. Ten picomoles of 5′-RACE RNA adaptor (provided in the kit) was added to the RNA sample, and ligation was performed in the presence of T4-RNA ligase for 1 h at 37°C. Retrotranscriptions were carried out with 0.5 μg of RNA ligated to the adaptor and gene-specific primer (EGR) using M-MLV reverse transcriptase. Two microlitres of portions of the reverse transcription reaction was used as templates for subsequent PCRs with a gene-specific primer (RAS) and a primer corresponding to sequences from the RNA adaptor. PCR products of about 200 bp (present only in the TAP treated samples) were isolated from agarose gels and cloned into the EcoRV site of the pBluescript vector (Stratagene) for sequencing. The first nucleotide following the adaptor sequence was taken as the tsp.

Acknowledgements

We thank B. Robert for his support, A. A. Pascal and P. Setif for critical reading of the manuscript and C. Cassier-Chauvat for fruitful discussions and critical reading of the manuscript. A. Wilde and D. Dienst are acknowledged for kindly providing the plasmid carrying the inactivated *hfq*. B. Ughy and L. Kaiser are acknowledged for preliminary work on this project. The CNRS, URA2096, PEPS Modutics (to GA) and the CEA, IBITEC-S financially supported this work. AON was the recipient of a doctoral fellowship from the French Ministry of Higher Education and Research (ED 387).

References

Aiba, H., Adhya, S., and de Crombrugghe, B. (1981) Evidence for two functional *gal* promoters in intact *Escherichia coli* cells. *J Biol Chem* **256:** 11905–11910.

Allen, M.M., and Smith, A.J. (1969) Nitrogen Chlorosis in Blue-Green Algae. *Arch Mikrobiol* **69:** 114–120.

Anderson, L.K., and Toole, C.M. (1998) A model for early events in the assembly pathway of cyanobacterial phycobilisomes. *Mol Microbiol* **30:** 467–474.

Asayama, M., and Imamura, S. (2008) Stringent promoter recognition and autoregulation by the group 3 sigma-factor SigF in the cyanobacterium *Synechocystis* sp. strain PCC 6803. *Nucleic Acids Res* **36:** 5297–5305.

Barne, K.A., Bown, J.A., Busby, S.J., and Minchin, S.D. (1997) Region 2.5 of the *Escherichia coli* RNA polymerase sigma70 subunit is responsible for the recognition of the 'extended-10' motif at promoters. *EMBO J* **16:** 4034–4040.

Benz, J.P., Lintala, M., Soll, J., Mulo, P., and Bölter, B. (2010) A new concept for ferredoxin-NADP(H) oxidoreductase binding to plant thylakoids. *Trends Plant Sci* **15:** 608–613.

Bowsher, C.G., Hucklesby, D.P., and Emes, M.J. (1993) Induction of Ferredoxin-NADP+ Oxidoreductase and Ferredoxin synthesis in pea root plastids during nitrate assimilation. *Plant J* **3:** 463–467.

Dienst, D., Dühring, U., Mollenkopf, H., Vogel, J., Golecki, J., Hess, W.R., and Wilde, A. (2008) The cyanobacterial homologue of the RNA chaperone Hfq is essential for motility of *Synechocystis* sp. PCC 6803. *Microbiology* **154:** 3134–3143.

Elhai, J., and Wolk, C.P. (1988) A versatile class of positive-selection vectors based on the nonviability of palindrome-containing plasmids that allows cloning into long polylinkers. *Gene* **68:** 119–138.

Golden, J.W., and Wiest, D.R. (1988) Genome rearrangement and nitrogen fixation in Anabaena blocked by inactivation of *xisA* gene. *Science* **242:** 1421–1423.

Lagarde, D., Beuf, L., and Vermaas, W. (2000) Increased production of zeaxanthin and other pigments by application of genetic engineering techniques to *Synechocystis* sp. strain PCC 6803. *Appl Environ Microbiol* **66:** 64–72.

Mazouni, K., Bulteau, S., Cassier-Chauvat, C., and Chauvat, F. (1998) Promoter element spacing controls basal expression and light inducibility of the cyanobacterial *secA* gene. *Mol Microbiol* **30:** 1113–1122.

Mitschke, J., Georg, J., Scholz, I., Sharma, C.M., Dienst, D., Bantscheff, J., *et al.* (2011) An experimentally anchored map of transcriptional start sites in the model cyanobacterium *Synechocystis* sp. PCC6803. *Proc Natl Acad Sci USA* **108:** 2124–2129.

Mohamed, A., and Jansson, C. (1989) Influence of light on accumulation of photosynthesis-specific transcripts in the cyanobacterium *Synechocystis* 6803. *Plant Mol Biol* **13:** 693–700.

Neuhaus, H., and Emes, M. (2000) Nonphotosynthetic metabolism in plastids. *Ann Rev Plant Physiol Plant Mol Biol* **51:** 111–140.

Obana, N., Shirahama, Y., Abe, K., and Nakamura, K. (2010) Stabilization of *Clostridium perfringens* collagenase mRNA by VR-RNA-dependent cleavage in 5′ leader sequence. *Mol Microbiol* **77:** 1416–1428.

Osanai, T., Imamura, S., Asayama, M., Shirai, M., Suzuki, I., Murata, N., and Tanaka, K. (2006) Nitrogen induction of sugar catabolic gene expression in *Synechocystis* sp. PCC 6803. *DNA Res* **13:** 185–195.

Prentki, P., and Krisch, H.M. (1984) In vitro insertional mutagenesis with a selectable DNA fragment. *Gene* **29:** 303–313.

Sauer, J., Schreiber, U., Schmid, R., Völker, U., and Forchhammer, K. (2001) Nitrogen starvation-induced chlorosis in *Synechococcus* PCC 7942. Low-level photosynthesis as a mechanism of long-term survival. *Plant Physiol* **126:** 233–243.

Schluchter, W.M., and Bryant, D.A. (1992) Molecular characterization of ferredoxin-NADP+ oxidoreductase in cyanobacteria: cloning and sequence of the *petH* gene of *Synechococcus* sp. PCC 7002 and studies on the gene product. *Biochemistry* **31:** 3092–3102.

Thomas, J., Ughy, B., Lagoutte, B., and Ajlani, G. (2006) A second isoform of the ferredoxin:NADP oxidoreductase generated by an in-frame initiation of translation. *Proc Natl Acad Sci USA* **103:** 18368–18373.

van Thor, J.J., Hellingwerf, K.J., and Matthijs, H.C. (1998) Characterization and transcriptional regulation of the *Synechocystis* PCC 6803 *petH* gene, encoding ferredoxin-NADP+ oxidoreductase: involvement of a novel type of divergent operator. *Plant Mol Biol* **36:** 353–363.

van Thor, J.J., Gruters, O.W., Matthijs, H.C., and Hellingwerf, K.J. (1999) Localization and function of ferredoxin-:NADP(+) reductase bound to the phycobilisomes of *Synechocystis*. *EMBO J* **18:** 4128–4136.
Ughy, B., and Ajlani, G. (2004) Phycobilisome rod mutants in *Synechocystis* sp. strain PCC6803. *Microbiology* **150:** 4147–4156.
Valladares, A., Muro-Pastor, A.M., Fillat, M.F., Herrero, A., and Flores, E. (1999) Constitutive and nitrogen-regulated promoters of the *petH* gene encoding ferredoxin:NADP+ reductase in the heterocyst-forming cyanobacterium *Anabaena* sp. *FEBS Lett* **449:** 159–164.
Valladares, A., Muro-Pastor, A.M., Herrero, A., and Flores, E. (2004) The NtcA-dependent P1 promoter is utilized for *glnA* expression in N2-fixing heterocysts of *Anabaena* sp. strain PCC 7120. *J Bacteriol* **186:** 7337–7343.
Waters, L.S., and Storz, G. (2009) Regulatory RNAs in bacteria. *Cell* **136:** 615–628.
Zuker, M. (2003) Mfold web server for nucleic acid folding and hybridization prediction. *Nucleic Acids Res* **31:** 3406–3415.

Supporting information

Additional supporting information may be found in the online version of this article.

Please note: Wiley-Blackwell are not responsible for the content or functionality of any supporting materials supplied by the authors. Any queries (other than missing material) should be directed to the corresponding author for the article.

A gene regulation mechanism that allows synthesis of two ferredoxin:NADP oxidoreductase isoforms from asingle gene in the cyanobacterium *Synechocystis* sp. PCC 6803

Ferredoxin:NADP oxidoreductase (FNR), encoded by the *petH* gene, provides NADPH for CO_2 fixation in photoautotrophic cells and oxidizes NADPH in heterotrophic cells. Whereas there is only one *petH* gene copy in the cyanobacterium *Synechocystis* sp. PCC6803, two FNR isoforms accumulate (FNR_L and FNR_S). It was proposed that FNR_L fulfills functions in linear electron transport while FNR_S is involved in cyclic electron transport and respiration. In addition, FNR_S was shown to be the product of an internal translation initiation within the FNR_L open-reading frame.

During my PhD, I revealed the mechanism by which *petH* translation leads to the accumulation of either one of the FNR isoforms. I showed that *petH* 5'noncoding region was essential for FNR_S accumulation. Deletions in the 5'noncoding region suggested that each isoform is produced from a specific mRNA. 5'-end mapping of the *petH* transcripts confirmed this fact and showed that under standard conditions -when FNR_L accumulates- two mRNAs carrying similar leaders (32 and 53 bases) are transcribed; while under nitrogen starvation -when FNR_S accumulates- an mRNA, carrying a longer leader (126 bases), is transcribed.

Transcriptional fusions of the *Escherichia colilac* promoter to *petH*, with different leader sequences, suggest that the translation regulation does not require a specific factor; but rather to a spontaneously occurring secondary structure, adopted by the longer leader. Such a structure could activate FNR_S translation initiation and prevent that of FNR_L. Toeprinting assays confirmed this hypothesis *in vitro*; translation-initiation complexes locations were mapped to the FNR_L initiator codon in the short mRNA and to the FNR_S initiator codon in the longer mRNA.

Thus we have uncovered a novel gene-regulation mechanism by which two isoforms are produced from a single gene in the cyanobacterium *Synechocystis* sp. PCC 6803.

Key words: Cyanobacteria, ferredoxin:NADP oxidoreductases, transcription, translation, genetic regulation

Un mécanisme de régulation génétique permettant la synthèse de deux isoformes de la ferrédoxine:NADP oxydoréductase, à partir d'un seul gène, chez la cyanobactérie *Synechocystis* sp. PCC 6803

La Ferrédoxine:NADP oxydoréductase (FNR), qui est codée par le gène *petH*, est une enzyme qui catalyse la production du NADPH dans les cellules photoautotrophes, ainsi que sa consommation dans les cellules hétérotrophes. Alors que le gène *petH* est unique, chez la cyanobactérie *Synechocystis* sp. PCC6803, deux isoformes de FNR sont synthétisées FNR_L et FNR_S. Il a été proposé que FNR_L soit impliquée dans les transferts linéaires de la photosynthèse, et que FNR_S soit impliquée dans les transferts respiratoires ainsi que dans les transferts cycliques de la photosynthèse. De même, il a été montré que FNR_S était le produit d'une initiation de traduction interne dans le même cadre de lecture que FNR_L.

Durant mon travail de thèse, j'ai découvert un mécanisme grâce auquel un gène peut coder deux isoformes. Tout d'abord, j'ai montré que la région 5' non codante de *petH* était indispensable à la synthèse de FNR_S. Des délétions dans cette région ont montré que chaque isoforme pouvait être codée par un transcrit spécifique. La cartographie de l'extrémité 5' des transcrits a confirmé cette hypothèse. En effet, en conditions standards (où FNR_L s'accumule) deux ARNm avec des séquences "leader" similaires (32 et 53 bases) sont transcrits alors qu'en conditions de carence en azote (où FNR_S s'accumule) un ARNm portant une séquence "leader" plus longue (126 bases) est transcrit.

Des fusions transcriptionnelles du promoteur *lac* de *Escherichia coli* avec les différentes régions transcrites de *petH*, nous ont permis de montrer que cette régulation ne nécessitait pas de facteur spécifique et qu'elle pourrait être accomplie par des structures secondaires adoptées par la région leader des ARNm. De telles structures pouvant activer l'initiation de traduction de FNR_S et inhiber celle de FNR_L. La cartographie des complexes d'initiation de traduction montre que dans l'ARNm le plus long le complexe se trouve dans la région initiatrice de FNR_L, alors que dans les ARNm plus courts celui-ci est localisé dans la région initiatrice de FNR_S.

Ainsi, nous avons mis en évidence un nouveau mécanisme de régulation génétique qui permet, dans une bactérie, la synthèse de deux isoformes à partir d'un seul gène.

Mots-clés : Cyanobactéries, ferrédoxine:NADP oxydoréductases, transcription, traduction, régulation génétique